Instituto Superior Técnico
Universidade Técnica de Lisboa

Characterisation of mixing in order to develop a scale--down approach for a two-liquid phase bio-oxidation reaction

Ana Catarina da Silva Damas Pinto

Dissertação para a obtenção do Grau de Mestre em
Engenharia Biológica

Júri

Presidente:	Prof. Luís Joaquim Pina da Fonseca, Departamento de Engenharia Química e Biológica (DEQB), IST
Orientação:	Prof. Duarte Miguel de Franca Teixeira dos Prazeres, Departamento de Engenharia Química e Biológica (DEQB), IST Dr. Frank Baganz, UCL Biochemical Engineering Department
Vogais:	Prof. Pedro Carlos de Barros Fernandes, Centro de Engenharia Biológica e Química do DEQB, IST

Dezembro 2009

Acknowledgements

I want to laud Instítuto Superior Técnico (IST) for everything that I am today. This school give me so many life and academic skills that I almost can say that built me as a individual that is very well prepared to face and be great at my prossifinal life.

I am truly grateful for the opportunity gave by IST Biological and Chemistry Engineering Department (DEQB) to do an international experience by doing my Biological Engineering Master Degree at the University College London (UCL) Biochemical Engineering Department in London.

At UCL, I met amazing people both in Roberts and Katz Building that welcomed me and helped me into find solutions and reasons for the many project bottlenecks. However, I have to truthfully thank all the support, interest and almost nursing that was given by Dr. Frank Baganz and Mr. Christopher Grant. I have really to give my thanks to Mr. Christopher Grant that always helps me both during the project and for reviewing my Master degree thesis.

Cannot describe how I am so thankful to the most important people in my life, my family. They give me all the support to live in London, but most of all for all the kindness and support in the hardest times that I faced.

To my family

Abstract

The biocatalysis oxidation of long chain alkanes is a key commercial target. The bio-oxidation studied was the *E.coli* pGEc47ΔJ *n*-dodecane bioconversion into 1-dodecanol. It was made the mixing characterisation in order to develop a scale-down approach for a two-liquid phase bio-oxidation reaction. It involved high speed camera (HSC) imaging, perform bioconversions and apply DoE software. From the HSC imaging it was identify an apparently good mixing in SFs and the 24-DSW are the best for mixing but still show a mixing limitation. That can be overcome by using surfactants or the Duetz system. The 24-SRW was considered inadequate. In all bioconversions performed dodecanoic acid was present indicating over-expression of the plasmid. The interface began to be analysed. The Triton X-100 and PPG addition reduced the liquid loss in sacles. In SFs bioconversions using Triton X-100 demonstrate a 3fold bioconversion improvement (0,8 $g/L_{organic\ phase}$) compared with other SFs and 2L-fermenter using *n*-octane. The use of Deutz system with the rigid silicone sandwich cover layer also is equal a good solution (0,3±0,3 $g/L_{organic\ phae}$). The alternative use of Duetz System with gas permeable membrane with 24-DSW with half sphere without surfactants prove also a high bioconversion (0,2±0,2 $g/L_{organic\ phase}$). In conclusion, it was achieved a scale-down method which is considered a breakthrough and a platform for more in-depth studies.

Keywords: Two-liquid phase systems, bio-oxidation reaction, Triton X-100; 1-dodecanol, DoE

Resumo

A bio-oxidação de alkanos de longa cadeia tem elevada importância comercial. A bio-oxidação estada foi a bioconversão de *n*-dodecane em 1-dodecanol por *E.coli* pGEc47ΔJ. Foi efectuada a caracterização da mistura para desenvolver a miniaturização da bio-oxidação de um sistema de duas fases líquidas. Para tal foi usado imagens de alta velocidade, fermentações e o recurso ao software DoE. Das imagens de alta velocidade detectou-se uma boa mistura nos erlenmeyers e o poço rectangular é o melhor apesar de apresentar ainda problemas na mistura, os quais podem ser resolvidos através da adição de surfactantes e/ou da aplicação do *Duetz system*. Os poços cilíndricos são considerados inadequados. Em todas as fermentações o ácido dodecanóico estava presente evidenciando a sobre-expressão do plasmidio. A análise à interface começou a ser feita. A adição de Triton X-100 e PPG implicaram a diminuição da perda do líquido em todas as escalas. No erlenmeyer de 1L a adição do Triton X-100 aumentou em 3 vezes a produção de 1-dodecanol (0,8 g/$L_{fase\ orgânica}$). A aplicação do *Duetz system* com a membrana de silicone rígida alcançou-se bons níveis de bio-oxidação (0,3±0,3 g/$L_{fase\ orgânica}$). A alteração no Duetz sytem ao adicionar a membrana permeável com fundo esférico provou alcançar elevada bioconversão (0,2±0,2 g/$L_{fase\ orgânica}$). Em conclusão, foi alcançado um novo progresso para a miniaturização de sistemas de dois líquidos e criou-se uma plataforma de arranque para novos desenvolvimentos.

Palavras-chave: Sistemas de dois líquidos, bio-oxidação, Triton X-100; 1-dodecanol, DoE

Table of Contents

List of Figures

long-chain-length integral membrane alkane hydroxylase ; dioxyg Acinetobacter sp. M-1 dioxygenase; CHA0 inferred alkane oxygenase in *P. fluorescens* CHA0. Image adapted from van Beilen J.B., *et. al.*, 2007.

Figure 11: Structural representations of the alkane-hydroxylating enzyme systems. Integral membrane non-heme di-iron alkane hydroxylase systems: i) crystal structure of the C-terminal domain of rubredoxin; ii) rubredoxin reductase modelled on the structure of putidaredoxin reductase; and iii). model for the AlkB alkane hydroxylase. The enzyme is proposed to have six transmembrane helices arranged in a hexagonal distribution that would define a long, hydrophobic pocket into which the linear alkane molecule can slip. The four histidine clusters (H) believed to bind the two iron atoms (Fe) would lie on the cytoplasmic side. In *P. putida* GPo1 AlkB, residue W55 lies in transmembrane helix 2 and extends its bulky arm towards the hydrophobic pocket (left). This hampers the proper insertion of alkanes longer than C13. The replacement of W55 by a serine residue (S55) (right), which has a shorter arm, allows longer alkanes to enter the pocket without impeding the proper alignment of the terminal methyl group relative to the histidine clusters. Sizes are not to scale. The soluble components of the alkane hydroxylase complex, rubredoxin and rubredoxin reductase, are not shown. Image adapted from van Beilen J.B.and *et. at.* (2004) and Rojo F. and *et. at.,*2005.

Figure 12: Struture of the alkane hydroylase system. The alkane hydroxylase system consists of three components: a membrane–bound mono-oxygenase (alkane hydroxylase AlkB), rubredoxin (AlkG) and rubredoxin reductase (AlkT). The alkane hydroxylase AlkB is an integral cytoplasmic membrane protein containing a diiron cluster. Rubredoxin (AlkG) transfers electrons from the flavoprotein rubredoxin reductase (AlkT) to AlkB. The functions of AlkF and AlkL are unclear. Image adapted from Staijen I. E. and *et. at.*, 1987, van Beilen J. B. and *et. at*., 1994, Wubbolts M.G. and *et. at.*1996 and Panke S. *et. at.*,1999.

Figure 13: Steps involved in the oxidation reaction catalyzed by alkane hydroxylase. Image adapted from Ayala M. and *et. at.*,2004.

Figure 14: Molecular genetics and pathway of alkane oxidation by *Pseudomonas oleovorans GPo1 (TF4- 1L; ATCC 29347 oleovorans.* The *alk-genes are* organized in two clusters: the *alkST* locus and the *alkBFGHJKL* operon, both located on the OCT plasmid. Proteins are identified by their gene name (see Table 2 for full name and function). Image adapted from van Beilen J. B. and *et. at.*,1994. For more detailed information about the alkBFGHJKL operon van Beilen J. B. and *et. at.* (1994) paper has a extensible description.

Figure 15: Schematic illustration of three possible mass-transfer mechanisms of apolar substrate from the organic phase to cell. A, direct droplet-cell interation; B, transfe mediated by organic carrier molecules; C, transfer via dissolution in the aqueous phase. Image adapted from Schmid A. *et.al.*, 1998.

Figure 16: Organization of the *alk* genes and plasmids carrying various *alk* constructs. (A) The *alk* genes are organized in the *alkST* and the *alkBFGHJKL* clusters. The expression of the *alkB-L* operon is positively regulated by AlkS. (B) pLAFRI-derived plasmids carrying different *alk* genes. The solid bars border deletions of specific *alk* genes. The effects of growth with (1) or without (2) DCPK on the growth rate and physiology of GPo12 recombinants carrying these plasmids are indicated as follows: 2, no detectable effects; 1, clear effects. Image adapted from Chen Q and *et.al*. (1996)

Figure 17: Process of using the Duetz system with sandwich covers for deepwell MTPs[3].

Figure 18: Visualisation of mixing conditions of a fermentation of *E.coli* pGEc47ΔJ in 20 % (v/v) of n-dodecane in 2L fermenter (two Ruston impellers and the air input) with 90% of head space.a) t=0h with no cells at 500 rpm; b) t=3h at 500 rpm; c) t=24h at 1000pm;d) t=48h 1000 rpm.

Figure 19: 2L Fermenter mimicking the usual components condition (20% (v/v) organic phase) with 1L of water and 200 mL *n*-dodecane with a stirrer agitation rate between 100 rpm and 700rpm and no air input. At the smaller agitation rates the laminate layer between the water and dodecane is not disrupt, but as agitation rate increases the laminar layer is broken by the first Ruston impeller forming organic droplets with 1-5 mm then the bottom Ruston impeller reduces the size of the droplets, helping to the complete mixture of the two phases at 700 rpm.

Figure 20: 2L Fermenter with 1L of water and 20% (v/v) of n-dodecane with no air supply after stirrer agitation. a) agitation rate of 1000 rpm; b) agitation rate of 650 rpm and with the addition of 100 µL of Polypropylene glycol (PPG). It is clear by b) that PPG creates an emulsion.

Figure 21: Visulisation of liquid hydrodynamics: of 1L SF with 100mL of Wubbolts media and 20% (v/v) of *n*-dodecane in a 25 mm throw diameter orbital shaker at 200rpm a), 250rpm b), 300rpm c) and 350rpm d).

Figure 22: Visulisation of liquid hydrodynamics: of 500mL SF with 50mL of Wubbolts media and 20% (v/v) of n-dodecane in a 25 mm throw diameter orbital shaker at 200rpm a), 250rpm b), 300rpm c) and 350rpm d).

Figure 23: Visulisation of liquid hydrodynamics: of 1L SF with 100mL of Wubbolts media and 20% (v/v) of *n*-dodecane in a 50 mm throw diameter orbital shaker at 50rpm a),100rpm b), 150rpm c), 200rpm d) and 250rpm e).

Figure 24: Visulisation of liquid hydrodynamics: of 500mL SF with 100mL of Wubbolts media and 20% (v/v) of *n*-dodecane in a 50 mm throw diameter orbital shaker at 50rpm a), 100rpm b), 150rpm c), 200rpm d), 250rpm e and 300rpm

Figure 25: Visulisation of the evoluation of agitation in the liquid hydrodynamics of 24-DSW with 10%(v/v) of Wubbolts media and 20%(v/v) of *n*-dodecane in a 50mm throw diameter orbital shaker at 220rpm and V_{liq} of 4,5mL a), 240rpm V_{liq} of 2,5mL b) and 240rpm with 48h fermentation broth*, V_{liq} of 2,5mL c). * Fermentation in 2L-Bioreactor where the fermentation of *E.coli* pGEc47∆J was using *n*-dodecane as substrate

Figure 26: Visualisation of the evolution of the agitation in the liquid hydrodynamics of 24-DSW with 10%(v/v) of Wubbolts media, 20%(v/v) of *n*-dodecane in a 12,5mm throw diameter orbital shaker at 360rpm V_{liq} of with 2,5mL a) and 0,1% TritonX-100 at 345rpm V_{liq} of with1,5mL b).

Figure 27: Visulisation of the evoluation of agitation in the the liquid hydrodynamics of 24-DSW with 2,5mL of 10%(v/v) of Wubbolts media, 20%(v/v) of *n*-dodecane in a 3mm throw diameter orbital shaker at 500rpm.

Figure 28: Visualisation of liquid hydrodynamics of 24-DSW with 2mL of 10%(v/v) of Wubbolts media, 20%(v/v) of *n*-dodecane and the fermentation emulsifying material collected at the interface after centrifugation** in a 3mm throw diameter orbital shaker at 300rpm a), 400rpm b), 500rpm c), 600rpm d). **Emulsifying material from 2L-Bioreactor two-phase fermentation of *E.coli* pGEc47∆J using *n*-dodecane as substrate after 48hours. The material was collected from the interface of the two-phases after centrifugation.

Figure 29: Visulisation of liquid hydrodynamics of 24-DSW with 2mL of 10%(v/v) of 48 h Broth cells with new media **, 20%(v/v) of *n*-dodecane and the fermentation emulsion*** in a 3mm throw diameter orbital shaker at 300rpm a), 350rpm b), 400rpm c), 500rpm d) and 600rpm e). ** Cells from a fermentation in 2L-Bioreactor where the fermentation of *E.coli* pGEc47∆J was using *n*-dodecane as substrate;***Emulsion from the previous fermentations.

Figure 30: Visulisation of the evoluation of agitation in the the liquid hydrodynamics of 24-SRW with 2,5mL of 10%(v/v) of Wubbolts media, 20%(v/v) of *n*-dodecane in a 3mm throw diameter orbital shaker at 520rpm.

Figure 31: 1L SFs with the different culture conditions after 30hours. In this picture is clear the importance of be concern with the evaporation rate and the formation of emulsion..

Figure 32: Image of the support of Duetz System and the gas permeable membrane from [3;6]

Figure 33: 3D surface plot showing that the higher 1-dodecanol concentration in the organic phase happens in two different situations. The one with maximum aqueous volume and the minimum of the *n*-dodecane. which correspond to higher evaporation rate (figure??). The other is the minimum aqueous volume and the *n*-dodecane maximum addition. The last it is the better conditions.

Figure 34: 3D surface plot showing that the highest 1-dodecanol concentration in the interface is reached combining the maximum of *n*-dodecane addition with the minimum of aqueous volume.

Figure 35: Schematic of face-centred composite design used. This is an extension of the full factorial design that requires 6 additional runs, one in the centre (axis) of each face of the cubic design space.

Figure 36: Showing a flat plateau region for achieving maximum yield exists with a growth period of 2hours, an induction agitiaton in the range of 275-325rpm and a growth agitation of 150rpm to 225rpm.

Figure 37: 3D surface plot showing how further reduction in growth period may lead to increased yield; fluctuations in growth period may also be expected to change the yield since the relationship is not flat around this region of the plot. The contour plot indicates that for maximum consistency an induction agitation of 310rpm should be used with a growth agitation of 185rpm.

Figure 38: DCW half-normal plot of effects, where it is chosen the effects to be included in the model.

Figure 39: 3D surface plot showing the weak relationship between the parameters. It seems that with the higher concentration of glucose the DCW is higher.

Figure 40: Evaporation rate half-normal plot of effects, where it is chosen the effects to be included in the model.

Figure 41: 3D surface plot showing that the higher evaporation rate is achieved at the maximum aqueous volume and the minimum *n*-dodecane volume.

Figure 42: 1-dodecanol in the organic phase half-normal plot of effects, where it is chosen the effects to be included in the model.

Figure 43: 1-dodecanol in the organic phase half-normal plot of effects, where it is chosen the effects to be included in the model.

Figure 44: 3D surface plot showing the weak relationship between the parameters.

Figure 45: 1-dodecanol in the organic phase half-normal plot of effects, where it is chosen the effects to be included in the model.

Figure 46: 1-dodecanol in the organic phase half-normal plot of effects, where it is chosen the effects to be included in the model.

Figure 47: 3D surface plot showing the weak relationship between the parameters. It seems that with the higher concentration of glucose the DCW is higher.

List of Tables

Table 20: Table showing ANOVA for response 6: dodecanoic acid in the interface. The model is not significant.

Table 21: GC Chromatogram (50 % (v/v) sample/ethyl acetate)of the 1-Dodecanol Standards of Experience 1. Blue: Ethyl acetate, Orange: *n*-dodecane GC peak area and Pink: 1-Dodecanol peak area. t:time (minutes)and peak area: peak area (µV s).

Table 22: GC Chromatogram (50 % (v/v) sample/ethyl acetate) of the 1-Dodecanol Standards of Experience 2. Blue: Ethyl acetate, Orange: *n*-dodecane GC peak area and Pink: 1-Dodecanol peak area. t:time (minutes)and peak area: peak area (µV s).

Table 23: GC Chromatogram (20 % (v/v) sample/ethyl acetate) of the Dodecanoic Acid of Experience 2. Blue: Ethyl acetate, Orange: *n*-dodecane GC peak area and Green: Dodecanoic Acid peak area. t:time (minutes)and peak area: peak area (µV s).

Table 24: GC Chromatogram (20 % (v/v) sample/ethyl acetate) of the 1-Dodecanol Standards from experiences 3, 6 and 7 . Blue: Ethyl acetate, Orange: *n*-dodecane GC peak area and Pink: 1-dodecanol peak area. t:time (minutes)and peak area: peak area (µV s).

Table 25: GC Chromatogram (20 % (v/v) sample/ethyl acetate) of the Dodecanoic Acid Standards from experiences 3, 6 and 7. Blue: Ethyl acetate, Orange: *n*-dodecane GC peak area and Green: Dodecanoic Area Peak area. t:time (minutes)and peak area: peak area (µV s).

Table 26: GC Chromatogram (20 % (v/v) sample/ethyl acetate) of the 1-Dodecanol Standards at 24hours from experience 5. Blue: Ethyl acetate, Orange: *n*-dodecane GC peak area and Pink: 1-Dodecanol peak area. t:time (minutes)and peak area: peak area (µV s).

Table 27: GC Chromatogram (20 % (v/v) sample/ethyl acetate) of the 1-Dodecanol Standards at 48hours from experience 5. Blue: Ethyl acetate, Orange: *n*-dodecane GC peak area and Pink: 1-Dodecanol peak area. t:time (minutes)and peak area: peak area (µV s).

Table 28: GC Chromatogram (20 % (v/v) sample/ethyl acetate) of the Dodecanoic Acid Standards at 24hours from experience 5. Blue: Ethyl acetate, Orange: *n*-dodecane GC peak area and Green dodecanoic peak area. t:time (minutes)and peak area: peak area (µV s).

Table 29: GC Chromatogram (20 % (v/v) sample/ethyl acetate) of the Dodecanoic Acid Standards at 48hours from experience 5. Blue: Ethyl acetate, Orange: *n*-dodecane GC peak area and Pink: 1-Dodecanol peak area. t:time (minutes)and peak area: peak area (µV s).

Table 30: GC Chromatogram (20 % (v/v) sample/ethyl acetate) of the 1-Dodecanol Standards from experience 7. Blue: Ethyl acetate, Orange: *n*-dodecane GC peak area and Pink: 1-Dodecanol peak area. t:time (minutes)and peak area: peak area (µV s).

Table 31: GC Chromatogram (20 % (v/v) sample/ethyl acetate) of the Dodecanoic Acid Standards from experience 7. Blue: Ethyl acetate, Orange: *n*-dodecane GC peak area and Green dodecanoic peak area. t:time (minutes)and peak area: peak area (µV s).

Table 32: GC Chromatogram (20 % (v/v) sample/ethyl acetate) of the 1-Dodecanol Standards from experience 8. Blue: Ethyl acetate, Orange: *n*-dodecane GC peak area and Pink: 1-dodecanol peak area. t:time (minutes)and peak area: peak area (µV s).

Table 33: GC Chromatogram (20 % (v/v) sample/ethyl acetate) of the Dodecanoic Acid Standards from experience 8. Blue: Ethyl acetate, Orange: *n*-dodecane GC peak area and Green: Dodecanoic Area Peak area. t:time (minutes)and peak area: peak area (µV s).

Table 34: GC Chromatogram (50 % (v/v) sample/ethyl acetate) of the samples of the 1L SFs at the different time points from experience 1. Blue: Ethyl acetate, Orange: *n*-dodecane GC peak area, Pink: 1-Dodecanol peak and Green: Dodecanoic Acid (proved later). t: time and peak area: peak area (µV s).

Table 35: GC Chromatogram (50 % (v/v) sample/ethyl acetate) of the samples of the 1L SFs at the different time points from experience 1. Blue: Ethyl acetate, Orange: *n*-dodecane GC peak area, Pink: 1-Dodecanol peak and Green: Dodecanoic Acid (proved later). t:time (minutes)and peak area: peak area (µV s).

Table 36: GC Chromatogram (20 % (v/v) sample/ethyl acetate) of the 1L SFs samples of organic phase at the different time points from experience 2. Blue: Ethyl acetate, Orange: *n*-dodecane GC peak area, Pink: 1-Dodecanol peak and Green: Dodecanoic Acid. t:time (minutes)and peak area: peak area (µV s).

Table 37: GC Chromatogram (20 % (v/v) sample/ethyl acetate) of the 500mL SFs samples of organic phase at the different time points from experience 2. Blue: Ethyl acetate, Orange: *n*-dodecane GC peak area, Pink: 1-Dodecanol peak and Green: Dodecanoic Acid. t:time (minutes)and peak area: peak area (µV s).

Table 38: GC Chromatogram (20 % (v/v) sample/ethyl acetate) of the 1L SFs samples of interface at the different time points from experience 2. Blue: Ethyl acetate, Orange: *n*-dodecane GC peak area, Pink: 1-Dodecanol peak and Green: Dodecanoic Acid. t:time (minutes)and peak area: peak area (µV s).

Table 39: GC Chromatogram (20 % (v/v) sample/ethyl acetate) of the 500mL SFs samples of interface at the different time points from experience 2. Blue: Ethyl acetate, Orange: *n*-dodecane GC peak area, Pink: 1-Dodecanol peak and Green: Dodecanoic Acid. t:time (minutes)and peak area: peak area (µV s).

Table 40: GC Chromatogram (20 % (v/v) sample/ethyl acetate) of the 1L SFs samples of organic phase at the different time points from experience 3. Blue: Ethyl acetate, Orange: *n*-dodecane GC peak area, Pink: 1-Dodecanol peak and Green: Dodecanoic Acid. t:time (minutes)and peak area: peak area (µV s).

Table 41: GC Chromatogram (20 % (v/v) sample/ethyl acetate) of the 1L SFs samples in the interface at the different time points from experience 3. Blue: Ethyl acetate, Orange: *n*-dodecane GC peak area, Pink: 1-Dodecanol peak and Green: Dodecanoic Acid.t:time (minutes)and peak area: peak area (µV s).

Table 42: GC Chromatogram (20 % (v/v) sample/ethyl acetate) of the well samples at 24hours in the organic phase from experience 5. Blue: Ethyl acetate, Orange: *n*-dodecane GC peak area, Pink: 1-Dodecanol peak and Green: Dodecanoic Acid. t:time (minutes)and peak area: peak area (µV s).

Table 43: GC Chromatogram (20 % (v/v) sample/ethyl acetate) of the well samples at 24hours in the interface from experience 5. Blue: Ethyl acetate, Orange: *n*-dodecane GC peak area, Pink: 1-Dodecanol peak and Green: Dodecanoic Acid. t:time (minutes)and peak area: peak area (µV s).

Table 44: GC Chromatogram (20 % (v/v) sample/ethyl acetate) of the well samples at 48hours in the organic phase from experience 5. Blue: Ethyl acetate, Orange: *n*-dodecane GC peak area, Pink: 1-Dodecanol peak and Green: Dodecanoic Acid. t:time (minutes)and peak area: peak area (µV s).

Table 45: GC Chromatogram (20 % (v/v) sample/ethyl acetate) of the well samples at 48hours in the interface from experience 5. Blue: Ethyl acetate, Orange: *n*-dodecane GC peak area, Pink: 1-Dodecanol peak and Green: Dodecanoic Acid. t:time (minutes)and peak area: peak area (µV s).

Table 46: Average GC Chromatogram (20 % (v/v) sample/ethyl acetate) of the well samples in the organic phase from experience 6. Blue: Ethyl acetate, Orange: *n*-dodecane GC peak area, Pink: 1-Dodecanol peak and Green: Dodecanoic Acid. t:time (minutes)and peak area: peak area (µV s).

Table 47: Average GC Chromatogram (20 % (v/v) sample/ethyl acetate) of the well samples in the interface from experience 6. Blue: Ethyl acetate, Orange: *n*-dodecane GC peak area, Pink: 1-Dodecanol peak and Green: Dodecanoic Acid. t:time. and peak area: peak area (µV s).

Table 48: GC Chromatogram (20 % (v/v) sample/ethyl acetate) of the well samples in the organic phase from experience 7. Blue: Ethyl acetate, Orange: *n*-dodecane GC peak area, Pink: 1-Dodecanol peak and Green: Dodecanoic Acid. t:time (minutes)and peak area: peak area (µV s).

Table 49: GC Chromatogram (20 % (v/v) sample/ethyl acetate) of the well samples in the interface from experience 7. Blue: Ethyl acetate, Orange: *n*-dodecane GC peak area, Pink: 1-Dodecanol peak and Green: Dodecanoic Acid. t:time. and peak area: peak area (µV s).

Table 50: GC Chromatogram (20 % (v/v) sample/ethyl acetate) of the well samples in the organic phase from experience 8. Blue: Ethyl acetate, Orange: *n*-dodecane GC peak area, Pink: 1-Dodecanol peak and Green: Dodecanoic Acid. t:time (minutes)and peak area: peak area (µV s).

Table 51: GC Chromatogram (20 % (v/v) sample/ethyl acetate) of the well samples in the interface from experience 8. Blue: Ethyl acetate, Orange: *n*-dodecane GC peak area, Pink: 1-Dodecanol peak and Green: Dodecanoic Acid. t:time (minutes)and peak area: peak area (µV s).

Table 52: GC Chromatogram (20 % (v/v) sample/ethyl acetate) of the well samples by a new extraction method from experience 8. Blue: Ethyl acetate, Orange: *n*-dodecane GC peak area, Pink: 1-Dodecanol peak and Green: Dodecanoic Acid. t:time (minutes)(minutes) and peak area: peak area (µV s).

Table 53: Cell Density on the samples from experience 2

Table 54: Cell Density on the samples from experience 3

Table 55: Volume of the three separated phases on the samples from experience 5

Table 56: Final volumes of the three phases from experience 6.

Table 57: Final volumes of the three phases from experience 7.

Table 58: Final volumes of the three phases from experience 8.

Abbreviations

BMO	Butane monooxygenase
CER	Carbon dioxide evolution rate
CMC	Critical micelle concentration
DCPK	Dicyclopropylketone
DCW	Dry cell weight
DEQB	Departamento de Engenharia Química e Biológica
DoE	Design experience
DOT	Dissolved oxygen tensions
DSW	Deep Square Well
DX7	Design-Expert®, version 7 software
E.coli	*Escheria coli*
Fe	Iron
GC	Gas chromatography
H_2O	Water
HLB	Hydrophile-lipophile balance
HPLC	High performance liquid chromatography
HSC	High speed camera
HT	High-throughput
IST	Instituto Superior Técnico
MBCR	Miniature bubble column reactor
MBRs	Miniature bioreactors
MSBRs	Miniature stirred bioreactors
MTPs	Microtitre plates
NADH	Nicotinamide adenine dinucleotide (reduced form)
NADPH	nicotinamide adenine dinucleotide phosphate (reduced form)
O_2	Oxygen
OD	Optical density
ORM	Optical Reflectance Measurement
OTR	Oxygen transfer rate
pAH1	Medium-chain-length integral membrane alkane hydroxylase
pAH2	Long-chain-length integral membrane alkane hydroxylase
pAHs	Particulate alkane hydroxylases
pMMO	Particulate methane monooxygenase
PMO	Propane monooxygenase
POE	Propagation of error
PPG	Polypropylene glycol
RQ	Respiratory quotient
RSM	Response surface methods
SA	Static surface area available for gas– liquid mass transfer
SDS	Sodium n-dodecyl sulfate
SFs	Shake flasks
sMMO	Soluble methane monooxygenase
SRW	Shallow Round Wells
STRs	Stirred tank reactors
t	Time
UCL	University College London
UHTS	Ultra high-throughput screening
V_W	Total well volume

Introduction

The oxidation of long chain alkanes is a key commercial target and would be particularly attractive via biocatalysis to avoid the difficulties of conventional oxidation. For example, stereo-region- and reaction-specific catalysts, operating under mild conditions, enable reactions difficult to perform chemically to be carried out effectively with minimum side reactions and by-products.

There are four areas of particular importance: oxygen supply, substrate access; two-phase operation and product recovery. It is crucial in aerobical fermentation that supply of oxygen to the cells and this factor is not only related with poor gas-liquid mass transfer in two-liquid phase biotransformation but also with the method of supply and for safety reasons. As alkane chain length increases the limitations for access into the cell may limit the bio-oxidation rate. Permeabilization methods may give a partial solution but will compromise cell stability. The solubility of the alkanes is very low, thus using an auxiliary phase may help. It is also essential to establish an environmentally compatible solution to the downstream removal of the product. Obtaining a high concentration of the target product is crucial to the economics of the process. The ability to separate the phases and carry out extraction and/or distillation is function of upstream and process parameters.

This project was focused in the bottleneck of substrate access. The first concern was to know in which shaken incubator conditions total homogenous mix between the aqueous and organic phase were achieved. The second was related with the permeabilization of the cell membrane. For that intention surfactants and biosurfactants were used.

The two-lliquid phase system study was *E.coli* pGEc47ΔJ *n*-dodecane bioconversion where the mixing characterisation was done in 500 mL shake flaks (SFs), 1L SFs with the same geometry, with four baffles, 24-DSW (inverted inverted pyramid bottom and half sphere) and 24-SRW in order to develop a scale-down approach for a two-liquid phase bio-oxidation reaction. It involved high speed camera imaging of mixing and performing two-phase bio-oxidation reactions at different scales, GC analysis of substrate and product and application of statistical experimental design (DoE) software.

The products from an *n*-dodecane bio-oxidation reaction are 1-dodecanol, dodecanal and dodecanoic acid. Althougth, in this work the target product is 1-dodecanol.

1-dodecanol is a medium-priced fine chemical with a large market; it is used in the production of surfactants, lubricating oils and widely applied for the personal care ingredients. The total European fatty alcohol market was worth €1billion in 2008 and this is growing at an average of 6% per year. 1-dodecanol accounts for a large proportion of this market but the natural sources of it are comparatively scarce compared to longer chain alcohols [12].

However, in particular, dodecanoic acid as a medium–length fatty acid is widely used as a lubricant, as an additive in industrial preparations, in the manufacture of metallic stearates, pharmaceuticals, soaps, cosmetics, and food packaging [11]. Therefore, it is also a possible target product.

Literature Review

Two-Liquid Biocatalytic Systems

Biocatalysis offers some advantages over traditional chemical catalysis from the viewpoint of both the organic chemist and process engineer. For example, stereo- region- and reaction-specific catalysts, operating under mild conditions, enable reactions difficult to perform chemically to be carried out effectively with minimum side reactions and by-products. In the past years biocatalytic processes have come to find applications in the pharmaceutical and fine chemical industries as an alternative to chemical synthesis for high value products (in particular optically pure compounds) and today several processes are operating commercially throughout the world. However, the majority of these processes are hydrolytic resolutions of racemic compounds to produce chiral synthons or optically pure products. Recent developments in biocatalysis will now enable the application of biologically mediated carbon-carbon bond forming reactions and redox conversions which is where real power of biocatalysis lies [Lye G. L., *et. al.*,2001].

The application of two-liquid phase biocatalysis presents some difficulties biochemical engineering challenges including the selection of an appropriate reaction medium, reactor design and operating parameters. These selections also have critical implications for subsequent downstream processing operations such as phase separation and product recovery. Besides the use of a multiphasic liquid-liquid medium also presents a number of unique problems for scaling-up such a process. As well, environmental constrains may also lead to the development of alternatives to organic solvents as the second liquid phase, which including the possibility of using room temperature ionic liquids. The potential advantages and disadvantages of two-liquid phase biocatalytic processes are summarised in (Table 1).

For each class of biocatalytic process the medium in which the conversion occurs is dependent on the properties of the reactants and products. In many cases the reaction components have relatively low water solubilities (less than 50mM), so they are called hydrophobic. Increasingly, the substracte(s), product(s), or both are novel compounds which may be aromatic, multicyclic or bulky molecules. These compounds bear little relationship in size, shape or hydrophilicity to the natural substrates of a given enzyme [Lye G. L., *et. al*., 2001]. Normally, the medium for hydrocarbon bioconversion consists of an apolar-organic phase, typically 20% (v/v), and a polar phase composed of nutrients, salts, glucose and cells [Mathys R. G., *et. al*., 1999; Schmid A., *et.al*., 1998]. The fact of the reactant is a poorly water-soluble implies that the biocatalytic conversions rates are low. Consequently, the process streams leaving the reactor frequently contain low product concentrations, making a difficult problem downstream.

However, the use of a two-liquid phase medium to effects bioconversions at higher overall concentrations has clear advantages for those reactions where one or more of the reaction components are poorly water-soluble. It has been also found to have particular benefits where

these compounds are inhibitory and/or toxic to the biocatalyst by providing a reservoir for the molecules away from the vicinity of the biocatalyst.

Table 1: Potential advantages and disadvantages of two-liquid phase biocatalysis. Table adapted from Lye G. L., *et. al.,*2001.

Process feature	**Advantages (+) and disadavantages (-)**
Reactor Operation	+ Solubilisation of poorly water-soluble molecules + Reduced inhibition/toxicity + Excellent substrate/catalyst contact - Reduced activity per unit volume - Diffusional limitations - Liquid-liquid interfacial damage to biocatalyst - Dissolved organic phase damage to biocatalyst
Downstream Processing	+ Isolation of reactant from product + Higher product concentration - Emulsification

Fundamentals

In two liquid-liquid phase biocatalysis processes a virtually water-immiscible organic solvent is added to an aqueous phase (at a concentration well above the aqueous phase saturation limit) containing the biocatalyst. Therefore a biphasic reaction medium is created. Where the substrate is hydrophobic the organic phase will be initially rich in substrate which will then partition into the aqueous phase. Once in the aqueous phase the substrate will be acted upon by the biocatalyst which can only operate at concentrations up to the aqueous phase saturation limit of the substrate. Due to the action of the biocatalyst more substrate will subsequently partition out of the organic phase in order to maintain a thermodynamic equilibrium. A second substrate may also be present, either preferentially present in the organic phase or alternatively supplied from another phase (for example oxygen from the gas phase or water from the aqueous phase). Depending upon its solubility, the product may either remain in the aqueous phase or partition into the organic phase. The basic mass transfer and biocatalytic reaction steps are summarised in Figure 1.

At a fundamental level, a considerable amount of work has addressed the issue of how microorganisms respond when exposed to an organic solvent. Hence organic solvents (whether dissolved in an aqueous phase or present as a discrete second liquid phase) have long been known to be harmful to biocatalytic activity [Lye G. L., *et. al.*, 2001; Laane C. *et al*., 1987]. The toxic effect of the solvent in the cells can be divided in two different processes: one it is the result of the diffusion of the solvent molecules throughout the citoplasmatic membrane - molecular toxicity- and the other is associated with the direct contact between the solvent and the biocatalyst – phase

toxicity. The former one can provoke enzymatic inhibition, protein denaturation and DNA damage and modification of the citoplasmatic membrane fluidity. [Aires-Barros M.R. *et. al*., 2003]

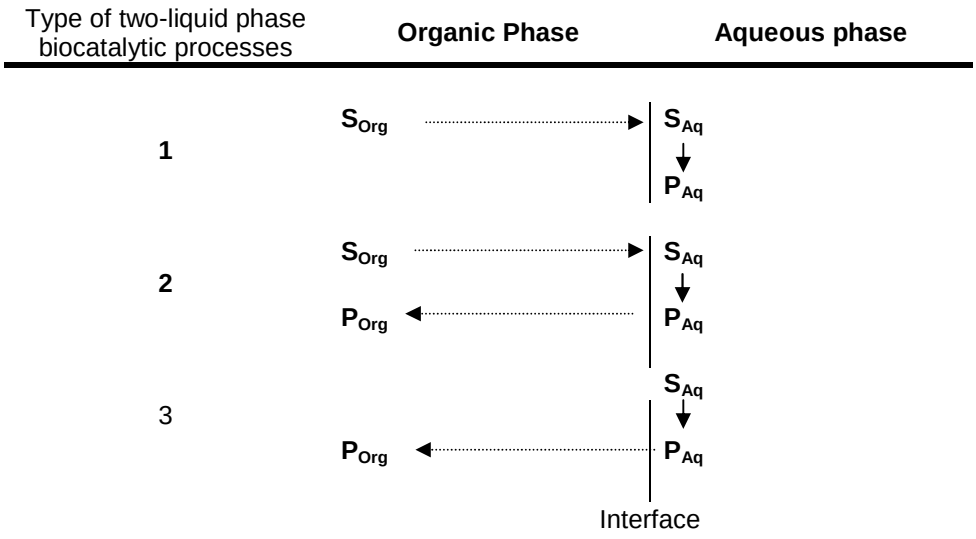

Figure 1: Classification of two-liquid phase biocatalytic processes on the solubility of both the substrate (S) and product (P) molecules. The biocatalyst may be a whole-cell or an immobilized enzyme and is assumed to be present in the aqueous phase. Dashed lines represent mass transfer processes. Image adapted from Lye G. L., *et. al.,* 2001.

The solvent molecular toxicity is usually evaluated through the logarithm of the partition coefficient of an organic solvent in a standard octanol-water system (logP, known as *Hansch parameter*, which is an indicator of the hydrophobic degree of a solvent. This value can be experimental determined or estimated. Many works demonstrated that, the application of different hydrophobicities on several biocatalysts show a tendency between the biocatalytic activity and the solvent hydrophobicity as being a sigmoidal curve. Therefore, it is considered that logP< 2 is toxic and so biocatalysis in organic solvents is low, biocatalysis is moderate at LogP between 2 and 4 and high at LogP>4. Nonetheless, these correlations are depended on the biocatalyst, microorganism, agitation rate, etc. and then have empirical nature and only can provide guidance.

The major toxicity of the polar organic solvents is because they reduce the water activity. In the other way the apolar organic solvents do not interact with water molecules creating biphasic systems, so the water activity is not disturbed. It is known that molecular toxic solvent-resistant bacteria typically possess a number of physiological mechanisms to counteract the presence of solvents in the cytoplasmic membrane. These mechanisms include the rapid synthesis of *trans*-unsaturated fatty acids to alter membrane fluidity and the active pumping of solvents out of the membrane [Aires-Barros M.R. *et. al*., 2003; Laane C. *et al*., 1987; Lye G. L., *et. al.*, 2001].

The solvent phase toxicity is associated to the disorganization of the citoplasmatic membrane and its permeabilization, with the lost of essential metabolites and co-factors, could lead to the extraction of nutrients, cellular aggregation and emulsification. This type of toxicity can be

reduced trough the use of more concentrated nutrients and inoculums to compensate the lost of nutrients, and diminish the interfacial area, using a smaller agitation rate and/or decreasing the volumetric ratio of organic/aqueous phase, in order to reduce aggregation phenomenal and emulsifications. The immobilisation of the biocatalyst, the use of hydrophobic membranes and the biocatalyst reactor design are some of the possible solutions for the decrease of the phase toxicity [Aires-Barros M.R. *et. al*., 2003; Laane C. *et al.*, 1987].

Two-liquid phase biocatalysis process

In the two-liquid phase biocatalysis process, as in any other bioprocess, biocatalysis and reactor selection, design and operation all have an impact on subsequent product recovery and in the economics of the process. It is possible recycle either the biocatalyst or the organic phase. It is important therefore that design methods incorporate such reasoning. Figure 2 shows a schematic integrated process design strategy [Lye G. L., et. al., 2001; Lye G. L., et. al., 2003; Duetz W. A., 2007].

Target productivity together with preliminary selection of the biocatalyst form defines the required mass transfer coefficient. Currently, the initial identification of a desired biocatalytic activity and its subsequent improvement (over-expression of enzyme activities) is made by microscale techniques. Having identified a biocatalyst, optimisation of fermentation conditions for more efficient production of the biocatalyst is made. This step usually occurred in shake flask formats. When these conditions are optimised the kinetics, product inhibition, evaporation rate, etc. are made at microscale. This then sets guidelines for initial reactor selection which subsequently set operating parameters (for example, in a stirred tank reactor: stirrer speed and phase volume ratio). The effects of these decisions on the rest of the process must then be considered and if there are problems for product recovery then either the catalyst selection or reactor selection or (operation or some combination of these) may need to be re-examined. The scheme also shows that this is an iterative procedure and indicates where molecular genetics methods may be applied to overcome design constrain associated with biocatalyst. Using graphical technique many of the “what if” studies can be done prior to the experimentation so as to guide the development effort. A number of experimental design tools, normally in miniature bioreactors (MBRs), can also be used here. The automation of these approaches holds the possibility to efficiently examine the activity of large numbers of biocatalysts acting on a wide range of parameters.

Two-liquid phase biocatalysis classification

The two-liquid biocatalyst systems could be grouped by theirs mixture nature (Figure 3):

Homogeneous mixture of the organic and aqueous phase

The best way to increase the solubility of a hydrophobic substrate in an aqueous biotransformation environment is by adding an organic solvent that is well miscible in water

(methanol, ethanol). Although, the high polarity of such solvents (LogP<2) give them a toxic character.

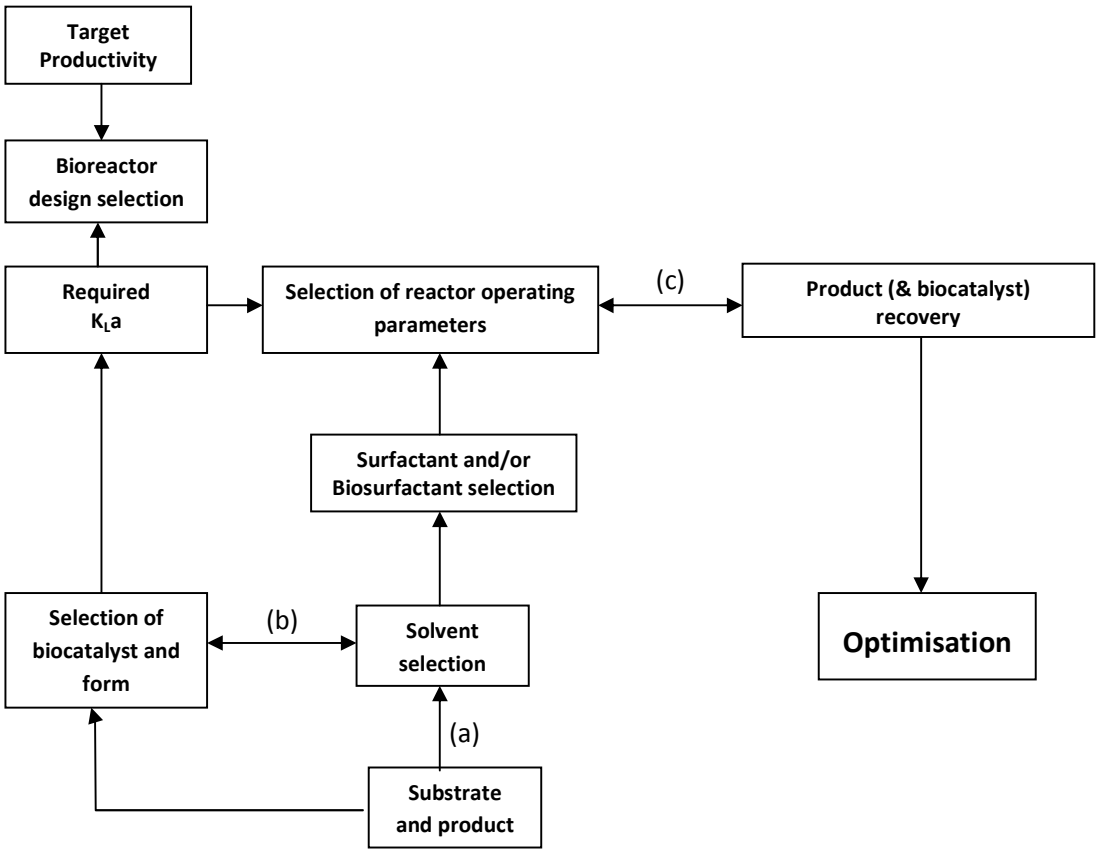

Figure 2: Integrated design strategy for two-liquid phase biocatalytic processes: (a) may need to compromise on solvent selection to satisfy solubility constraints; (b) opportunities for protein/genetic engineering; (c) may need to compromise on reactor operation to satisfy downstream processing constraints. Image adapted from Lye G. L., *et. al*., 2001.

Two-liquid phases mixture

The biocatalyst stability in an organic solvent can be improved using a water immiscible solvent (LogP>4). The result is biphasic system with the biocatalyst and the hydrophilic components in the aqueous phase and the substrate(s) and the hydrophobic compounds in the organic phase. It is considered that the organic phase is continuous and the aqueous is dispersed in the aqueous phase (Figure 3 A)). In other cases the continuous phase is the aqueous phase and the organic phase is disperse in the former one (Figure 3 B)). At both cases the biocatalyst remains in the aqueous phase. Yet, it could be possible to add a third phase (immobilised biocatalyst) in the previous situations (Figure 3 C), D)).

In these systems is necessary that the interfacial area is higher enough to ease the mass transfer between substrate/product through the liquid-liquid interface and liquid-solid interface (if the biocatalyst is immobilised) and agitation rate and phase ratio (organic volume/aqueous volume). The mass partition of the substrate(s) and product(s) between the phases is mediated by the

selection of the organic solvent. The preferential accumulation of substrate(s) and product(s) on organic phase minimizes the inhibition action for the biocatalyst.

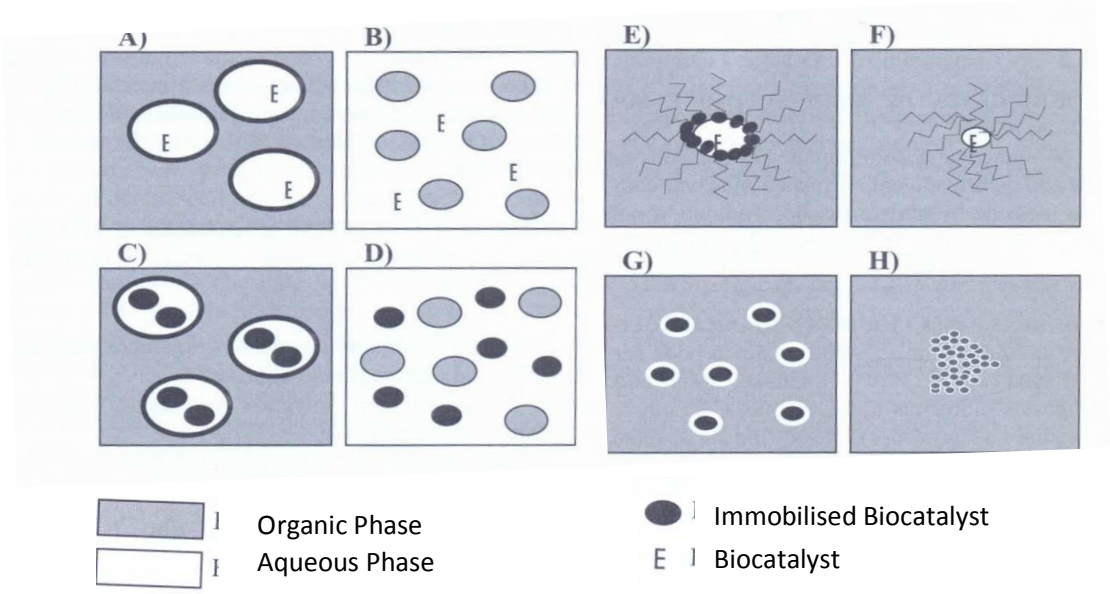

Figure 3: Classification of the two-liquid biocatalytic systems. A) Two-liquid phase mixture: emulsion of the aqueous phase in the organic; B) Two-liquid mixture: emulsion of the organic phase in the aqueous; C) and D) Immobilised biocatalyst in a porous support on a biphasic system; E) Microencapsulated Biocatalyst in a inverse micelle; F) Modified biocatalyst with Polyethylene glycol (PEG) and dissolved on organic phase; H) Lyophilized biocatalyst and in crystal from, suspended on the organic phase. Image adapted from Aires-Barros M.R. *et. al*., 2003.

Biocatalysts dissolved in organic phase: inverse micelles and covalently modified enzymes

The systems of inverse micelles are particular cases of microemulsions, in which the aqueous phase is not macroscopically visible in the organic phase (continuous phase) (Figure 3 E)). Inverse micelles are almost spherical surfactant molecules with a diameter of 15-20A□, where the polar "heads" remain on the inside due to unfavourable interactions. The lipophilic tails due to favourable interactions with the organic phase, form a hydrophobic outer later that in effect protects the hydrophilicity core (Figure 3 E)). In this way, inverse micelles allow the solubilisation of biocatalyst in the inner aqueous core and the mass partition of substrate(s)/product(s) between the aqueous nucleus and the organic solvent, depending on the surfactant hydrophobicity. So the enzyme is located in finely dispersed aqueous pools which are encapsulated by a surfactant within the nonpolar solvent [Singh A. *et al*., 2007].

The elevated interfacial area of the inverse micelles minimise the mass transfer limitations. Though, the presence of the surfactant can inactivate enzymes and cause problems at the downstream process. Alternatively, the enzymes can be solubilised in organic solvents by covalent modification of enzyme surface with PEG (Figure 3 F)).

Biocatalysts suspended in organic phase with low water quantity: immobilised biocatalysts.

The reduction of the amount of water at vestigial quantities can be useful in some biocatalytic systems. The selection of the solvent is critical as a competition between the solvent and the enzyme for water. The use of hydrophilic solvents can lead to the removal of the hydration layer of the enzyme, then there is structural modification and consequently lost of catalytic activity. The use of these almost anhydrous environments, in biotransformations implies the use of immobilised enzymes in a solid support (Figure 3 G)) or as powder (lyophilized or in crystals) (Figure 3 H)). In the choice for the type or support it is needed to have in accounted its affinity towards water, because water will be shared between the immobilization matrix, the enzyme and the reaction environment, and so condition the available water in the microenvironment.

Two-liquid phase biocatalysis process reactors

The keys to the design or select a two-phase biocatalytic reactor are [Lye G. L., *et. al*., 2001] :

- Match the rate of substrate supply to (or product removal from) the biocatalyst with the rate of the reaction itself such that the aqueous phase concentration of any inhibitory substrate (or product) is maintained below a critical level and maximum use is made of the available activity;
- Establish sufficient interfacial area between the aqueous and organic phases to enable adequate substrate or product mass transfer;
- Be able to readily control the interfacial area.

The reactors that achieve these requirements are two-phase bioreactors, which include the stirred tank and the liquid-impelled loops, and membrane reactors.

Downstream of two-liquid phase biocatalysis process

The whole process flowsheets for the conversion of a poorly water-soluble substrate into either a poorly water-soluble product or a water-soluble product are shown in Figure 4 (options for recycling of the phases and the biocatalysts are also included). In both cases the key initial downstream processing step is the separation of the product-containing phases from both the second phase are the biocatalyst [Lye G. L., *et. al*., 2001].

There are several downstream processes to two-liquid biotransformation: microporous microfiltration membranes; centrifugation; heating and cooling treatment; dense phase membranes and distillation [Schmid A. *et.al.*, 1998].

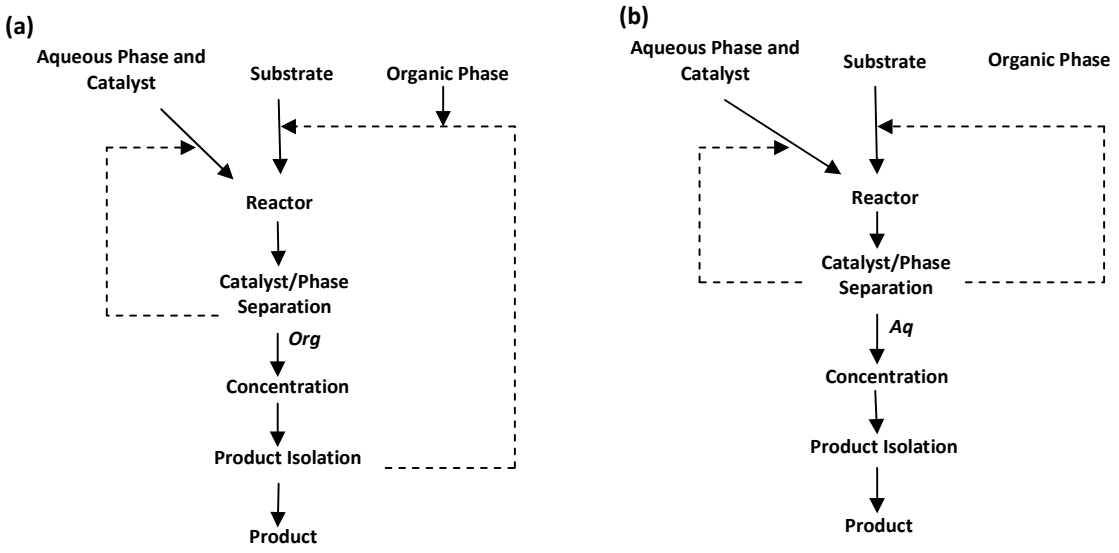

Figure 4: Process flowsheets for (a) conversion of a poorly water-soluble substrate into a poor water-soluble product, and (b) conversion of a poorly water-soluble substrate into a water-soluble product..Dashed lines, represent options for organic phase recycle while dotted lines represent options for biocatalyst recycle. Image adapted from Lye G. L., *et. al.*, 2001.

Scale-up of a two-liquid phase biocatalysis

In order to reliably scale-up a two-liquid phase process an understanding of how the individual parameters within the model will vary as a function of scale is required. Generally it would be expected that the kinetic constants of the biocatalyst and substrate/product partition coefficients would be scale independent. While the substrate/product mass transfer coefficients may vary somewhat, it would be expected that the most significant parameter with respect to scale-up would be the maintenance of a constant interfacial area per unit volume. This will be critical in determining solute mass transfer rates (flux being proportional to area per unit volume) and hence the maintenance of substrate/product concentrations in the vicinity of the biocatalyst below toxic levels. Rules for scale-up of two-liquid phase biocatalytic process are currently lacking [Lye G. L., *et. al.*, 2001; Cull S.G., *et. al*., 2002].

The majors bottlenecks for the scale of a two-liquid phase biotransformation are [Schmid A. *et.al.*, 1998]:

1. The maximum apolar substrate transfer rates from the organic phase to the cells could limit the volumetric bioconversion rates, thus negatively influencing the attainable space-time yield;
2. Downstream processing could present a major challenge because of the strong emulsification or organic solvents in the two-liquid phase culture medium;
3. The combination of aerobic operation and flammable solvents in two-liquid phase precesses presents an explosion hazard. Unless means are found to operate two-liquid phase systems efficiently and safetly, scale-up of such bioprocesses will not be feasible;

4. The major cost of operating two-liquid phase biotransformation.

Safety Considerations

In aerobic bioconversions, where organic solvents are used, the potential to form explosive atmosphere at large scales of operation raises serious issue. Clearly reactors for such processes must be housed in special facilities designed to comply with both explosion-proof and biological containment regulations. First, high pressure reactors can be built capable of containing the pressure generated by an air-solvent vapour explosion (e.g. >6 bar). Secondly, the generation of an explosive atmosphere can be prevented by a range of operating strategies. These include the dissolution of volatile solvents in inert carrier solvents, reduction of the oxygen concentration in the inlet gas and operation above critical pressures or below critical temperatures. The need to ensure the safe operation of two-phase biotransformations will lead to increased capital and operating costs compared to traditional fermentation processes [Lye G. L., et. al., 2001; Schmid A. *et.al.*, 1998].

Mass transfer in two-liquid phase biocatalysis process

In a multiphase system, mass and heat transfer processes provide the cells with nutrients and remove products and heat created by the whole-cell biocatalysis (Figure 5). In two-liquid phase cultures, one of the phase barriers is the liquid-liquid interface between the organic solvent and the aqueous medium. Apolar substrates, dissolved in the organic phase, are transported from the solvent droplets to the cells and apolar products are transferred from the cells to solvent droplets [Schmid A. *et.al.*, 1998]. Clearly intimate contact of the aqueous and organic phases is necessary in order to effectively transfer reactants and/or products from one phase to the other. Therefore, the isolated enzymes are favored over whole cell systems [Lye G. L., *et. al.*, 2001].

An important question in this context is under which conditions apolar substrate transfer from organic phase to the cells will limit productivities and how will maximal transfer rates relate to the biocatalaytic potential of the cells. That is, if it could be possible to design a high-quality at high cell densities, could be possible transfer substrate to the biocatalyst from apolar phase across phase, boundaries at a sufficiently high rate to take full advantage of the biocatalytic potential?

To answer to this question it is necessary to determine the organic mass transfer rate from apolar phase to the cells in two-liquid phase cell cultures growing on organic substrate as the sole carbon source [Schmid A. *et.al.*, 1998]. There is an apparatus known as *Lewis cell* that the rate of mass transfer of substrate from organic to aqueous phase under defined conditions can be measured and thus a mass coefficient obtained. These data can be combined with measurements of aqueous phase biocatalyst kinetics (measured in all aqueous phase solution with dissolved levels of poorly water-soluble organic substrate beneath the saturation concentration) to predict substrate and product concentration-time profiles in a Lewis cell with biocatalyst present. These can then be compared with those measured experimentally. This technique is valid both for microbial and

enzymically cataysed biotransformations. The Lewis cell may also be used to measure the partitioning of substrates and products between phases. The generic use of the Lewis cell lies in the ability it gives to expose biocatalyst to defined amounts of interface and consequently the Lewis cell has a role in determining interfacial effects not only upon biocatalyst kinetics as illustrated here but also upon biocatalyst stability.

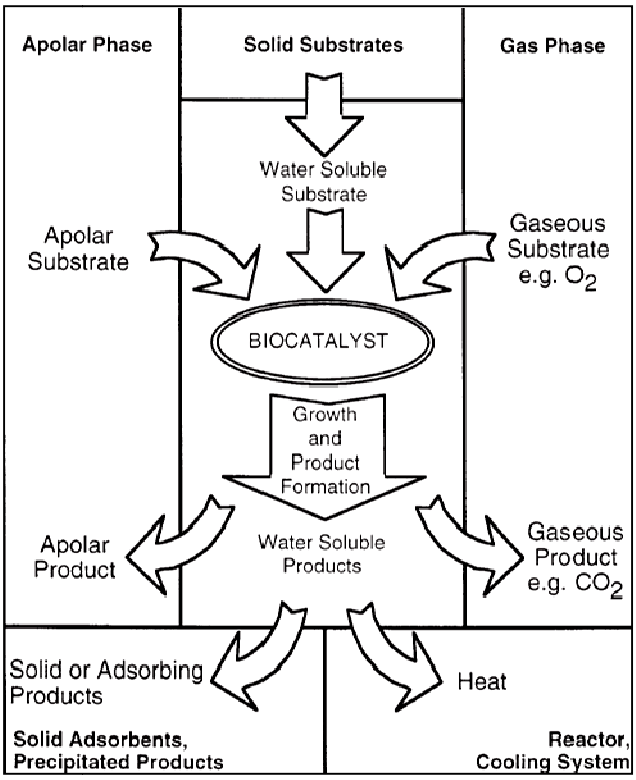

Figure 5: Schematic diagram of substrate, product, and heat fluxes throughout a multiphase bioreactor medium. Gaseous, apolar, and solid substrates must cross phase boundaries to be taken up by cells. Likewise, products excreted by cells, if they do not accumulate in the aqueous phase, are extracted into the organic solvent phase, stripped by the continuous flow of gas through the reactor, or adsorbed to a solid absorbent. Heat produced by the culture is transferred to the cooling system of the reactor. In a mass-heat transfer-limited culture one of these fluxes indicates by the *shaded arrows*, is rate limiting. Image adapted from Schmid A. *et.al.*, 1998.

Substrate concentration profiles of the two-liquid phase biocatalysis

The film theory is a useful model to describe and study the mass transfer between two phases. In this model it is assumed that the mass transfer takes place in a thin film (interface) and that the two phases are totally mixed (constant concentration), but near the interface the fluid is stagnated. So, the principal mass transfer resistance is near the interface [Fonseca M.M., *et. al.*, 2007].

In Figure 5 it is shown the substrate concentration profiles for two-liquid phase biocatalysis [Aires-Barros M.R. *et. al*., 2003]. Figure 5 A) represents the substrate concentration profile for the

two-liquid phase (aqueous and organic) system with the biocatalyst dissolved in the aqueous phase. The aqueous phase could be the continuous phase or the disperse phase (Figure 3 A, B). In the interface there is a substrate concentration variation because the substrate is hydrophobic and has low affinity to the aqueous phase and so its concentration decrease, not only by mass transfer effects but also by partition effects.

When the biocatalyst is immobilized, besides the two liquid phases (aqueous and organic), a third phase (solid) have to be considered which are the enzymes or whole cells immobilized. In Figure 5B)), it is the substrate concentration profile where the immobilized biocatalyst in a hydrophobic porous support is not dissolved in the aqueous phase (Figure 3 C, D). In this case, besides the mass transfer and partition effects at the liquid-liquid interface there are also the mass transfer and partition effects at the immobilized biocatalyst. The fact of the support is hydrophobic or hydrophilic is very important. For example, the use of a hydrophobic support increases the substrate concentration near the enzyme. If the volume of the aqueous phase is reduced compared with the organic phase and to the insoluble biocatalyst, the aqueous phase is no longer discrete. This situation is represented in the Figure 5C) and embrace the biocatalyst systems resuspended in organic solvent (Figure 3 G,H). In this case, the mass transfer between the organic and the not dispersed aqueous phase will depend on the biocatalyst particle specific area and not on the interfacial area between the two-liquid phases. The biocatalytic systems solubilized in the organic solvents, inverse micelles and chemical modification with PEG, are unique cases of the biphasic biosystems (Figure 3 E), F)), where macroscopically there is only one phase, (Figure 5 A)).

Options to overcome mass transfer limitations

Few two-liquid phase biocatalysis processes have so far reached industrial application because of their often uncompetitive low space-time yields. One important step on the way to more efficient processes is to overcome mass transfer limitations. Identification of these limitations is indispensable for optimal reactor design and successful scale-up. However, laboratory an industrial practice have shown, that in two-liquid phase whole phase systems it is sometimes difficult to predict transfer rates due to the complex interactions of the solvent and microorganisms [Kollmer A. and *et. at*., 1999].

To attain high volumetric biotransformation and biosynthesis rates in two-liquid bioprocesses it is necessary to maintain high substrate mass transfer rates and improve these where they are limiting. Options to achieve this include increasing the organic-aqueous interfacial area by [Schmid A. *et. al*., 1998]:

- Using surfactants;
- Increasing the volume fraction of the dispersed organic phase;
- Increasing the agitator power input.

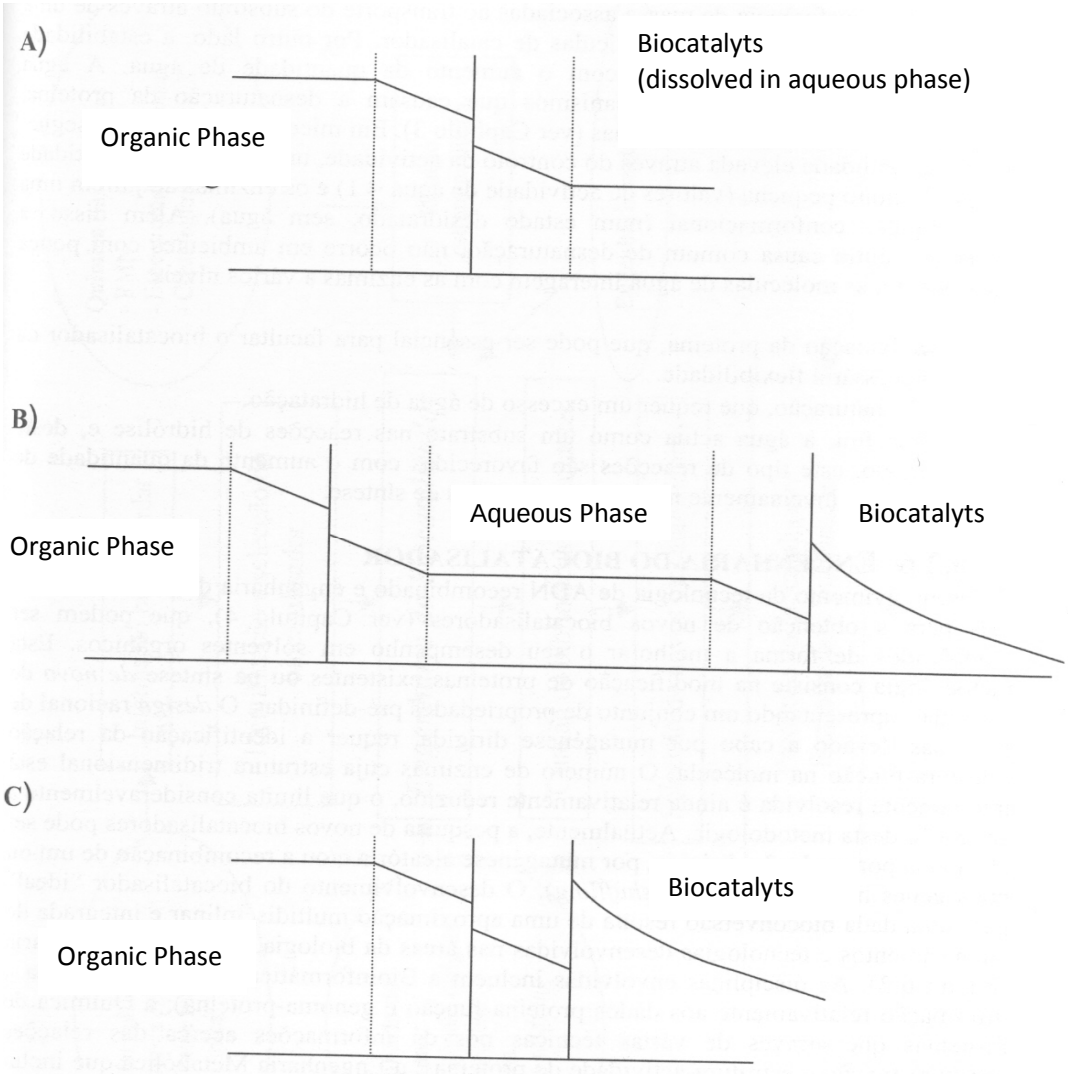

Figure 6: Theoretical hydrophobic substrate concentration profiles to several biocatalytic systems. Image adapted from Aires-Barros M.R. *et. al*. (2003).

Use of Surfactants

Surfactants, both chemical and biological, are amphiphilic compounds which can reduce surface and interfacial tensions by accumulating at the interface of immiscible fluids and increase the solubility, mobility, bioavailability and subsequent biodegradation of hydrophobic or insoluble organic compounds. They form aggregates structures such as micelles. They are generally characterised by properties such as the critical micelle concentration (CMC), the hydrophile-lipophile balance (HLB), chemical structure and charge, as well as by source. An interface is any boundary between two different phases (e.g. air–liquid, liquid–liquid, solid–liquid, etc.) and microbial life may be more common at interfaces as evidenced by microbial biofilms, surface films, and aggregates. Below the cmc, a surfactant may increase bioavailability by decreasing surface tension.

Above the cmc, micelles or other aggregates are formed that partition hydrophobic substrates and may enhance biodegradation by allowing for closer cell–substrate interactions, or may fuse directly with microbial membranes resulting in direct substrate delivery. However, they can be toxic and can damage very type of environments because of human excessive use of surfactants [Bognolo G., 1999; Singh A. *et.al.*, 2007; Van Hamme J.D. *et. al.*, 2006; Schmid A et.al., 1998; Kollmer A. et. al., 1999].

The chemical surfactants are available in many forms, and are generally classified based on charge as anionic (e.g. Alkyl sulfates (includes sodium dodecylsulfate, SDS), nonionic (Ethoxylated alcohols (includes Triton X-100), cationic (Amidoamine quaternaries) and amphoteric. Investigations on their impacts on microbial activity have generally been limited in scope to the most common and best characterized surfactants. Chemical surfactants can interact with microbial proteins and can be manipulated to modify enzyme conformation in a manner that alters enzyme activity, stability and/or specificity. Familiar examples of chemical surfactants routinely used in the biology laboratory include sodium n-dodecyl sulfate (SDS), which is an anionic alkyl sulfate, and Triton X-100, which is a nonionic ethoxylated alcohol. Chemical surfactants may be exploited to mimic some of the roles of biosurfactants. Chemically synthesized surfactants are commonly used in the petroleum, food and pharmaceutical industries as emulsifiers and wetting agents.

Recently a number of new biosurfactants have been described and accelerated advances in molecular and cellular biology are expected to expand our insights into the diversity of structures and applications of biosurfactants [Bognolo G., 199].

Scale-Down Process and mixing conditions in minibioreators

Microscale processing techniques are rapidly emerging as a means to increase the speed of bioprocess design and reduce material requirements. Automation of these techniques can reduce labour intensity and enable a wider range of process variables to be examined.

The challenge that biotech companies, especially pharmaceutical industry face is the will to establish biocatalytic processes quickly yet the biocatalysis is often slow to implement whereas chemical routes, although often more expensive and less selective, can currently be developed more quickly. This is because of the need to first screen a large biocatalyst library in shake flask cultures for the required catalytic activity from this do further testing of the successful candidates in bench-top bioreactors prior to pilot-scale studies and then subsequently collect the necessary design data for each step of the design process. The need to carry out a vast number of development cultivations has resulted in the advance and increasingly widespread deployment of small-scale bioreactor systems (miniature bioreactors (MBRs) that offer a miniaturised, high-throughput (HT) solution to process development.

The advantages of such an approach to overcome this process development bottleneck would include:

- the evaluation of large biocatalyst libraries in shorter periods of time;
- a reduction in the quantity of often expensive synthetic substrates required for process development;
- the rapid generation of design data for use in process and economic models;
- the potential to operate automated whole process sequences in microwell formats;
- a more rapid translation of processes from discovery to pilot plant scale.

At present, there are several constraints on the use of microscale techniques for biocatalyst improvement, in particular, the requirement for a rapid and sensitive activity assay. The variability in growth often seen between microwells on a single plate can render assays too insensitive to distinguish between improved biocatalysts with less than a tenfold difference in activity. This is often compounded by the need to maintain HT, which effectively limits the number of measurements of activity in each well to only one. Techniques for enhanced and reproducible microbial cultivation in microwells are thus essential. To date, the screening problem has mainly been addressed by choice of biocatalytic systems that are amenable to rapid and sensitive screening strategies. These include colorimetric or fluorimetric assays or the monitorization *via* a change in pH of the reaction. In practice, however, such an assay is often not available and the assay of choice becomes high performance liquid chromatography (HPLC), possibly coupled with mass spectrometry, which is more generic but reduces throughput. Recent developments in high-throughput detection methods could extend the range of biocatalytic reactions that can be effectively monitored in microwell formats. As a result, MBRs typically are currently less instrumented and also have limited opportunity for off-line sampling due to the small volumes used (ranging from 0.1 ml to approximately 100 ml); this means that there is currently a trade-off between information content in terms of data quality and quantity available from the bioreactor obtained by both online and off-line measurement and experimental throughput, illustrated in Figure 7 [Jonathan I. B., *et. at.,* 2003].

Besides technical problems there is the impact of miniaturisation on the cells. For an individual cell there are two indirect physical miniaturisation effects that have significant consequences. One is the intrinsically higher ratio of the gas–liquid exchange area to the volume of the bulk of the liquid, which results in relatively high specific OTRs under static conditions. The second physical effect of miniaturization is an increased importance of the surface tension, which counteracts the flow and movement of the liquid under the impact of bubbling or g-forces arising from orbital shaking. However, this two effects have counter consequence in the improve [Wouter A. D., 2007].

Types of Miniature bioreactors

The MBRs can be grouped on the basis of their agitation method (e. g. shaking, stirring or gas-sparging) with reference to the type of conventional bioreactor they either mimic or are derived from [Jonathan I. B., *et. at.,* 2003]. It is clear that some seek to replicate large-scale bioreactors in their

geometries. Furthermore, devices that agitate cultures through shaking typically exhibit a lower OTR capability relative to stirring, making these mechanically-agitated devices most promising for the cultivation of fast-growing microorganisms or cell cultivations that reach a high-cell density; however, there is typically not the same degree of parallelism available in stirring type. Besides the agitation method, the type of cell also influence the type of bioreactor used for process development. Bacterial cells (most frequently used in the two-liquid phase biocatalystis processes) are generally robust and not susceptible to shear damage, meaning that highly-shearing radial impeller systems (e.g. Rushton turbines) and high agitation rates can be employed. This provides such bioreactors with a high mass transfer capability, allowing rapidly metabolising, high-cell density microbial cell cultivations to be supported and increasing the amount of product that such bioprocesses can yield.

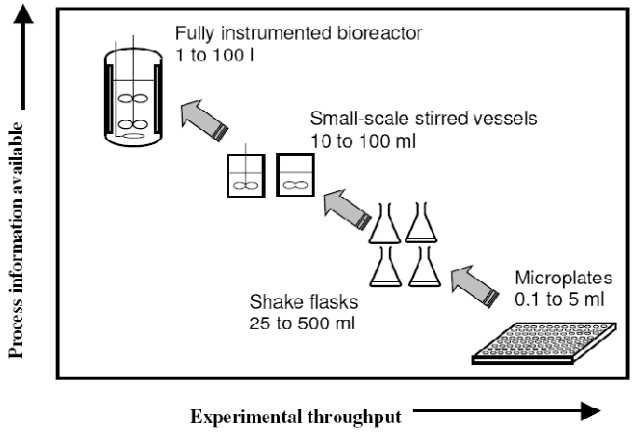

Figure 7: Illustration of the trade off in information output versus HT capability that currently exists for various cell cultivation devices at different scales. This figures shows that as bioreactors increase in scale, typically more process information is available due to improved monitoring a control systems. Image adapted from Jonathan I. B., *et. at.*, 2003.

Miniature shaken bioreactor systems:

Shaken systems have been used in bioprocessing from the very first attempts to grow antibiotic-producing microbial cultures. They are still widely used in industry and academia as a tool for drug discovery; media, strain and product optimisation; and process development. They comprise many different designs and volumes, ranging from shake flasks of hundreds of millilitres right down to microtitre plates (MTPs) of a few microlitres in volume.

Shake flasks (SFs)

For the past fifty years, scientists have used cell cultivation in SFs as a means of process development on a small scale, with volumes ranging from 10 ml to 500 ml. Shake flasks come in a variety of guises, can be made out of glass or plastic and some have baffles to aid aeration and mixing. They can be agitated using either orbital or linear shaking and can be housed in a

temperature-controlled cabinet. Factors that affect shake flask cultivations include vessel size, fill volume, construction material, geometry of baffles, shaking frequency and type of plug used to seal the vessel. They are widely used because they are an inexpensive and effective way of reproducibly performing many types of industrially-relevant cell cultivations for process development and, are easy to operate and largely impervious to mechanical complications. At the moment, online monitoring of cultures and manual additions and sampling are made. It is possible to control pH, measured online DOT, oxygen transfer rate (OTR), carbon dioxide evolution rate (CER) and consequently the respiratory quotient (RQ). Having such parameters monitored online would allow for more sophisticated cell-cultivation strategies to be carried out such as substrate feeding based on changes in culture broth pH due to cell metabolism and increase the scope of parallel bioprocess [Jonathan I.B. and *et. al*., 2006].

For the purpose of cultivations where the oxygen demand is high, the introduction of baffles can increase OTR at lower shaking frequencies. Though, high speeds can lead to excess splashing which can cause the gas-permeable plug (often made of cotton wool) at the top of the flask to become blocked through liquid saturation. Such an obstruction has been shown to severely reduce the oxygen transfer capability of the system, which could cause problems if a rapidly-respiring aerobe was being grown. Oxygen starvation could slow down the growth rate, alter production formation rates and/or generate unwanted toxic by-products e.g. acetate formation by *Escherichia coli.* However, a major limitation of shake flasks is their reliance on surface aeration, leading to reduced oxygen transfer relative to stirred tank reactors (STRs). Other issue is the measurement of the power consumption. It was demonstrated that the SF design was evolved in these problems [Büchs, J., 2001].

Microtitre plates (MTPs)

MTPs were first introduced in 1951 as a platform for diagnostic tests and are still widely used in the life sciences. They have the advantage of the ability to perform many identical reactions in parallel and at a very small scale. It is this advantage that has led to MTPs being used as miniature shaken bioreactors in the screening stage of process development for cell-line evaluation. Microtiter plates can now be considered a mature alternative to Erlenmeyer shake flasks.

Plates are usually fashioned out of plastic (polypropylene or polystyrene), although glass and metal versions exist. Mixing can be achieved using pipette aspiration or magnetically-agitated stirrer bars; however, orbital shaking of the entire plate on a heated block capable of controlling culture temperature is by far the most common method. The number of wells contained in MTPs is typically 6, 12, 24, 96 and 384, with up to 1536 and 3456 wells now available for ultra high-throughput screening (UHTS). Wells can either be rectangular or cylindrical (round) (Figure 8).

Square geometries aid mixing and oxygen transfer by mimicking the action of baffles. Square-bottomed plates act in a similar way by limiting vortexing of liquid inside the well and thus

increasing the turbulence of the system. However, this turbulent flow pattern results in wave-like structures at the surface causing an increase in the air-liquid surface area and probably an increase in the steepness of the oxygen gradient at the surface. In addition, the turbulent liquid flow seems to 'break' the surface tension, which does not exert a visible negative effect on the air–liquid area. The material of the square shape of the wells is normally polypropylene, which can consist in a problem as the leakage of toxic compounds from the plastic during incubation.

Polystyrene round-well MTPs (especially 96- and 48-well plates) has received much attention in more recent years. The advantages of polystyrene MTPs include their transparency, which enables the direct reading of optical densities, the absence of toxic substances leaking out from polystyrene and the presence of two walls separating the wells rather than one, which further minimizes the risk of cross-contamination. It might be concluded that MTPs with round wells give rise to lower OTRs than square-well MTPs at the same filling height and shaking conditions but that this disadvantage can be compensated for readily by using smaller culture volumes. The logistic advantages of the use of nontoxic and disposable polystyrene round-well MTPs – in combination with ever more sensitive assays – make it likely that they will gradually replace square-well MTPs for those applications where turbulence is not a major issue [Wouter A. D., 2007, Lye G.J. et.al., 2003].

Due to the increase in surface area caused by greater fluid dissipation up the sides of each microwell and the increased driving force for oxygen caused by better mixing, OTR is proportional to shaking amplitude and frequency, therefore increasing these parameters can be beneficial. In addition, OTR is inversely proportional to fill volume, particularly at higher shaking frequencies. However, there is a point beyond which any increase in agitation results in spillage of process liquid (unless the well is capped – which has it own problems, with reduced oxygen transfer into the well). As with shake flasks, the relatively low oxygen- transfer capacity of MTPs stems from the fact that they are shaken systems and rely upon surface aeration for mass transfer.

MTPs also suffer to a degree from the very feature that makes them attractive as a high-throughput device–small volume–because evaporation can remove a significant proportion of the fluid in the well. Breathable membranes can be placed on top of the plates to limit this evaporation, yet then the oxygen transfer capabilities are reduced. Duetz and co-workers (2000) (Figure 8) described a closure system consisting of a soft silicone layer with a small hole above the center of each well and a layer of cotton wool. Such a sandwich cover prevented spillage of the culture fluid during orbital shaking and ensured that exchange of headspace air is sufficient and occurs solely through the center holes. Evaporation rates of 20 ml per well per day (at 50% humidity and 30 ℃) were reported for 6 mm long holes with a diameter of 1.5 mm. Although evaporation is a potential problem in all MBRs, MTPs appear to be more susceptible to this due to typically using the smallest process volumes [Lye G.J. et.al., 2003].

Although, MTPs are used extensively in discovery research they have suffered from a lack of instrumentation limiting the range of data that can be collected. However, recently techniques have

been developed like multipipettes, pipetting robots, microplate readers and autosamplers. Besides, MTPs are designed based on a standard footprint, are mechanically-simple and the very standardisation of their design makes them ideal to build into automated, robotic platforms that truly take such technologies into the HT domain, conferring upon them the ability to perform hundreds of cell-cultivations in parallel, using a footprint not much larger than that of a conventional pilot-scale bioreactor.

A)

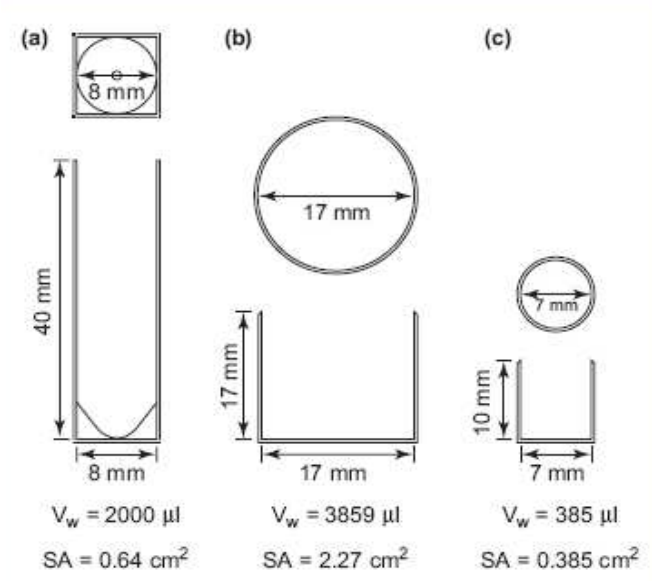

B)

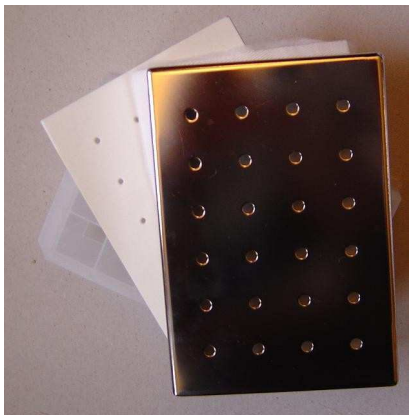

Figure 8: A) Schematic diagram of individual microwell formats: (a) 96-deep square well format; (b) 24-round well format; (c) 96-round well format. V_W represents the total well volu me, SA represents the static surface area available for gas–liquid mass transfer. Image adapted from Lye G.L. *et. al.,*2003. B). Duetz and coworkers (2000) described a closure system consisting of a soft silicone layer with a small hole above the center of each well.

The challenge of using microtitre plates for this application is how to translate the micro-scale process information to laboratory or pilot-scale. Characterisation of the engineering environment is a key step toward successful scale translation [Zhang H, et. al., 2008].

Miniature stirred bioreactor systems (MSBRs) and Miniature bubble column reactors (MBCR)

Miniature stirred bioreactors (MSBRs) based on conventional STRs have been developed as an alternative to shaken MBR systems for early-stage process development and cell characterisation (Figure 9).It has been shown to be capable of mimicking conventional STRs in cell cultivations of varying rheology, shear-sensitivity and oxygen demand. One of the advantages of this MSBRs is that it is possible to operate 4–16 MSBRs in parallel. Miniature bubble column reactor (MBCR) utilise gas sparging instead of agitation as a means of promoting mixing and oxygen mass transfer for cell cultivation (Figure 9). One of the benefits of this type of device is that, unlike an MTP,

aeration is via direct sparging. This has the effect of increasing the oxygen mass transfer capability of the system relative to an MTP because sparging increases the surface area available for gas-liquid mass transfer relative to surface aeration alone. Furthermore, the device is stationary, as opposed to shaken, which allows for easier instrumentation as agitation of most MTP systems has to be stopped before measurement in a plate reader can take place [Jonathan I. B. (2003)].

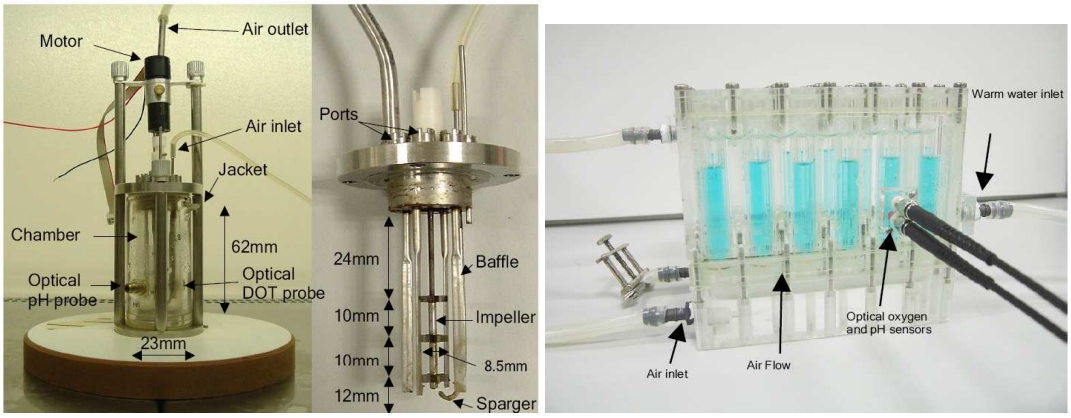

Figure 9: Prototyps from MSBR and MBCR developed in UCL. A) Technical illustration of an 18 ml working volume miniature stirred bioreactor (MSBR) prototype. B) Diagram of the miniature bubble column reactor (MBCR) prototype. Image adapted from Jonathan I. B. and *et. al*. 2003.

Bacterial metabolism of long-chain n-alkanes

Degradation of alkanes (aerobic or anerobic) is a widespread phenomenon in nature, and numerous microorganisms, prokaryotic and eukaryotic, capable of utilizing these substrates as a carbon and energy source have been isolated and characterised [Wentzel A. and *et. at.*, 2007; van Beilen *et al.*,2004; van Beilen J. B. and *et. at.*, 1994; Rojo F. and *et. at.,* 2005; van Beilen J.B., *et. al.*, 2007; Wubbolts M.G. and *et. at.*, 1996; Funhoff E. G. and *et. at.*, 2006; van Beilen J.B.and *et. at.*, 2005]. Since the 1960s, potentials have been discussed and attempts have been undertaken to channel capabilities of these microorganisms to convert aliphatic compounds like *n*-alkanes into commercial biotechnological applications [Wentzel A. and *et. at.*, 2007; Wubbolts M.G. and *et. at.*, 1996].

Alkanes are saturated hydrocarbons (highly reduced) that can be linear (n-alkanes), circular (cyclo-alkanes), and branched (iso-alkanes), and are virtually insoluble in water. Besides their high inflammability, alkanes are probably the least reactive class of organic compounds. The physical properties of linear alkanes are very important for the rate with which these compounds are oxidized and metabolized. Longer alkanes are progressively less soluble with increasing chain-length, which results in decreasing oxidation rates. With decreasing chain length, short-chain alkanes in the range of C_5 to C_{10} become increasingly soluble and consequently increasingly toxic. Branched alkanes are considered to be more recalcitrant to degradation than linear alkanes. As carbon and hydrogen atoms are almost equally electronegative, the chemical bond between them shows slight polarity. Moreover, all electrons between the two atoms are shared. As a consequence, alkanes display low

chemical reactivity, especially in the terminal positions [van Beilen *et al.*,2004; Ayala M. and *et. at.*,2004].

As main components in fuels and oils (20%-50%), they are of outstanding value for modern life, but the relative inertness of alkanes poses ecological problems upon their release to the environment. They are also produced by geochemical processes from decaying plant and algal material, end up in the environment by natural oil seeps and human activities (oil-spills and run-off due to dispersed sources), and then disappear due to physical and biological degradation, a process estimated to amount to several million tons of alkanes per year. A probably much larger quantity (predominantly long-chain linear compounds) is produced throughout the biosphere by living organisms (plants, animals and bacteria) as a structural element, vapour barrier, waste product, defence mechanism, or chemoattractant.

Consequently, these compounds are a reliable carbon and energy source for microorganisms of many different genera belonging to the high- and low- (G+C) Gram-positives, and the α-, β-, and γ-Proteobacteria. Frequently mentioned genera are *Mycobacterium*, *Rhodococcus*, *Bacillus*, *Acinetoacter*, and *Pseudomonas*. The last genera plays a proeminent role. A large number of microorganisms belonging to the phyla of eubacteria, yeast, and fungi and also some algae capable of using long-chain n-alkanes as carbon and energy source have been described, Thermophilic long-chain n-alkane-degrading strains are of special interest for future biotechnological applications.

The low reactivity of alkanes has constrained their direct conversion to high-value chemicals such as alcohols or amines. However, biotechnology offers alternatives that are already applied to industry, particularly in the pharmaceutical, agrochemical and food fields. The advantages of biotechnological processes arise from the ability of enzymes or microorganisms to catalyze at physiological pressure and temperature and to generate, due to their high selectivity, few or no side-products. Therefore, it results in a reduction in the production costs due to higher process efficiency, less waste production, safer raw material, energy savings and higher quality product, resulting in an improved competitiveness especially in highly regulated countries [Ayala M. and *et. at.*,2004].

During the past decades, research related to alkane degradation has focused on the identification and characterization of enzymes involved in the initial step of aerobic bacterial catabolic pathways. In most described cases, the n-alkane is oxidized to the corresponding primary alcohol by substrate-specific terminal monooxygenases/hydroxylases. However, subterminal oxidation has also been described both for long-chain n-alkane substrates up to C_{16} and for *n*-alkanes of shorter chain lengths. The resulting secondary alcohols are converted to the corresponding ketones, which can be oxidized to an ester by Baeyer-Villiger monooxygenases. The esters in turn are hydrolyzed by an esterase to an alcohol and a fatty acid [van Beilen *et al.*,2004; van Beilen *et al.*, 2007].

Depending on the chain-length of the alkane substrate, different enzyme systems (type of oxygenases) are required to introduce oxygen in the substrate and initiate biodegradation. For simplicity, There are three categories: C_1–C_4 (methane to butane, oxidized by methane monooxygenase-like enzymes), C_5–C_{16} (pentane to hexadecane, oxidized by integral membrane non-heme iron or cytochrome P450 enzymes), and C_{17+} (longer alkanes, oxidized by essentially unknown enzyme systems). The substrate ranges of the enzyme systems sometimes overlap and may cover more than one group of alkanes [van Beilen J.B., *et. al*., 2007] (Figure 10).

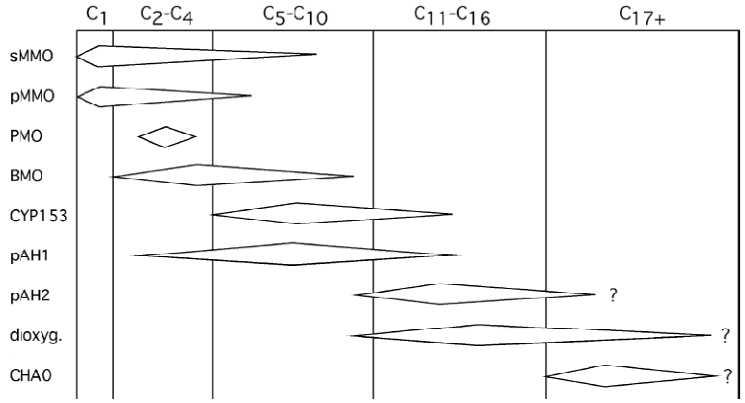

Figure 10: Overview of the substrate range of alkane hydroxylase with respect to alkanes. sMMO Soluble methane monooxygenase; pMMO particulate methane monooxygenase; PMO propane monooxygenase; BMO butane monooxygenase; CYP153; pAH1 medium-chain-length integral membrane alkane hydroxylase ; pAH2 long-chain-length integral membrane alkane hydroxylase ; dioxyg Acinetobacter sp. M-1 dioxygenase; CHA0 inferred alkane oxygenase in *P. fluorescens* CHA0. Image adapted from van Beilen J.B., *et. al*., 2007.

In several Pseudomonas isolates, particulate alkane hydroxylases (pAHs) were detected. The alkane hydroxylase of one particular Pseudomonas isolate, now known as *Pseudomonas oleovorans* GPo1 (TF4- 1L; ATCC 29347), has been characterized in great detail. The oxidation of medium chain length alkanes and alkenes (C_6 to C_{12}) by *Pseudomonas oleovorans* GPo1 (TF4- 1L; ATCC 29347) encoded by the OCT plasmid and related, biocatalytically active recombinant organisms, in two-liquid phase cultures can be used for the biochemical production of several interesting fine chemicals. The alkane hydroxylase system is able to carry out a wide range of stereoselective and regioselective oxidation reactions, giving it considerable commercial potential as a biocatalyst [Schmid A. and *et. at.,* 1998; Chen Q. and *et. at.*,1995; Staijen I. E., *et. al.*, 1997].

Most alkane oxygenases are relatively complex and difficult to use in vitro, as they consist of multiple components, leading to low electron transfer rates. They are co-factor dependent, sensitive to inactivation by activated oxygen species, and sensitive to product inhibition. Moreover, the substrates as well as the products of these enzymes tend to be quite hydrophobic and toxic to the host cell. This calls for careful substrate feeding protocols to keep the substrate concentration below toxic limits and *in situ* extraction set-ups consisting of a second hydrophobic but non-toxic liquid phase or a solid extractant. Evidently, high volumetric productivities are required for an economical process [van Beilen J.B., *et. al*., 2007].

Alkane hydroxylases also serve as models for chemical catalysts and mechanistic studies; robust chemical catalysts for regio- and stereoselective hydrocarbon activation, equaling or surpassing the selectivity and activity of biological catalysts would indeed be very valuable tools [van Beilen J.B., *et. al*., 2007].

Genetic and Enzymology of Alkane Hydroxylation System

Alkanes are chemically inert and must be activated before they can be metabolized. In the presence of oxygen, activation is usually achieved by oxidation of one of the terminal methyl groups to generate the corresponding primary alcohol, which is further oxidized by dehydrogenases to render fatty acids. Several unrelated enzymes can catalyze the terminal activation of alkanes. The best known of these enzymes encode on the OCT plasmid is the *Pseudomonas putida* GPo1 alkane hydroxylase system [Rojo F. and *et. at.,* 2005; Wentzel A. and *et. at.*, 2007].

Biochemical charaterisation of the alkane hydroxylase system showed that it consist of three components; a particulate hydroxylase; and two soluble proteins, which act as electron carriers between NADH and the hydroxylase (Figure 11).

The alkane hydroxylase system (Figure 12), which catalyzes the hydroxylation of alkanes and alkenes, consists of three components: a cytoplasmic membrane alkane hydroxylase (AlkB) (an inducible enzyme system) and two soluble proteins: rubredoxin (AlkG), and rubredoxin reductase (AlkT), which act as electron carriers between NADH and the hydroxylase [Rojo F. and *et. at.,* 2005; Chen Q. and *et. at.*,1995; van Beilen J. B. and *et. at.*, 1994; Ayala M. and *et. at.*,2004; Smits T. H. M. and *et. at.*, 2003; Funhoff E. G. and *et. at.*, 2006].

AlkB transfers one oxygen atom from O_2 to one of the terminal methyl groups of the alkane molecule, rendering an alcohol, while the other oxygen atom is reduced to H_2O by the electrons transferred by rubredoxin. Besides hydroxylating terminal methyl groups in aliphatic and alicyclic hydrocarbons, AlkB generates epoxides from alkenes and other chemicals with a terminal double bond, oxidizes alcohols to aldehydes, and catalyzes demethylation and sulfoxidation reactions [Kok M. and *et. at.,* 1988]. So, the alkane is oxidized to an alcohol, further oxidation to the corresponding aldehyde and carboxylic acid, all catalyzed by different enzymes. The carboxylic acid enters the fatty acid degradation pathway and is used as an energy source (e.g. The carboxylic acid then serves as a substrate for acyl-CoA synthetase, and the resulting acyl-CoA enters the β-oxidation pathway). In order to make use of the alkane hydroxylase system for the production of oxidized intermediates, these metabolic reactions must be interrupted, so that the desired product accumulates [Ayala M. and *et. at.*,2004; Smits T.H.M., *et. al*., 1999].

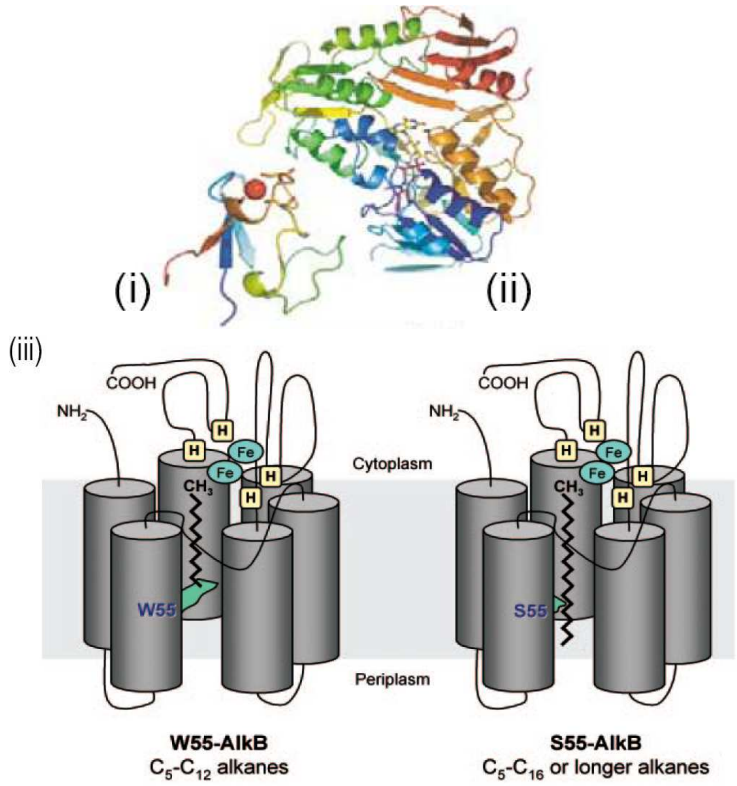

Figure 11: Structural representations of the alkane-hydroxylating enzyme systems. Integral membrane non-heme di-iron alkane hydroxylase systems: i) crystal structure of the C-terminal domain of rubredoxin; ii) rubredoxin reductase modelled on the structure of putidaredoxin reductase; and iii). model for the AlkB alkane hydroxylase. The enzyme is proposed to have six transmembrane helices arranged in a hexagonal distribution that would define a long, hydrophobic pocket into which the linear alkane molecule can slip. The four histidine clusters (H) believed to bind the two iron atoms (Fe) would lie on the cytoplasmic side. In *P. putida* GPo1 AlkB, residue W55 lies in transmembrane helix 2 and extends its bulky arm towards the hydrophobic pocket (left). This hampers the proper insertion of alkanes longer than C13. The replacement of W55 by a serine residue (S55) (right), which has a shorter arm, allows longer alkanes to enter the pocket without impeding the proper alignment of the terminal methyl group relative to the histidine clusters. Sizes are not to scale. The soluble components of the alkane hydroxylase complex, rubredoxin and rubredoxin reductase, are not shown. Image adapted from van Beilen J.B.and *et. at.* (2004) and Rojo F. and *et. at.,*2005.

The alkane hydroxylase (AlkB) is an integral membrane protein that requires phospholipids and iron for activity, and is inhibited by cyanine. Its primary sequence contains six transmembrane helices. Four highly conserved sequence motifs histidines that are essential for catalytic activity, and are conserved in alkane hydoxylase and xylene monooxygenase sequences as well as in the much more distantly related desaturases. The conserved histidines probably form the nitrogen-rich coordination sphere for two iron atoms. The two electron transfer proteins that supply electrons for the monooxygenation reaction are rubredoxin (AlkG) and rubredoxin reductase (AlkT). The rubredoxin reductase is a flavoprotein that transfer electrons from NADH to rubredoxin. The latter belongs to a family of small electron-transfer proteins containing an iron coordinated by four cyteines (Figure 13) [van Beilen *et al.*, 2004]. AlkB and AlkG are both non-heme iron proteins. Interestingly, the alkane hydroxylase can also stereoselectively convert 1-alkenes to epoxyalkanes [Kok M. and *et. at.,* 1988].

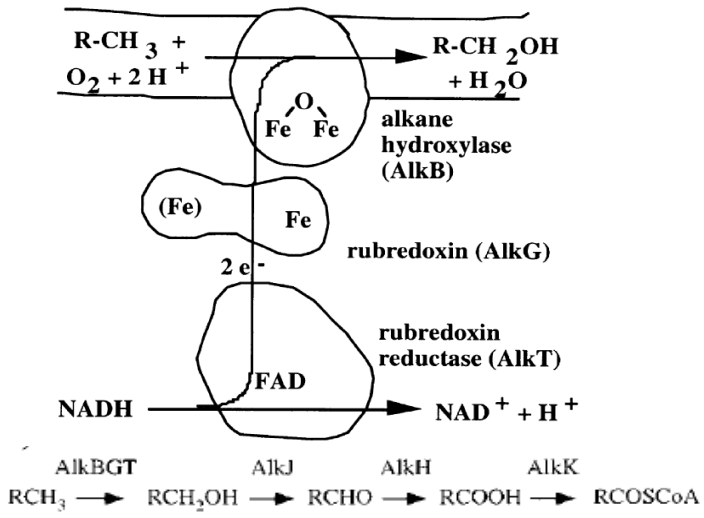

Figure 12: Struture of the alkane hydroylase system. The alkane hydroxylase system consists of three components: a membrane–bound mono-oxygenase (alkane hydroxylase AlkB), rubredoxin (AlkG) and rubredoxin reductase (AlkT). The alkane hydroxylase AlkB is an integral cytoplasmic membrane protein containing a diiron cluster. Rubredoxin (AlkG) transfers electrons from the flavoprotein rubredoxin reductase (AlkT) to AlkB. The functions of AlkF and AlkL are unclear. Image adapted from Staijen I. E. and *et. at.*, 1987, van Beilen J. B. and *et. at*., 1994, Wubbolts M.G. and *et. at.*1996 and Panke S. *et. at.*,1999.

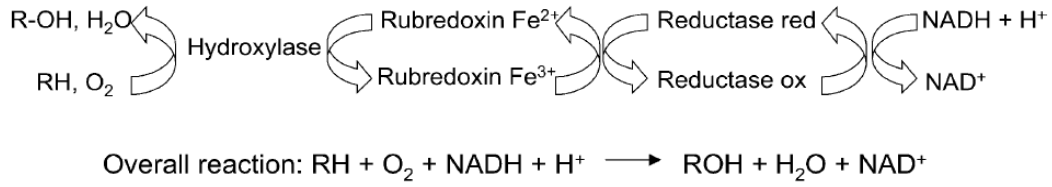

Figure 13: Steps involved in the oxidation reaction catalyzed by alkane hydroxylase. Image adapted from Ayala M. and *et. at.*,2004.

The alkane hydroxylase system and other proteins involved in alkane degradation are encoded by the alkST and alkBFGHJKL clusters located on the OCT plasmid. The expression of *alkBFGHJKL* is positively regulated by AlkS. AlkS is expressed poorly during the exponential phase of growth, while its expression increases considerably when cells enter the stationary phase. AlkS expression is controlled by two promoters, and that this protein regulates its own expression both positively and negatively. alkS is regulated by a positive feedback mechanism. Such mechanism should allow both rapid induction of the n-alkane utilization pathway, and a fast downregulation thereof when the nalkanes are consumed [Wentzel A. and *et. at.*, 2007]. The *alk* genes are induced with dicyclopropylketone (DCPK), a gratuitous inducer of the *alk* genes. DCPK is water soluble and hence is a convenient inducer in aqueous cultures, while alkanes are useful inducers in two liquid-phase cultures which contain an organic phase [Chen Q., *et. al.*, 1996; Staijen I. E., *et. al.*, 1987; Panke S. *et. at.*, 1999].

The alkane hydroxylase system, which catalyzes the first step of alkane oxidation, consists of alkB, alkG and alkT genes. The enzymes which catalyze the subsequent oxidation and catabolic steps are encoded by *alkJ*, *alkH*, and *alkK*. *alkF* encodes a non functional rubredoxin, while *alkL* encodes an outer membrane protein which is not essential for growth on alkanes[Chen Q., *et. al*., 1996; van Beilen J. B. and *et. at.*, 1994] (Figure 14 and Table 2).

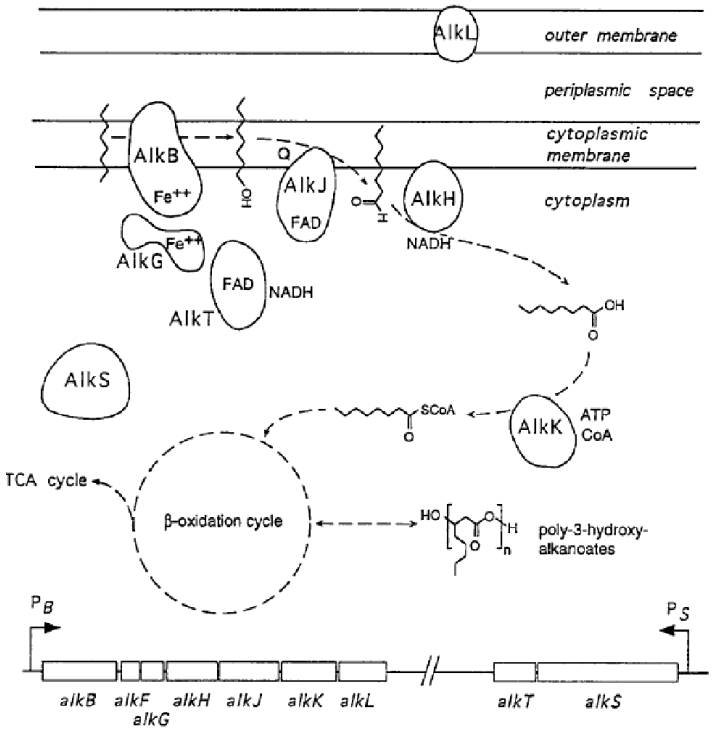

Figure 14: Molecular genetics and pathway of alkane oxidation by *Pseudomonas oleovorans GPo1 (TF4- 1L; ATCC 29347 oleovorans.* The *alk-genes are* organized in two clusters: the *alkST* locus and the *alkBFGHJKL* operon, both located on the OCT plasmid. Proteins are identified by their gene name (see Table 2 for full name and function). Image adapted from van Beilen J. B. and *et. at.*,1994. For more detailed information about the alkBFGHJKL operon van Beilen J. B. and *et. at.* (1994) paper has a extensible description.

Alkane Uptake and Solubilisation

The volumetric productivities that can be attained in two-liquid phase systems can be, in contrast to aqueous fermentations, limited by the transport of substrates from an apolar phase to the cells residing in the aqueous phase and by toxic effects of apolar solvents on microbial cells [Schmid A. and *et. at.,* 1998].

Generally, alkane uptake is supposed to take by three different mechanisms [van Beilen *et al.*,2004] (Figure 15):

a) By direct cell-droplet interaction;

b) By interaction of cells with solubilized or emulsified hydrocarbon micelles or microdroplets.

c) Via uptake of alkanes dissolved in the aqueous phase;

Table 2: Properties of the gene products of the *alkBFGHJKL* operon. Table adapted from van Beilen J. B. and *et. at.*, 1994.

	Nucleotide Position	Ribosomal binding site	Size (amino acids; calculated; minicells)	Protein or function	Localization[1]	pI [2]	Purified	N-terminus [3]
AlkB	622-1825	UGGAGA(7)AUG	401, 45.7 kDa, 41 kDa	alkane hydroxylase	CM	7.24	YES	YES
AlkF	2044-2439	AGGAGA(8)AU	132, 14.6 kDa, 14 kD	rubredoxin 1 (inactive)	cytoplasm	4.90	NO	NO
AlkG	2490-3008	UGGUGA(5)AU	172, 18.7 kDa, ?	rubredoxin 2	cytoplasm	4.0	YES	YES
AlkH	3058-4506	AGGACA(8)AU	483, 52.7 kDa, 49 kDa	aldehyde dehydrogenase	CM?	10.05	NO	NO
AlkJ	4548-6221	CGAGAA(6)AUG	558, 60.9 kDa, 58 kDa	alcohol dehydrogenase	CM	7.39	NO	YES [4]
AlkK	6284-7921	UGAGGC(7)AUG	546, 59.3 kDa, 59 kD	acyl-CoA synthetase	cytoplasm	5.72	NO	NO
AlkL	8026-8715	CGAGGG(7)AUG	230, 25.0 kDa, 20 kDa	unknow	OM	4.32	NO	NO
AlkS	628-3273	CGAGAA(7)AUG	882, 99.8 kDa, 99 kD	regulation of *Palk*	unknown	9.93	NO	YES 4
AlkT	3326-4476	GGAGAG(6)AUG	385, 41.0 kDa, 48 kD	rubredoxin reducta	cytoplasm	6.01	YE	YES

[1] CM: cytoplasmic membrane; OM: outer membrane. [2] The pI was calculated from the primary sequence using the PC/GENE software package (IntelliGenetics, Geel, Belgium).[3] YES: N-terminal sequence was determined, and agreed with the amino acid sequence deduced from the nucleotide sequence; NO: N-terminal sequence has not been determined. [4] N-terminal sequence has been determined from protein blotted on PVDF-membrane.

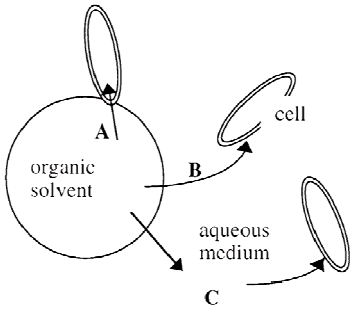

Figure 15: Schematic illustration of three possible mass-transfer mechanisms of apolar substrate from the organic phase to cell. A, direct droplet-cell interation; B, transfe mediated by organic carrier molecules; C, transfer via dissolution in the aqueous phase. Image adapted from Schmid A. *et.al.*, 1998.

Here, the cell contact with hydrophobic substrates is crucial because the initial step in aliphatic and aromatic hydrocarbon degradation is often mediated by oxidation reactions catalyzed by cell-surface-associated oxygenases. *Pseudomonas* isolates typically do not use the first option. In the case of short alkanes, the solubility is high enough to allow uptake from dissolved alkanes (e.g. the uptake of substrate dissolved in aqueous phase is applied). These short alkanes probably reach the alkane hydroxylase in the cytoplasmic membrane by passive diffusion and partitioning into the cytoplasmic membrane, not by an active uptake system. This is supported by the

observation that recombinant *E.coli* strains containing the *P.putida alk* genes grow well on alkanes, even though the wild-type *E. coli* does not possess pathways for the uptake and degradation of hydrocarbons or the production of biosurfactants. Longer alkanes are not soluble enough to support growth from dissolved substrate, and in many cases growth on such hydrocarbons is associated with the production of surface-active compounds (e.g. interaction of cells with solubilized or emulsified hydrocarbon micelles or microdroplets is applied) [van Beilen *et al.*,2004; Schmid A. and *et. at.,* 1998]. Substrate uptake presumably takes place through diffusion or active transport [Setti L. and *et. at.,* 1995; Wentzel A. and *et. at.*, 2007].

The mechanisms of *n*-alkane uptake by the aerobic microorganisms may be specific or non-specific. The latter are usually observed and there is a correlation between *n*-alkane chain length and susceptibility to biodegradation, in which lower molecular weight n-alkanes are more degradable than higher. Generally, biodegradation of aliphatic compounds is affected by biological and physico-chemical factors. The former include the enzymatic activity of the microorganism on the substrate and the transport limitation of the substrate through the membrane, while the latter include the fermentation conditions (agitation, aeration, etc.) and substrate characteristics such as water solubility, viscosity, diffusivity and surface tension of the substrate. Today, many authors are of the opinion that biological factors are more important than physico-chemical factors for hydrocarbon biodegradation [Setti L. and *et. at.,* 1995].

Qualitatively, the mechanisms involved in n-alkane degradation include: a lag period without compound degradation; a step with accelerating conversion rates; a step with constant conversion rates, limited by the mass-transfer rate of the substrate from the bulk of the organic phase to the absorbed microorganism on the oil-water interphase; and a decrease in the conversion rate, long before all the *n*-alkane is converted.

In conclusion, it was demonstrated that certain non-specific *n*-alkane degradation microorganisms present similar behavior, and that the *n*-alkane biodegradation rate depends on the fermentation conditions (agitation, aeration, etc.) and on the strain of microorganism, as is well-known. The pattern of n-alkane biodegradation was essentially bound to the substrate characteristics (molecular structure, molecular weight and density) [Setti L. and *et. at.,* 1995].

Physiology of Alkane-Degrading Pseudomonas

Growth on hydrophobic compounds such as alkanes or alkenes can have profound effects on the physiology of a bacterium, and bacteria have developed elaborate mechanisms to counter the effects of solvents on the cell membrane morphology and cell membrane properties [van Beilen *et al.*, 2004; Schmid A. and *et. at.,* 1998].

When *P. oleovorans* is grown on alkanes or alkenes, the changes of membrane lipid fatty acid composition resulted both from exposure of the cells to organic solvents and from the induction and expression of *alkB*. Induction of *alkB* and insertion of alkane hydroxylase into the cytoplasmic membrane have also been found to alter the physiology of *Escherichia coli alk*+ recombinants, by

inducing, for example, reductions in growth rate and appearance of membrane vesicles in the cytoplasm [Chen Q., *et. al*., 1996]. These changes in the membrane lipid fatty acid composition lead to a decrease in membrane lipid fluidity [van Beilen *et al.*,2004]. It is essential that these microorganisms can alter fatty acid compositions of theirs membrane lipids in order to adapt to the high activity of the alkane hydroxylase system for the accumulation of the target product [Chen Q. and *et. at.*, 1995].

One of several approaches to reduce substrate toxicity is to dissolve apolar substrates in a high boiling, high logP carrier solvent, added as a second-liquid phase. The effect of this action is the reduce growth inhibition by organic solvents. Then, it provides significant advantages for downstream processing, safety, and process economics [Schmid A. and *et. at.,* 1998].

Whole Cell and Immobilise Enzyme and Oxygenases limitations

There are four main reasons to use whole cells rather than purified enzymes, when using oxygenases [Schmid A. and *et. at.,* 1998]:

1- The use of whole cells is simply more economical; enzyme isolation and purification are significant cost-factors. In addition, the 'packaging' of enzymes in small 'bags' of membranes and cell walls (as nature does) protects the enzyme from shear forces, and might result in a longer half-life of enzyme activity in stirred bioreactors;

2- Second, the membrane-bound nature of the target enzyme may be a reason to use whole cells. Removal of an enzyme from a membrane environment often leads to full or nearly complete loss of activity. Alkane hydroxylase is a wellknown example of such an integral membrane protein;

3- Cascades of enzymatic reactions may be too complicated to perform *in vitro* because of the number of enzymes, cofactors and substrates that are involved;

4-- The stoichiometric consumption of NAD(P)H, NAD(P)+, ATP or other cofactors during the enzymatic reaction or chain of reactions may make the use of whole cells attractive. Important NAD(P)H-dependent processes include hydroxylations/epoxidations and the reduction of ketones to chiral alcohols.

Irrespective of the type of biocatalyst used (wild-type, mutant or recombinant strain), three themes determine the potential for practical applications; the intrinsic properties of the oxygenase, the impact of oxygenase expression on he physiology of the host strain, and the impact of oxygenase and host properties on bioprocess design (Table 3).

Several developments have helped to realize the commercial potential of oxygenases. Finally, the combination of metabolic engineering with efficient and stable oxygenase expression systems will enable the production of many oxygenated hydrocarbons [van Beilen J. B. and *et. at.,* 2003].

Table 3: Issues and challenges in the commercial application of oxygenases. Table from van Beilen J. B. and *et. at.,* 2003.

	Issue or challenge	Explanation, cause or comment	Solution or further action
Intrinsic oxygenase properties	**Low kcat**	Balance between optimal activity, selectivity and overoxidation (speculative)	Fusions between oxygenase and; electron transfer component directed evolution
	Uncoupling	Bad fit of substrate, Product binding to active site	Protein engineering and directed evolution. Product removal by in situ product recovery
	Overoxidation	Product might also be a substrate	Reduce electron transfer rate or partial oxygen pressure
Physiological aspects of oxygenase expression	**Heterologous expression**	Multiple components, co-factors, membrane-bound, hydrogen peroxide formation	Multicistronic expression vectors, Addition of co-factor Precursors, Protein engineering and directed evolution
	In vivo cofactor recycling	Capacity of cell metabolism may become limiting at higher specific oxygenase activities	Co-expression of suitable dehydrogenase. Reduce activity of terminal electron chain
	Substrate uptake and toxicity	-Hydrophobic compounds disrupt cell membranes; -General toxicity of more polar compounds; -Uptake systems for larger substrates have not been characterized yet.	Reduce effective aqueous phase concentration (reduced substrate feed rates, substrates and products dissolved in apolar phase adsorption of substrates and products to a solid-phase) In vitro application of the oxygenase. New hosts with altered uptake profiles. Co-expression of uptake systems/porins
Bioprocess engineering	**Limiting oxygen transfer rates**	-Relatively high K_M for oxygen -Competition with endogenous respiration -Low kLa of standard bioreactors	Increased oxygen pressure through added oxygen and increased pressure; Modify host strain to minimize maintenance requirements and hence, endogenous respiration
	Explosion hazard	Many hydrophobic substrates or enzyme inducers are volatile and flammable	Reduction of vapor pressure by operation above a critical pressure and below a critical temperature reactor engineering (explosion proof, explosion suppression)
	Limiting substrate mass transfer	Oxygenase substrates are often hydrophobic and/or insoluble in water	Two-liquid phase systems: the substrate is dissolved in an inert organic solvent Addition of cyclodextrins

Hosts for Alkane Hydroxylation

An efficient production requires both a high concentration of biomass and specific product formation rate. Increasing the productivity is therefore possible by increasing the specific productivity or the biomass concentration, or both. The tolerance of microorganisms to starting material, overflow and biotransformation products, and an appropriate bioprocess design determine the stability of a production process [Rothen S.A. and *et. at.*, 1998]. To reach these goals it is necessary to turn to genetic modified microorganisms.

Eschericia coli is the most frequently used prokaryotic host for high-level production of a wide range of heterologous proteins because of its industrial relevance and relatively well-known genetics, physiology, and cultivation conditions.

Pseudomonas are suitable candidates for the bioconversion of aromatic and aliphatic compounds. The most well studied examples are the alkane hydroxylase system from Pseudomonas oleovorans and the the *xyl* system of Pseudomonas *putida* mt-2. However, to avoid the consumption of desired products, it might be necessary to use mutants defective in the degradation of these compounds or to transfer the catabolic genes of interest into an organism such as *Escherichia coli* that is not capable of product consumption. Other reasons for using *E. coli* in biotransformations include the ease with which *E. coli* can be modified genetically, thus facilitating

the development of engineered pathways to produce specific compounds, and the fact that there is considerable experience with large scale fermentations of recombinant *E. coli* strains [Wubbolts M.G. and *et. at.*, 1996; Favre-Bulle O. and *et. at.*, 1993].

The genes enabling *Pseudomonas oleovorans* to oxidize alkanes have been cloned in various *Escherichia coli* strains (Figure 16).

The *E. coli* host serves only to produce and maintain the recombinant biocatalytic activity and to regenerate the required cofactor, generally NADH or NADPH while neither substrate nor product is consumed by host strain. These strains are unable to grow on medium-chain fatty acids because their β-oxidation system is repressed and not induced by medium-chain-length fatty acids. The cells must therefore be grown on a common carbon source such as glucose. In a two-liquid-phase system (aqueous and organic phase), alkanols are excreted and preferentially partition, according to the chain length to the organic phase and alkanoic acids are to the aqueous phase. These whole-cell biotransformation systems consist of four different phases, two liquid phases (apolar and polar phase), one solid phase (microorganisms), and one gaseous phase (air). The cells are growing only in the polar phase but are affected by the apolar phase. The substrate of the biotransformation is converted from the apolar phase to form an inhibiting product in the polar and/or apolar phase. [Rothen S.A. and *et. at.*, 1998; van Beilen *et al.*, 2004] However, despite considerable over expression of alkane mono-oxygenase in some E. coli hosts, the most active recombinants showed in vivo alkane-oxidation rates no higher than that of the native host strain [Staijen I. E. and *et. at.*, 1987].

However, the cloned enzyme system dos not function as well in E. coli as it does in P. oleovorans. This may be due to intrinsic factors that relate to the performance of the enzyme system as such, or to extrinsic factors, such as the availability of substrates and cofactors *in vivo.* High expression of Alk B as a heterologous protein in *E.coli* alk+ recombinant is responsible for triggering the heat-shock response in E. coli, which in turn induces elevated proteolysis. Thus, appears instability of AlkB in *E.coli* caused by increased protease expression as a result of cellular responses to its synthesis [Staijen I. E., *et. al.*, 1997; Staijen I. E. and *et. at.*, 1987].

Staijen I E. and et. al in 1987 found that alkane hydroxylation in E. coli recombinants is not limited by extrinsic factors but by intrinsic factors. Extrinsic factors include the transport of substrates to and products from the enzyme system, and a sufficient flux of electrons (Figure 12 and Figure 13). These are supplied by NADH, which is used stoichiometrically in the oxidation of alkanes by alkane monooxygenase, donating electrons to the mono-oxygenase AlkB via the reductase (AlkT) and rubredoxin (AlkG). Thus, the in vivo activity of the system depends on the available intracellular NADH, which must be regenerated continuously during alkane oxidation. As for the transport of alkane hydroxylase substrates, the alkB/G/T genes are sufficient to confer alkane uptake and oxidation capacity to E. coli and Pseudomonas putida strains, and no additional specific alkane uptake components have ever been described in P. oleovorans. Thus, it is most likely that medium-chain-length alkanes (C_6-C_{12}) simply traverse the cell membranes by diffusion. It can be use small

concentrations of non-ionic surfacts to help the diffusion, like Triton X-100 in the whole cell assay suspension.

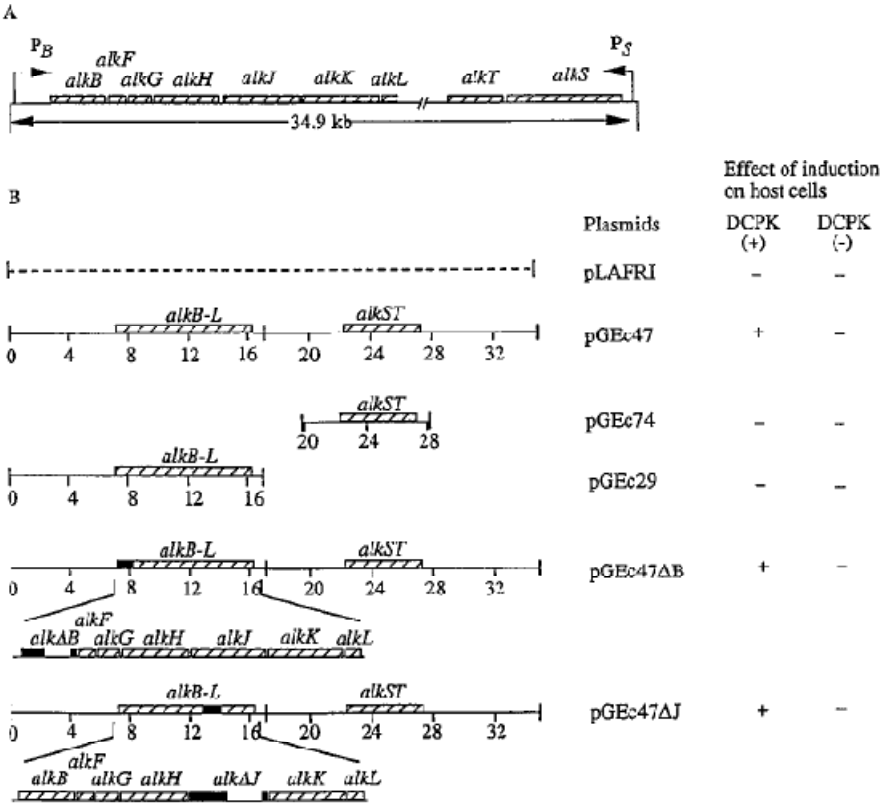

Figure 16: Organization of the *alk* genes and plasmids carrying various *alk* constructs. (A) The *alk* genes are organized in the *alkST* and the *alkBFGHJKL* clusters. The expression of the *alkB-L* operon is positively regulated by AlkS. (B) pLAFRI-derived plasmids carrying different *alk* genes. The solid bars border deletions of specific *alk* genes. The effects of growth with (1) or without (2) DCPK on the growth rate and physiology of GPo12 recombinants carrying these plasmids are indicated as follows: 2, no detectable effects; 1, clear effects. Image adapted from Chen Q and *et.al*. (1996)

Staijen I E. and et. al in 1987 found that alkane hydroxylation in E. coli recombinants is not limited by extrinsic factors but by intrinsic factors. Extrinsic factors include the transport of substrates to and products from the enzyme system, and a sufficient flux of electrons (Figure 12 and Figure 13). These are supplied by NADH, which is used stoichiometrically in the oxidation of alkanes by alkane monooxygenase, donating electrons to the mono-oxygenase AlkB via the reductase (AlkT) and rubredoxin (AlkG). Thus, the in vivo activity of the system depends on the available intracellular NADH, which must be regenerated continuously during alkane oxidation. As for the transport of alkane hydroxylase substrates, the alkB/G/T genes are sufficient to confer alkane uptake and oxidation capacity to E. coli and Pseudomonas putida strains, and no additional specific alkane uptake components have ever been described in P. oleovorans. Thus, it is most likely that medium-chain-length alkanes (C_6-C_{12}) simply traverse the cell membranes by diffusion. It can be use small concentrations of non-ionic surfacts to help the diffusion, like Triton X-100 in the whole cell assay suspension.

The composition and ultrastructure of P. oleovorans and *E. coli* membranes are similar, and there is no indication that such passive transport should be more difficult in *E. col*i than in *P. oleovorans.* The perform of E. coli alk+ recombinants show high cellular AlkB-synthesis and alkane hydroxylase activities implying that neither substrate or product transport nor NADH regeneration limited alkane oxidation, at least up to rates identical with those seen in the native host. Therefore, extrinsic factors did not affect the performance [Staijen I. E. and *et. at.*, 1987].

Incomplete iron incorporation in heterologously expressed proteins may explain the lower specific activity of the alkane hydroxylase system in E. coli hosts. One indication was less iron was found to be bound to AlkG isolated from *E. coli* alk+ recombinants than to AlkG from *P. oleovorans*. So, it is easily assumed that the insertion of iron into the mono-oxygenase is due to simple binding, but it is possible that *P. oleovorans* contains specific iron-transfer enzymes that catalyze the insertion of iron into iron-binding clusters in non-heme apoproteins. However, it was shown by other authors that incorporation of di-iron is not a problem. The problem may rely on the incorrect processing (*folding*) of the Alk proteins. Moreover, whereas the Alk proteins are very stable in the native host, this is not so for the E. coli alk+ recombinants, where the components can be rapidly degraded. As well, there are additional native host factors (components or processes) that are vital for optimal mono-oxygenase function and that these are not or only partially present in E. coli hosts. These factors are likely to include correct post-translational folding, processing of apoproteins and membrane interactions of AlkB [Staijen I. E. and *et. at.*, 1987; Staijen I. E. and *et. at.*, 1998]. However, the same author latter emphasize the importance of the iron supply in the media for the alkane hydroxylase activity. This requires the addition of yeast extract to the growth medium and so, higher the cost in large scale of bioconversion processes. Therefore, inexpensive chemically defined media that allow *E. coli alk*+ recombinants to express high alkane hydroxylase activities are of special interest [Staijen I.E. and *et. at.,* 1998].

In conclusion, both incorrect folding of AlkB and lack of iron affects the activity rate of the alkane hydroxylase system.

Economics

From an economic point of view for all types of biotransformations, the following conditions are very important for obtaining products from substrates using whole cells [Chan E-C, et. al., 1991; Schmid A. and *et. at.,* 1998]:

1. Relatively cheap substrate;
2. A high conversion rate of the substrate (e.g. high substrate yields);
3. High volumetric productivity;
4. A short reaction time;
5. A product-over producting microorganism.

In two-liquid phase processes these yields and productivities can be limited by toxic effects of solvents, substrates, and products or by low substrate transfer rates from the apolar liquid phase to the cells. At present, the best volumetric productivities with such systems range between 1 and 10 mmol L^{-1} h^{-1} further process development will eventually lead to volumetric productivities in the range of 10 to 60 mmol L^{-1} h^{-1}. High volumetric productivities depend not only on biocatalyst activity, but also on high fluxes of substrates and metabolites. In two-liquid phase cultures the volumetric rate of apolar substrate transfer from the organic phase to the cells can be limiting. The maximum obtainable mass transfer rate of apolar substrates across the liquid-liquid boundary to cells strongly depends on the system used: microorganism, organic solvent, concentration, reactor configuration, and power input as well as the mechanism of substrate transport from the organic phase to the cells have all been shown to influence these rates [Schmid A. and *et. at.,* 1998].

Therefore, at the present the two-liquid phase biocatalysis process appears to not be profitable. A study realised by Mathys and *et. al*. (1999) about *Pseudomonas* oleovorans and recombinant strains (e.g. *E.coli*) containing the alkane oxidation genes process design and economic evaluation showed that total costs for biochemically produced medium chain length alkanols (1-octanol) would be of the order of US$10 kg^{-1}, which compares well to the present cost of highly purified alkanols. The largest contribution to the total productions costs, 40 %, is from the medium components required for cell growth and 20%-25% from equipment. Improvements relevant for this process can be achieved by increasing the biocatalyst performance, which results in improved overall efficiency, decreased capital investment, and hence, decreased production cost.

Two-liquid phase biocatalysis processes examples

Wild-type cells of *P. putida* mt-2 are used by Lonza® to produce heteroaromatic acids on a commercial scale. Furthermore, xylene oxygenase is selective for the *si*-face of prochiral vinyl functions on aromatic ring systems, which leads to the formation of optically active epoxides, such as (*S*)-styrene oxide. *Escherichia coli* recombinants carrying the genes for xylene oxygenase have produced (*S*)-styrene oxide from inexpensive styrene in a 2-liter reactor. Unfortunately, so far the productivities displayed by such recombinants have been insufficient to commercially exploit their synthetic potential. A number of observations have indicated that expressing the xylene oxygenase genes via the *alk* regulatory system of *Pseudomonas oleovorans* GPo1 might provide suitable biocatalysis strains for two-liquid-phase cultures. It was observed a volumetric productivity of more than 2 g of styrene oxide per h per liter of aqueous phase was obtained; this value is very fortunate [Panke S. *et. at.*,1999].

Chan E-C and *et.al*. (1991) used non-ionic chemical surfactants (Triton X-100 and Tween 80) to alter the cell permeability of *P. aeruginosa* growing in *n*-pentadecane to produce tri-decane 1,13-dicarboxylic acid (DC-15). They determined that the higher the concentration of detergents added to the culture, the more non-viable cells were found. However, when the concentrations of

both surfactants exceed 5% (v/v), the number of viable cells remained at a constant level. They concluded that using an optimized Triton X-100 concentration yield of DC-15 increased. The reasons for that was the formation of the micelles with the substrate that became it more accessible to the cellular surface and the increased cell permeability, which accelerate the contact between the enzyme system in the cells and the substrate.

Schmid A and *et. al.* (1998) the grow Pseudomonas oleovorans cultures and cell-free emulsions containing n-decane. They observed that excessive surfactant concentrations are not beneficial. The enlarged decane-water interfacial area obtained by emulsification was apparently overcompensated by an increased apolar substrate transfer resistance across the liquid-liquid phase barrier. This effect is likely to be due to an increased mechanical stability and perhaps also of the thickness of the droplet stabilizing layer of surface-active material at the liquid-liquid interface, effects which have been observed to reduce transfer rates in liquid-liquid extraction processes, thus, there appears to exist an optimal surfactant concentration and composition for maximal interfacial transfer rates in microbial two-liquid phase cultures. Therefore, it can be advantageous to find ways to optimize surfactant synthesis rates during two-liquid phase cultivation in order to maximize volumetric growth rates and decane transfer rates. So, they found that the optimum surfactant concentration has to be below 1 g/l_{aq} . Maximal volumetric growth rates were determined in two-liquid phase *P. oleovorans* cultures grown on n-decane as the sole carbon source. In these cultures containing either only the surfactants produced by the bacteria during the cultivations or additional surfactant added beforehand, limited decane transfer from the apolar solvent phase to the cells led to linear growth. When stirred continuously at 500 rpm, the maximum volumetric growth rate under decane limitation, an indicator of the maximum decane transfer rate, was 0,7 g/l_{aq}. When the culture was emulsified at 2500 rpm during the initial 12 h and then stirred at 500 rpm and an addition of 1 g/l_{aq} biosurfactant isolated from previous cultures was added, maximal volumetric growth rates decreased to 0,4 and 0,25 g/l_{aq} , respectively. So, they concluded that efforts to maintain surfactant concentrations at low levels and to control surfactant composition should improve mass transfer of apolar substrates in two-liquid phase bioprocesses.

Material and Methods

Chemicals

Substance	Chemical Formula	Specifications	Company
Sodium phosphate dibasic	Na_2HPO_4	≥99%	Sigma Aldrich®
Dipotassium phosphate	K_2HPO_4	≥99.0%	Sigma Aldrich®
Monopotassium phosphate	KH_2PO_4	≥99.0%	Sigma Aldrich®
Ammonium sulfate	$(NH_4)_2SO_4$	≥99.0%	Sigma Aldrich®
Ammonium chloride	NH_4Cl	≥99.5%	Sigma Aldrich®
Yeast			Oxoid®
l-leucine	$C_6H_{13}NO_2$	99%	Alfa aesar®
l-proline	$C_5H_9NO_2$	99%	Alfa aesar®
Thiamine Hydrochloride	$C_{12}H_{17}N_4OS^+Cl^-.HCl$	99%	Sigma Aldrich®
Purified water		80Ω	
magnesium Sulfate heptahydrate	$MgSO_4.7H_2O$	98%	BDH®
Calcium Chloride Dihydrate	$CaCl_2.2H_2O$	99,5%	Alfa aesar®
Glucose	$C_6H_{12}O_6$	99%	Sigma Aldrich®
Tetracycline	$C_{22}H_{24}N_2O_{88}$	99%	Sigma Aldrich®
Ferrous Sulphate Heptahydrate	$FeSO_4.7H_2O$	100%	Sigma Aldrich®
Manganese Chloride Tetrahydrate	$MnCl_2.4H_2O$	99.5%	Sigma Aldrich®
Cobalt Sulphate heptahydrate	$CoSO_4.7H_2O$	99%	Fluka®
Copper Chloride dihydrate	$CuCl_2.2H_2O$	99%	Riedel-de Haen®
Zinc Sulphate heptahydrate	$ZnSO_4.7H_2O$	99%	VWR®
dicyclopropyketone (DCPK)		>95%	Merck®
n-Dodecane	$C_{12}H_{26}$	99%	Alfa Aesar®
1-Dodecanol	$C_{12}H_{26}O$	98%	P&G®
Dodecanoic Acid	$C_{12}H_{24}O_2$	98%	Alfa Aesar®
Triton X-100	$C_{14}H_{22}O(C_2H_4O)_n$ (n = 9-10)	100%	Alfa Aesar®
Polypropylene glycol (PPG)		100%	Alfa Aesar®
Ethyl Acetate		99%	Alfa Aesar®
Tris	$C_4H_{11}NO_3$	99,9%	National Diagnostics

Solutions

Trace mineral Stock:

(Filter sterilised)	Concentration (g/L)
$FeSO_4.7H_2O$	2,78
$MnCl_2.4H_2O$	198
$CoSO_4.7H_2O$	2,81
$CaCl_2.2H_2O$	1,47
$CuCl_2.2H_2O$	0,17
$ZnSO_4.7H_2O$	0,29

Medium [Wubbolts and at. al. 1996]

	Quantity/L
Purified Water (mL)	1000
Na_2HPO_4 (g)	7
K_2HPO_4 (g)	15,9
KH_2PO_4 (g)	4
$(NH_4)_2SO_4$ (g)	1,2
NH_4Cl	0,2
Yeast Extract (g)	5
l-Leucine (g)	0,6
l-Proline (g)	0,6
Thiamine Hydrochloride (g)	0,005
Above components are autoclaved	
$MgSO_4.7H_20$ (MgSO4 only) (ml of 0,5M sol)	5
Trace Minerals (112) (mL)	1
4% (w/v) $CaCl_2.2H_20$ (mL)	1
Glucose (mL of 500g/L)	20
Tetracycline (mL of 10mg/mL)	1
Above were filter sterilised and added after autoclaving	

Software

In this work it was used a statistical experimental design version 7.1.6 from State-ease® for the design experience (DoE). Design-Expert®, version 7 software (DX7) is a powerful and easy-to-use program for design of experiments (DoE). With it the user can quickly set-up an experiment, analyze your data, and graphically display the results. This intuitive software is a must for anyone wanting to improve a process or a product. It is used to screen for vital factors, identify ideal process settings with response surface methods (RSM), and discover optimal product formulations via mixture design. Design-Expert software offers an impressive array of design options and provides the flexibility to handle categorical factors and combine them with mixture and/or process variables. After building the design, generate a run sheet with your experiments laid out for you in randomized run order. Add, delete or duplicate runs in any design with the handy design editor. With annotated statistical analysis and an extensive context-sensitive help system, the user can easily interpret the outputs. Interactive 2-D color graphics support use of your mouse to drag contours or set flags that display coordinates and predicted responses. Rotatable 3-D color plots

make response visualization easy. With the powerful optimization features in Design-Expert, you can maximize desirability for dozens of responses simultaneously. There are also unique tools for generating and graphing propagation of error (POE), thus allowing you to achieve six-sigma objectives for reducing variation. Maximize, minimize or hit targets with factor levels set to give robust results. With this version 7 new design creation tools were created, enhanced design augmentation augmentation ability, powerful analysis and diagnostic capabilities, updated graphics, an improved user interface, more options for design evaluation, expanded help, and new import/export tools [8].

Devices

Device	Specifications and Comments	Company
Balance		Sartorius 61000
Analytical Balance		Ohaus Analytic plus®
Autoclave	Capacity: 25L	Boxer® 200
Laminar Flow cabinet		Heraeus®
pH meter	Bench pH meter model 510	Mettler Toledo Seveneasy®
Incubator (cell culture)	Kuhner ISF 1V; Throw Diameter: 25mm; Agitation rate: 250rpm	Kuhner AG®
Oven (DCW)		Heraeus® 6060
Centrifuge	Agitation Rate 13000rpm	Beckman Coulter 22rR
Vortex Shaker		Junke&Kunkel® VF2
Spectrophotometer [1]	Wavelength range, nm: 330–830 nm; Absorbance range, A: -0.3–2.500	Amerdham Novaspec plus®
Thermomixer [2]	This thermomixer is equipped with a rack that allows the simultaneous heating of up to 24 1.5 ml eppendorf Safe-Lock tubes. It is fully programmable, capable of heating or cooling samples from 1℃ to 99℃ and of agitatin g from 300 rpm to 1500 rpm (also has a no mixing mode).	Eppendorf® Thermomixer Comfort Sigma Aldrich®
Duetz Sytem [3]	The Duetz system was composed of a spongly silicon membrane and a rigid silicon membrane and the support that could be attached to the incubator platform.	Enzcreen®
24-Microwells	In the 24-well plate the individual wells have a maximum diameter of 17mm and a height of 60mm. The top of both wells is a square cross-section. The bottom was the shape of a four sided inverted inverted pyramid and a half sphere .It was used also the half sphere bottom.	Sigma Aldrich®
Permeable membrane [4]	An Adhesive Gas-Permeable, Cell Culture Membrane. Compose by polyurethane and UV transparent.	Breathe-Easy®
Gas Chromatograph	Autosystem XL.To quantify the concentration of the components in the organic phase and in the interface the following GC method was used: Split injection of the sample into a BPX5 capillary column (30 m long, 0.53 mm internal diameter, 1µm fil) with helium as carrier gas. Peak detection was by using a Flame ionisation (FID) .Elution**:** 200^{o}C for 2min, followed by linear increase of 10^{o}C per minute until final temp of 240^{o}C. Injector temperature of 280^{o}C and a detector temp of 280^{o}C. Compounds were quantified from the integrated GC signal by the internal standard method, using reagent grade standards.	Perkin Elmer®
High Speed Camera: Phantom® Miro® 4 [5]	The Miro® 4 has a high resolution 800x600 pixel CMOS sensor combined with a maximum full frame recording speed of 1,000 pictures per second. The continuously adjustable shutter supplies exposures as short as 2 microseconds for incredible motion freezing control. The Miro® 4 provides excellent image quality with the choice of color or monochrome sensors that deliver 8-bit pixel depth, (10-bit, or 12-bit are available as an option).	Vision research®
Shake Flask (SF)	There were used 1L SF and 500mL with the same geometry, with four baffles. In fermentations they were covered with cotton bung and foil and 90% of head space was used as well 20%(v/v) of *n*-dodecane.	
2L Fermenter	Glasss bioreactor with 2 ruston impeller and air spairger. There is a control software that permits to set and control several parameters like the control of agitation rate, oxygen concentration, etc.	Adaptative®

Methods

E.coli pGEc47ΔJ cell culture

E.coli pGEc47ΔJ with the plasmid pGEc47ΔJ. This plasmid contains the *alkBFGHJKL* operon and *alkST* genes, but with the deletion of the *alk*J (alcohol dehydrogenase), in order to only produce primary alcohols from the degradation of medium chain linear alkanes [Eggink G. and *et. at.*, 1987].

E.coli pGEc47ΔJ was stored as glycerol stocks (20% v/v glycerol) of 1 mL aliquots at -80ºC. After room temperature thawing, the stocks were used for inoculation. The inoculation was into 50mL Wubbolts medium in 500 mL SF. Overnight growth was conducted at 37ºC in a orbital shaken incubator. Before the inoculums (5% (v/v)) were used to cultivate other vessels the optical density (OD) of the cultures at 600nm was measured. It was important that all the experiments had the same growth conditions of the inoculum (37ºC, 250 rpm, 25 mm throw diameter) and an OD of 2,0 ±1 time=t_0.

Sample preparation

The cell cultivation in the SF or in MTPs were performed in the laminar flow cabinet. Then transported to the incubator and at particular time points samples were collected.

In the cell cultures in SFs, 5mL samples were taken, decanted into 5 pre-weighed eppendorsf spun at 28^{o}C for 15 minutes at 13000 rpm. The phases were carefully manually separated and volumes of each phase recorded. The organic phase was diluted (to 20% or 50%) in ethyl acetate and analysed by gas chromatography (GC). In microwell plates (MTPs) a whole well was sacrificed and the content of the well was subjected to the same procedures described above.

As the melting point of 1-dodecanol is 24°C [6] it is critical to process the samples above this temperature, for maximising the product recovery.

A characteristic of two-liquid phase fermentation is that with increasing fermentation time an emulsion starts to form. This fact added an interfacial phase in the system and the phase separation became more difficult. Moreover, when the samples are centrifuged due to the angle of orientation of the eppendorfs in the centrifuge the interface formation is not uniform and forms more on the upper side of the eppendorf.

The interface separated was diluted with ethyl acetate and shaking on the thermomixer for 15min at 50℃ and 1000rpm. The volume of ethyl acet ate added was the volume for fulfill the total volume after the phase separation. The dilution factor was calculated by subtracting the volume of added ethyl acetate from the final colourless organic component volume. As the organic phase this colourless organic from the interface was also analysed by GC.

Determination of cell density

Cell density was determined by the dry cell weight (DCW) method. Cell density measurements were typically taken by centrifuging 1ml two-phase samples at 13000rpm for 15 minutes, marking the aqueous volume on the side of the graduated eppendorf; washing the pellets with tris-HCL pH7.4 and drying in an 80℃ oven until a constant mass was reached (24-96hours).

Determination of 1-dodecanol and dodecanoic acid concentrations

The eppendorfs samples for GC analysis were prepared, according to the dilution, into GC vials. Then, these vials were vortexed before GC analysis to ensure homogeneity.

For 1-dodecanol and dodecanoic acid concentration determination present or in the organic phase or in the interface, the samples were eluted at an initial temperature of 200℃ for 2minutes, followed by a linear increase of 10℃ minute to reach a final temperature of 240℃. Injector and detector temperatures were both 280℃. The concentrations were determined by cross-referencing to a set of *n*-dodecane, dodecanoic acid and 1-dodecanol standards analysed in the same run. The form of calculation of the total concentrations is in Appendix 1.

Visualisation of liquid hydrodynamics by high speed video camera

To visualise the liquid hydrodynamic of the two-liquid phase system the high–speed camera was mounted next to the platform where the 500 mL, 1L SFs and microwell mimics were shaken in order to record the fluid motion and the droplet distribution.

Single well mimics with the same geometrical configuration as a single well from commercial 24-well plates (24-Deep Square Wells (DSW) and 24-Shallow Round Wells (SRW) were fabricated in the University College London (UCL) department of chemical engineering workshop.

Sterilisation and use of sandwich covers for deepwell microtitre plates (MTPs) (Duetz System)

The use of the Duetz system (was to ensure the decrease of liquid loss due to splashing observed with the high speed camera and previous work, whilst allowing sufficiently high agitation rates for effective mixing of the two phases. They were prepared following the Duetz Manual [3]:

1. Put sandwich cover on top of a suitable square-deepwell MTP;
2. Wrap the sandwich cover and MTP in aluminium foil (alternative: use a sterilization bag);
3. Autoclave for 15 minutes at 121 ºC;
5. The sandwich cover + MTP were then dried in an oven set at ~ 100-110 ºC for 1 hour, in order to dry the cotton layer;
6. Place the sandwich cover and MTP in a laminar flow cabinet;
7. Take off the aluminium foli;

8. Fill each well of the sterile MTP (using e.g. a multipipette or a filling station) with an appropriate sterile liquid growth medium (for advised volumes, see below);

9. Inoculate the wells of the MTP;

10. Put the sandwich cover on top of the MTP (Figure 17 a));

11. Slide the sandwich cover and MTP into the clamp (attached onto an orbital shaking platform), and turn the handle to the "CLOSED" position (Figure 17 b));. Start the shaker.

a) **b)**

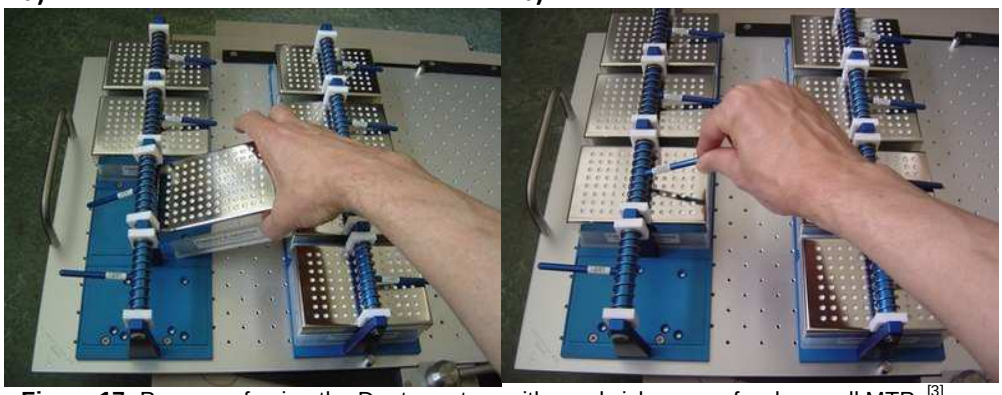

Figure 17: Process of using the Duetz system with sandwich covers for deepwell MTPs[3].

Results and Discussion

Visualisation of liquid hydrodynamics: Phase mixing and droplet size distribution

The objective here was to start at the large scale and end at the small scale, in order to visualise the relationship between the mixing condition with the volumetric product yields. As the 2L fermenter is where the higher volumetric product yield is reached because of the better mixing by , in this case, two ruston impellers and the air sparger. These mixing conditions are not at all present in SF or in a MTPs where the only way of mixing is, in this case, orbital shaking. By reasons mentionened before, the interest is in performing the reaction at the smaller scale. Therefore, by observing the effects of different agitation rates, throw diameters, addition of biosurfactnats and chemical surfactants on the phase mixing it is hoped that the best mixing conditions, mimicking the fermenter volumetric productivity, can be established.

2L Fermenter

At a large scale, the first purpose was to picture how the fluid hydrodynamics inside of a 2L fermenter, where there is OTR control, was. The intention was to measure the droplet size distribution but the path-length of the fermenter was too large to accurately measure this; distinguishing air bubbles from *n*-dodecane droplets (Figure 18).

In Figure 18 it can be seen very roughly the droplet distribution and the fluid distribution, because of the difficulty in distinguishing air bubbles from *n*-dodecane droples at least at figure ! a). In the rest of the pictures is humanly impossible distinguished anything. For more quantitative data an Optical Reflectance Measurement (ORM) particle size analyser should be use that can provide *in-situ* and on-line measurements, although this would be in a more localized region in the fermenter and so heterogeneity would not be detected [Cull S.G. and *et. al.*, 2002].

However, some useful qualitative observations could be made. In Figure 18 a) is clear that there are no phase mixing. After only 3hours the two-liquid media started to become emulsified, but the media still appears heterogeneous. After 24hours the two-liquid media is opaque, homogenous and completely emulsified. From these observations it can be said that potential mass transfer limitations can occur in the fermenter under these conditions.

Since it is desirable to know the droplet size dristribuition as it is intrinsically related to liquid-liquid mass transfer, another experience was set up with the same 2L-fermenter with 20% (v/v) *n*-dodecane but with no cells and air input (Figure 19). However, this observation was qualitative.

During the two-phase fermentation in the fermenter polypropylene glycol (PPG) is added to reduce foaming but, as a surfactant, is likely to have an effect on the liquid-liquid mixing. Figure 20 shows the effect of PPG addition it can be seen that PPG addition creates emulsification of the

organic phase but it remains unclear whether this is beneficial (due to increased liquid-.liquid interface) or detrimental (due to increased resistance) to mass transfer.

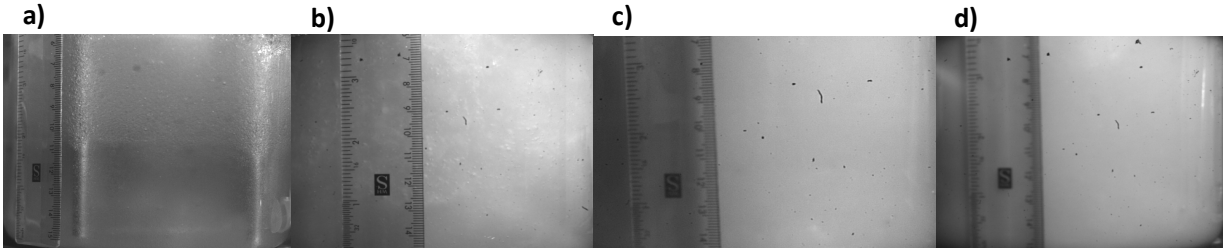

Figure 18: Visualisation of mixing conditions of a fermentation of *E.coli* pGEc47ΔJ in 20 % (v/v) of n-dodecane in 2L fermenter (two Ruston impellers and the air input) with 90% of head space.a) t=0h with no cells at 500 rpm; b) t=3h at 500 rpm; c) t=24h at 1000pm;d) t=48h 1000 rpm.

During the two-phase fermentation in the fermenter polypropylene glycol (PPG) is added to reduce foaming but, as a surfactant, is likely to have an effect on the liquid-liquid mixing. Figure 20 shows the effect of PPG addition it can be seen that PPG addition creates emulsification of the organic phase but it remains unclear whether this is beneficial (due to increased liquid-.liquid interface) or detrimental (due to increased resistance) to mass transfer.

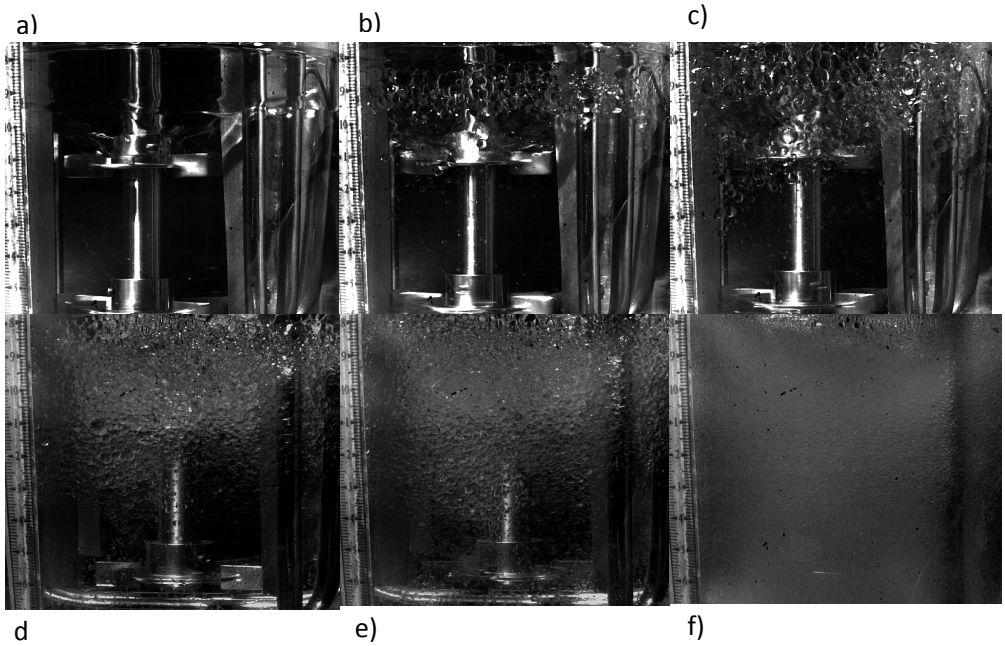

Figure 19: 2L Fermenter mimicking the usual components condition (20% (v/v) organic phase) with 1L of water and 200 mL *n*-dodecane with a stirrer agitation rate between 100 rpm and 700rpm and no air input. At the smaller agitation rates the laminate layer between the water and dodecane is not disrupt, but as agitation rate increases the laminar layer is broken by the first Ruston impeller forming organic droplets with 1-5 mm then the bottom Ruston impeller reduces the size of the droplets, helping to the complete mixture of the two phases at 700 rpm.

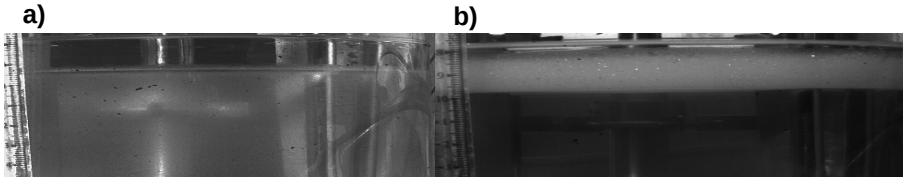

Figure 20: 2L Fermenter with 1L of water and 20% (v/v) of n-dodecane with no air supply after stirrer agitation. a) agitation rate of 1000 rpm; b) agitation rate of 650 rpm and with the addition of 100 µL of Polypropylene glycol (PPG). It is clear by b) that PPG creates an emulsion.

Shake flask: 500mL and 1L

Shake flasks are widely used in bioprocess development and optimization due to their ease of handling and low operating costs. The liquid distribution gives important information about the momentum transfer area, which is the contact area between the liquid mass and the flask inner wall, and the mass transfer area, which is the surface exposed to the surrounding air, including the film on the flask wall. The shake flask performs a circular translatoric movement with the radius equal to half the shaking diameter keeping its orientation relative to the surrounding. Moreover, in reality a liquid film remains at the flask wall after the liquid sickle has passed. During fluid motion, power is dissipated due to internal friction. In shake flasks, the compensating mechanical power is introduced over the flask wall, which can therefore be regarded as the power inducing element (comparable to the stirrer in an agitated tank). The contact area between the liquid bulk and the flask is the liquid covered surface of the wall. The total momentum transfer area therefore consists of two parts: first, the area on the flask bottom and second, the area on the flask wall. The liquid sickle within a shake flask periodically moves on the inside of the wall leaving a thin liquid film. Hence, the gas/liquid mass transfer area consists subsequently of the sickle surface itself and the surface of the wetted glass wall. The total gas/liquid mass transfer area therefore consists of three parts: first, the area on the flask bottom periodically covered by the liquid bulk, second the inner surface area of the liquid bulk facing the parabolic and finally the area of the film on the flask wall wetted periodically by the liquid bulk [Büchs J and *et. al*., 2007]

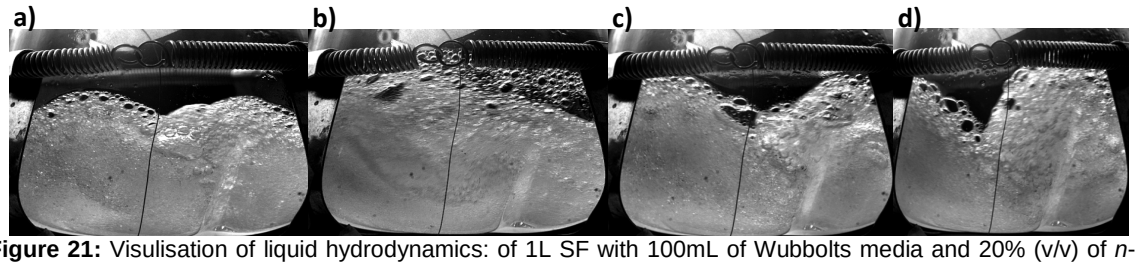

Figure 21: Visulisation of liquid hydrodynamics: of 1L SF with 100mL of Wubbolts media and 20% (v/v) of *n*-dodecane in a 25 mm throw diameter orbital shaker at 200rpm a), 250rpm b), 300rpm c) and 350rpm d).

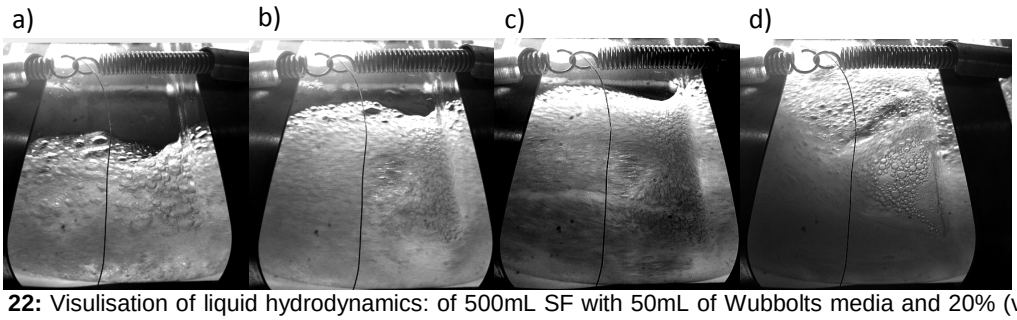

Figure 22: Visulisation of liquid hydrodynamics: of 500mL SF with 50mL of Wubbolts media and 20% (v/v) of n-dodecane in a 25 mm throw diameter orbital shaker at 200rpm a), 250rpm b), 300rpm c) and 350rpm d).

The Figure 21 and Figure 22 are mimics of the throw diameter that are normally used in the cell cultivation. Evidently, with the increase of agitation rate the liquid height, turbulency and foam creation also increase. Increasing liquid height and turbulency is very desirable for improved oxygen transfer, however excessive turbulency could damage the cells. So, a balance should be attaining. Apparently, a good mix is achieved in all the rotation rates. Therefore, it is not need to use excess of power input. So, for 1L and 500mL SF the "ideal" agitation rate, for this system, is 250rpm, which was the agitation rate used in all the cell cultivations in this work. Besides, it is the most used.

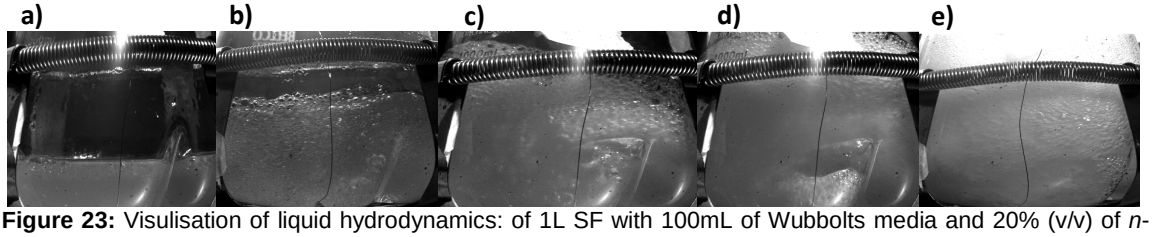

Figure 23: Visulisation of liquid hydrodynamics: of 1L SF with 100mL of Wubbolts media and 20% (v/v) of *n*-dodecane in a 50 mm throw diameter orbital shaker at 50rpm a),100rpm b), 150rpm c), 200rpm d) and 250rpm e).

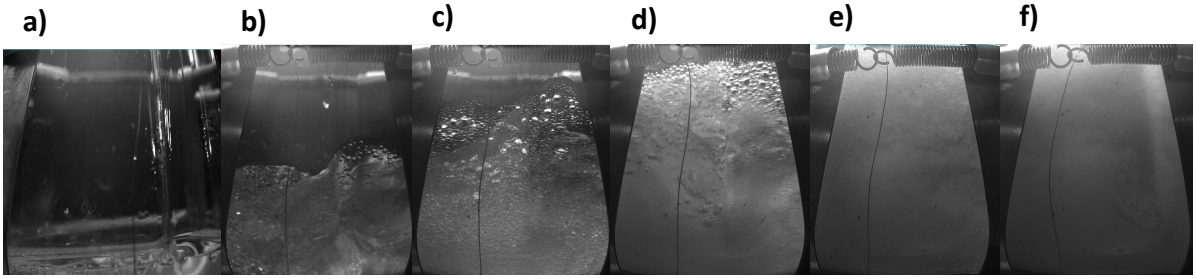

Figure 24: Visulisation of liquid hydrodynamics: of 500mL SF with 100mL of Wubbolts media and 20% (v/v) of *n*-dodecane in a 50 mm throw diameter orbital shaker at 50rpm a), 100rpm b), 150rpm c), 200rpm d), 250rpm e and 300rpm

Figure 23 and Figure 24 are a mimics of the throw diameter used in some cell cultures. It is clear that at the lower agitation rate (50rpm) there is no mixing, the two liquids moves one on the top of the other never breaking the phase boundary. Therefore, the "ideal" agitation rate, for this system, is 150rpm. It is advisable to not do cell cultivation above this agitation rate, for only one reason–the liquid height could reach the cotton cover and saturate the cotton wool leading to poorer oxygen transfer and increased risk of contaminating the culture.

Microwell plates

A sufficiently high exchange rate of headspace air is a pre-requisite but not a guarantee that the cells growing in the wells are supplied with an adequate amount of oxygen; gas–liquid transfer is usually the chief limiting factor in this respect [Deuty W. A., 2007].

In a one liquid phase condition, the imposed shaking conditions for both MTPs bioreactors promote significant deformation and motion of the gas–liquid interface. The gas–liquid (oxygen) mass transfer will primarily occur at the interface between the two phases since there is no dispersion of the gas phase in the bulk liquid. It is noticeable that as the liquid moves orbitally from side to side, any liquid film on the side-walls of the microwell is exposed to air increasing the potential for gas–liquid mass transfer. Gas–liquid mass transfer at the wall however would require the presence of a liquid film adhering to the surface of the microwell as the bulk liquid moves away from the wall. The formation of such a liquid film is critically affected by the hydrophobicity and hydrophilicity of the wall material and the wetting characteristics of the fluid. [Zhang H, et. al., 2008]. It can be assumed that a similar behaviour occurs in a two-liquid phase, however the fact that second phase is present is likely to improve the gas-liquid (oxygen) mass transfer simnce oxygen is more soluble in *n*-dodecane than in water. As the two liquid is hydrophobic most likely this phase adhere to the walls of the MTPs instead of the aqueous phase, where the cells are growing. Nevertheless, if a totally homologous mixture is present a better gas-liquid (oxygen) mass transfer is achieved. It is critical to ensure a good gas-liquid (oxygen) mass transfer since without cell growth there is no product formation. Then, another difficulty appears the liquid-liquid mass transfer between the substrate and the product.

Consequently, it was very interesting to observe the hydrodynamic of the two-liquid phase system. This study was performed in 24-Standard Round Well (SRW) and 24-Deep Square Well (DSW), but in more detail in the last. Even so, this study was only qualitative.

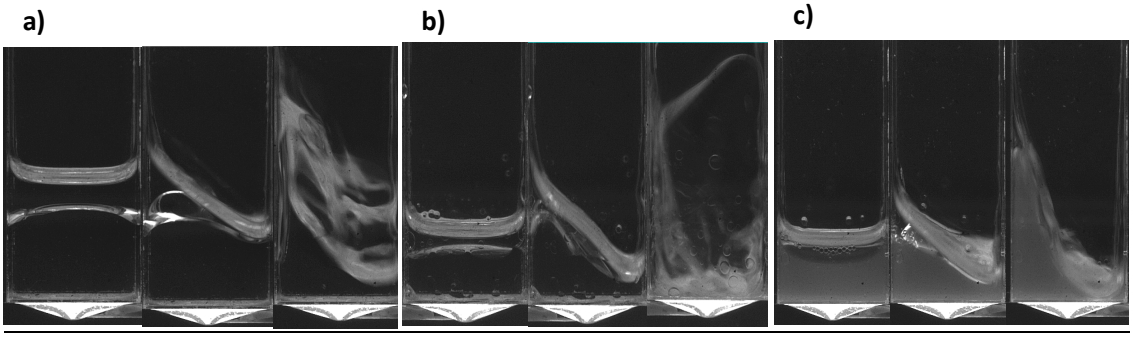

Figure 25: Visulisation of the evoluation of agitation in the liquid hydrodynamics of 24-DSW with 10%(v/v) of Wubbolts media and 20%(v/v) of *n*-dodecane in a 50mm throw diameter orbital shaker at 220rpm and V_{liq} of 4,5mL a), 240rpm V_{liq} of 2,5mL b) and 240rpm with 48h fermentation broth*, V_{liq} of 2,5mL c). * Fermentation in 2L-Bioreactor where the fermentation of *E.coli* pGEc47ΔJ was using *n*-dodecane as substrate

In Figure 25 a), where there is the higher liquid volume, it was demonstrated that at 220rpm there is no mixing between the two liquid phases. It is clear the separation of the phases. Therefore,

the volume was reduced and the agitation rate slightly increased to test if it was the volume the key for the no mixing. Still, watching Figure 25 b) no mixing during the evolution to reach the 240rpm was observed. However, at the 240rpm the turbulence is so intense that it is impossible see if there is or not mixing. A fact to keep is the thin film of *n*-dodecane at the polypropylene wall of the well. Therefore, this last experience is inconclusive. As during fermentation of *E.coli pGEc47ΔJ* and *P. oleovorans* there are surface- active substances released helping to reduce the surface tension of *n*-alkanes. In Figure 25 c) it was added a fermentation broth instead of the culture medium. Even so, the mixing was not improved.

As a consequence, the throw diameter was reduced, in order to increase fluid motion. In Figure 26 a) it can be seen a slight mixture between the two phases. However, the addition of a non-ionic surfactant, Triton X-100, could do a total mix between the two phases, pointing out for more research about if these mixing conditions could increase the 1-dodecanol production.

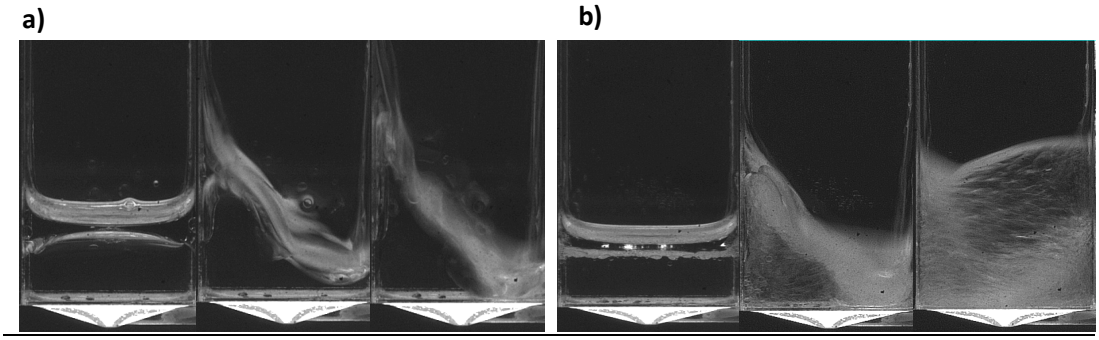

Figure 26: Visualisation of the evolution of the agitation in the liquid hydrodynamics of 24-DSW with 10%(v/v) of Wubbolts media, 20%(v/v) of *n*-dodecane in a 12,5mm throw diameter orbital shaker at 360rpm V_{liq} of with 2,5mL a) and 0,1% TritonX-100 at 345rpm V_{liq} of with1,5mL b).

Nevertheless, the throw diameter was diminished. In figure Figure 27 a semi-total mixing is achieved, but the shear force could be too high for the cells.

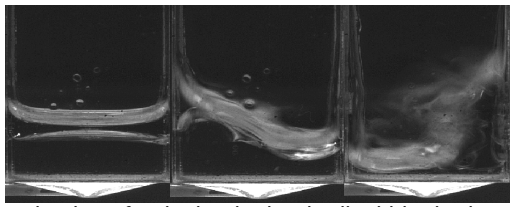

Figure 27: Visulisation of the evoluation of agitation in the the liquid hydrodynamics of 24-DSW with 2,5mL of 10%(v/v) of Wubbolts media, 20%(v/v) of *n*-dodecane in a 3mm throw diameter orbital shaker at 500rpm.

As it was accomplished a good result by adding chemical surfactant, it was test adding biosurfactant from E.coli pGEc47ΔJ fermentation using *n*-dodecane as substrate. First, the interface (biosurfactant) was added to the culture medium (Figure 28) and at last at the fermentation broth (Figure 29) both with a fresh addition of *n*-dodecane. It was noted that total mixing appeared at 400 rpm in the first case and at 350rpm for the last. This could be explained by the decrease in interfacial tension between the phases allowing for breaking of the phases boundary at a lower

agitation rate. In conclusion, the addition the biosurfactant is beneficial for mixing either on media or broth, although the components in the broth ease more the emulsification.

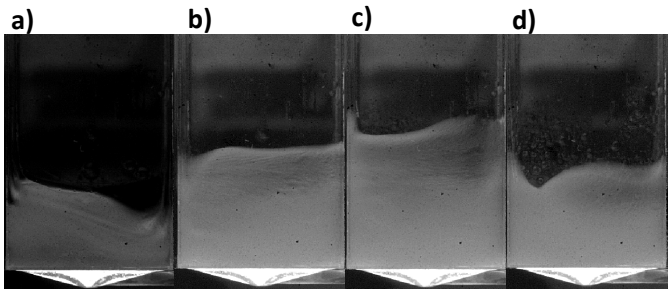

Figure 28: Visualisation of liquid hydrodynamics of 24-DSW with 2mL of 10%(v/v) of Wubbolts media, 20%(v/v) of *n*-dodecane and the fermentation emulsifying material collected at the interface after centrifugation** in a 3mm throw diameter orbital shaker at 300rpm a), 400rpm b), 500rpm c), 600rpm d). **Emulsifying material from 2L-Bioreactor two-phase fermentation of *E.coli* pGEc47ΔJ using *n*-dodecane as substrate after 48hours. The material was collected from the interface of the two-phases after centrifugation.

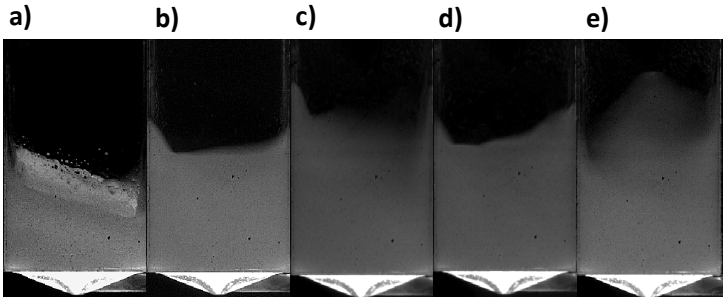

Figure 29: Visulisation of liquid hydrodynamics of 24-DSW with 2mL of 10%(v/v) of 48 h Broth cells with new media **, 20%(v/v) of *n*-dodecane and the fermentation emulsion*** in a 3mm throw diameter orbital shaker at 300rpm a), 350rpm b), 400rpm c), 500rpm d) and 600rpm e). ** Cells from a fermentation in 2L-Bioreactor where the fermentation of *E.coli* pGEc47ΔJ was using *n*-dodecane as substrate;***Emulsion from the previous fermentations.

Same tests also was realised in the 24-SRW, but the main conclusion is that for the system in interest is not adequate as the mixing is lacking and the liquid height is too high at this agitation rate (520rpm). Even at lower agitation rates the two liquid phases did not mixed (data not shown) (Figure 30).

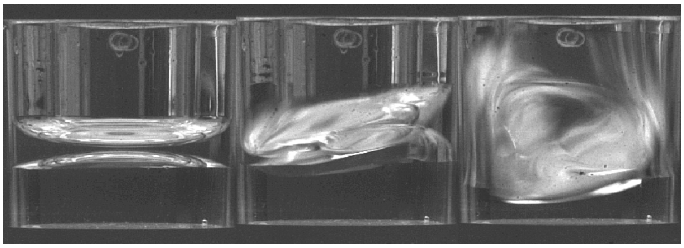

Figure 30: Visulisation of the evoluation of agitation in the the liquid hydrodynamics of 24-SRW with 2,5mL of 10%(v/v) of Wubbolts media, 20%(v/v) of *n*-dodecane in a 3mm throw diameter orbital shaker at 520rpm.

In summary, in all different scales it was achieved a homogeneous mixing conditions. However, some limitations also be noticed. Notice that the same conditions were used in all (10% (v/v) aqueous phase and 20% (v/v).

In an *E.coli* pGEc47ΔJ fermentation on a 2L-fermenter, only after 24hours was observed a homogenous and completely emulsified. Therefore, there is not a good mixing between the two liquid phases during the first 24hours. The result of these mass transfer limitations reflects on a low bioconversion yield. Even without cells and air sparger a full homogenous phase was achieved only at 700rpm, establishing, in a way, the minimum agitation rate that could be used. With the addition of a small volume of the surfactant, PPG, it was observed a faster homogeneity (data not shown) and also a formation of an interface, which in the system water-*n*-dodecane took a long time to disappear. This communion between the surfactant and the organic phase, shape the droplet size distribution because the action of PPG is to low the surface tension, in order to increase the solubility of the organic phase on the aqueous phase. The effect of PPG was not fully understood. However, in a later experience with a *E.coli* pGEc47ΔJ fermentation of *n*-dodecane where it was added 0,1% (v/v) of Triton X-100 show a bottleneck of the use of surfactants in 2L-fermenter (data not shown). Immediately, intense foaming was produced making this fermentation impracticable. So, different surfactants have different impacts. To sum up, more studies should be done to determine the exact concentration and conditions for the use of surfactants in large scale. Those are made at small scale.

About the SFs it was tested the two throw diameters most used (25mm and 50mm). In this experience it was establish an operational agitation rate for each throw diameter The overall conclusion is that the size of the SF little interfered in the fluid motion, perhaps the only important effect was that the liquid height is higher. Again, it was impossible to distinguish air bubbles from *n*-dodecane droplets and with the increasing of the agitation rate, in the two throw diameters, the foaming intensifying. Another important achievement was to confirm that the later E.coli pGEc47ΔJ fermentations were realised at the optimal operational agitation rate for the throw diameter (25mm) of the incubator.

Continuing in the scale–down, it was study at three different throw diameters (50mm, 12,5mm and 3mm) in a 24-DSW mimic. At 50mm higher liquid volume difficult the mixing and even when the volume of the liquid decrease the best mixing was achieved with the Wubbolts media. The components, for example, active –surface substances present on a 48hours broth did not reduced the surface tension as was expected. Again, in the 12,5mm throw diameter it was verified that a higher volume difficult the mixing, yet it is accomplish a better mixing conditions. With the addition of 0,1% (v/v) of Triton X-100 the success is complete. It was proved that a homogenous phase can be reached in MTPs. In the throw diameter of the thermomixer (3mm), where normally is realised the fermentations in MTPs, it was got a reasonable good mixing without the addition of the surfactant (which maybe one of the reasons for the thermomixer use). At this same throw diameter was tested the effect of using biosurfactants (emulsion from the fermentation). The conclusion was that it is beneficial, but at 3mm the 48hour broth has a surface tension reducer action. About the 24-SRW mimic the only thing to say is that this geometry is not adequate for this system.

An overall analysis of surfactant addition is that the splashing reduces and the mixing between phase is hugely increased. Although, oxygen transfer, mixing and evaporation. Another factor is that lower liquid volume liquid in the microwell the best is the mixing and oxygen mass transfer. Therefore, in the below MTPs experiences with *E.coli* pGEc47 ΔJ *n*-dodecane bioconversion was used the wells with V_{liq} of 2,5mL.

Therefore, it was proved the feasibility for scale-down for the two liquid phase bioconversion, with the low throw diameter and with the addition of surfactants at microwells (24-SRW). However, there is a correlation between the better mixing that may imply higher agitation rate and so more splashing, and evaporation rate. These will affect the bioconversion of *n*-dodecane.

E.coli pGEc47 ΔJ n-dodecane bioconversion

After having a reasonable understanding how liquid hydrodynamics on 2L-Fermeter, 500mL and 1LSFs and 24-SDW AND 24- SRW mimics, it was interesting to quantitatively know the *n*-dodecane bioconversion in the 500mL and 1L SFs and in the 24-DSW MTPs.

Several approached were done. First, it was done *E.coli* pGEc47 ΔJ *n*-dodecane bioconversion with several culture conditions in 500mL and 1L SFs. Then, MTPs were used. In this, first was performed the bioconversion on the thermomixer and then in the incubator, where a number of tests were performed: the effect of the MTP cover in evaporation rate and in the splashing by using two different type of sandwich cover from the Duetz system and the permeable membrane. After, the visualisation of the effects of surfactants in the mixing of two liquid phase, it was desirable to test that both in SFs and MTPs. In this work all the cultivations of *E.coli* pGEc47 were peformed with 10 % (v/v) of Wubbolts media, 5% (v/v) inoculums, 20% (v/v) of *n*-dodecane, 0,05% (v/v) or 0,1% (v/v) of DCPK (inducer) in SFs or in MTPs, respectively, 0,01% (v/v) of PPG (1:100) and 0,1% (v/v) of Triton X-100 (1:10). The incubator used for all the fermentation has a 25mm throw diameter, 250rpm and constant temperature at 37℃. The DCW, 1-dodecanol and dodecanoic acid concentrations in organic phase and in the interface, evaporation rate and formation of interface from all the experiences done in this section are in Table 5.

E.coli pGEc47ΔJ *n*-dodecane bioconversion in Shake flasks

It was performed *E.coli* pGEc47ΔJ *n*-dodecane bioconversion where it was tested the effect of the SF volume (500mL and 1L) in the bioconversion of *n*-dodecane during 48hours, as from the images from high speed camera (HSC) the fluid hydrodynamic seems identical. It was only measured the cell density and the 1-dodecanol (target product) in the organic phase (Table 4).

Table 4: Experienceal results from *E.coli* pGEc47 ΔJ *n*-dodecane bioconversion in 500mL and 1L SFs.

SF	Time (h)	DCW (g/Laqueous)	1-Dodecanol (g/Lorganic)
1L	6	0,15±0,071	0
	24	1,15±0,071	0,10±0,142
	48	0,1	0,95±0,512
500 mL	6	$0,2\pm7,85x10^{-14}$	0
	24	1,2±0,141	1,72±0,178
	48	0,25±0,212	2,49±0,6423

The cell grow is slightly higher in the 500mL SFs and produced more 48% of 1-dodecanol than 1L SFs. Another observation is that there is an indirect relationship between the cell density and the product formation, as the maximum cell density was achieved at 24h though the maximum product concentration occurred at 48hours. However, it was verified in the GC chromatograms (Appendix 3: Experience 1) that another reasonable large GC peak appeared after the 1-dodecanol, indicating that the alcohol was not the only product produced. Therefore, it was important to find out what was. Using standards of dodecanoic acid it was confirmed that dodecanoic acid was produced. This clearly shows that there is an over-expression of pGEc47ΔJ plasmid. Other observation was that the emulsion formation was high. Therefore, 1-dodecanol and dodecanoic acid was GC analysed in the organic phase and in the interface (emulsion) in all after experiences.

No measurements of the volume phases on the SFs was made, and still not made because the collect method of a sample in the SFs is very inaccurate and the volumes gathered vary. The attempt was to collect organic and/or interface, in order to have enough volume for analysis (which in some case it was not sufficient) is a procedure very imprecise. Nevertheless, to accomplish the determination of total quantities in SFs and MTPs, it was measured, with a rule the volume fraction of each phase, in the eppendorfs. Again, this technique is not the ideal. An alternative process but more morose is pipette each phase and so determine the exact volumes.

E.coli pGEc47ΔJ *n*-dodecane bioconversion in 500mL and 1L SFs

To know what was the importance of 1-dodecanol in the interface and to measure the over-expression, by GC analysis of the organic phase and interface for dodecanoic acid, it was performed an *E.coli* pGEc47ΔJ *n*-dodecane bioconversion in two SFs (500mL and 1L) during 48hours. From this experience it was observed that in the 1L SF the DCW shows a parabolic curve and in the 500mL tend to a plateau. Unlike the previous experience, 1L SFs had higher DCW that 500mL SFs. About the bioconversion, in organic phase, there is not conversion of *n*-dodecane until the 24 hours and 30 hours for 500mL SFs and 1L SFs, respectively. The PCL_{Total}(0,2g/L) is the same in the two type of SFs. However, 1L SFs reach the pcl total at 48 hours and 500mL SFs at 30hours, but in these SFs there is no 1-dodecanol at 48hours. Relative of the presence of 1-dodecanol in the interface is small in both SFs. Still, in the 1LSFs at 24hours there is 1-dodecanol in the interface and none in the organic phase and in the 500mL at 6hours there is a very small

amount of 1-dodecanol in the interface and none in organic phase. Therefore, this can indicate that the 1-dodecanol pathway from the aqueous phase to the organic phase pass through the interface. In the 500mL SFs at 48hours there are no target product, revealing that the bioconversion is already done or the evaporation of the 1-dodecanol was total. Regarding the over-expression, at 1L SFs is irrelevant, but in 500mL SFs could provoke problems in the posterior product recovering. In conclusion, as the pcl total is equal in both SFs, because the presence of dodecanoic acid is smaller to perform this type of bioconversion it is best work with the 1L SFs although the fermentation time is higher.

E.coli pGEc47ΔJ *n*-dodecane bioconversion in 500mL and 1L SFs with PPG and Triton X-100

It was performed an *E.coli* pGEc47ΔJ *n*-dodecane bioconversion with the addition of surfactants (PPG and Triton X-100) in 500mL SFs and 1L SFs during 48hours. Relatively to DCWs the 1L SFs show again a parabolic curve and the 500mL a tendency for the formation of a plateau. The DCW in the 1L SFs with Triton X-100 is higher than in the one with PPG, but in 500mL SFs is the opposite. However, it is shown that the concentrations added of these surfactants are not toxic as, they present similar cell density with the SFs without surfactants. In organic phase, the bioconversion in 1L SFs with PPG presented the same behaviour of the previous SFs with no surfactants, the 1-dodecanol starts to appear only at 30hours and increases. With 1L SFs with Triton X-100 the bioconversion began earlier (24hours) and the concentration of 1-dodecanol increases. Concerning to the 500mL SFs the addition of PPG harms the bioconversion although with the SFs with Triton X-100 there was a plateau of high 1-dodecanol concentration during 24 and 48 hours, after decreased astoundingly at 48hours. The highest PCL_{Total} (0,8 g/L) was achieved with the Triton X-100 in both SFs, though at different time, 48hours for 1L SFs and 30 hours for 500mL. The 1-dodecanol concentration in the interface is, in all the cases similar, slightly lower. Therefore, a reasonable amount of 1-dodecanol is stuck in the interface. The dodecanoic acid presence in the organic phase was increased, but higher in the SFs with Triton X-100. In the interface, the addition of PPG increased the dodecanoic acid concentration in there, but the Triton X-100 decreased it. Therefore, it seems that the action of the PPG is put the 1-dodecanol and the dodecanoic acid in the interface and Triton X-100 helps the transfer between the aqueous and organic phase. In conclusion, for the surfactant PPG, the best volume to perform the bioconversion is in 1L, because it was in there that was achieved the higher 1-dodecanol concentration in organic phase. Relative with the Triton X-100 the 500mL SFs there are a plateau with the pcl total between 24hours and 48hours.

E.coli pGEc47ΔJ bioconversion of *n*-dodecane in 1L SFs.

It was repeated the same experience that the previous one but only using only 1L SFs and during until 30hours. The decision of the time was because of the lack of the target product at

48hours. Besides it was performed an *E.coli* pGEc47ΔJ *n*-dodecane bioconversion without the inducer (DCPK) during 30hours. This was done to observe the effect of bioconversion of *n*-dodecane in cell density and in the evaporation rate (Figure 31). Obviously, the cell density is higher although the presence of *n*-dodecane, indicating a low toxicity of *n*-dodecane. Therefore, when the bioconversion occurs the products produced seems to be toxic to the cells. Observing the Figure 31, it can be taken several interesting observations. Visually, after 30hours of fermentation, the evaporation rate is higher in the follow sequence: normal culture condition, culture with PPG, culture with Triton X-100 and normal culture condition without DCPK. Another, parameter visually prominent is the interface formation. The interface fraction is higher is this sequence: culture with Triton X-100, normal culture condition without DCPK, culture with PPG and normal culture condition. About the evaporation rate it is clear that the presence of surfactants help to reduce, but diminishing the surface tension and from the 1L SFs without DCPK shows that when the 1-dodecanol evaporates carries the *n*-dodecane, the substrate explaining the low 1-dodecanol formation in SFs in normal conditions. About culture with Triton X-100, this created a white emulsion of the culture, improving the contact of *n*-dodecane with alkane hydroxylase system. In conclusion, what stunts this system is the lack of control of the evaporation rate

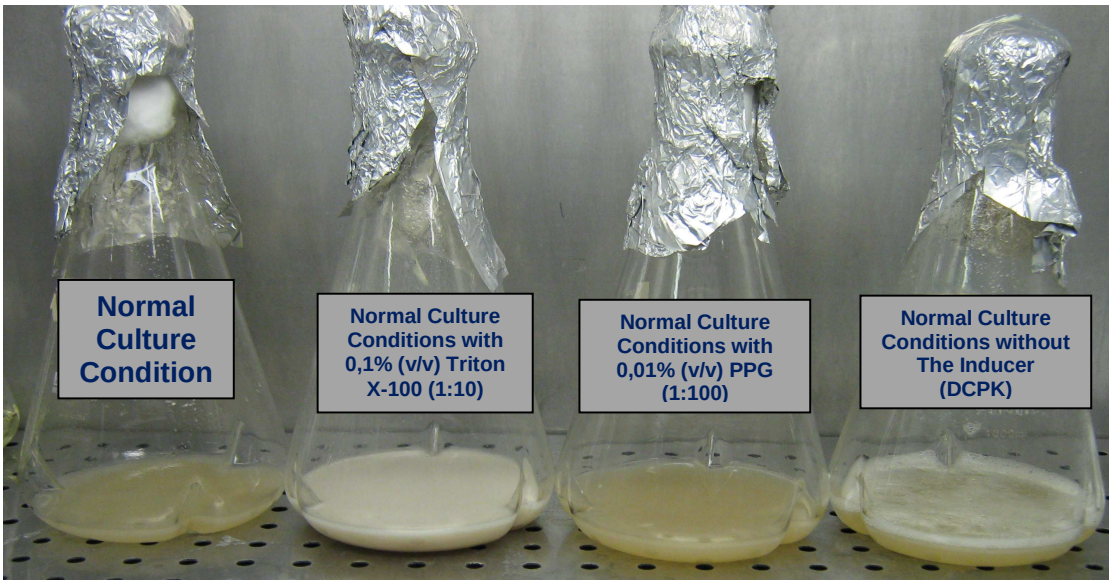

Figure 31: 1L SFs with the different culture conditions after 30hours. In this picture is clear the importance of be concern with the evaporation rate and the formation of emulsion..

E.coli pGEc47ΔJ *n*-dodecane bioconversion in MTPs

After the bioconversion in SFs it was decided to do the bioconversion of *n*-dodecane in 24-DSW MTPs The first attempt was to do the E.coli pGEc47ΔJ n-dodecane bioconversion in 24-DSW MTP covered by a gas permeable membrane in the thermomixer at 1000rpm and with a 3mm of throw diameter inside of the incubator to maintaining the temperature (37℃) constant for 24h. No

data was collected because the excessive turbulency, splashing and elevated evaporation rate. Nevertheles, samples from the organic phase of all wells were collected and analysed, but any product were there. Therefore, the *E.coli* pGEc47ΔJ bioconversion of *n*-dodecane did not occur in the conditions above. For solving the problem there are several hypotheses. One could be diminished the agitation rate, increase the throw diameter or use other type of cover for the 24-DSW MTP, like the Duetz System.

E.coli pGEc47ΔJ *n*-dodecane bioconversion in MTPs using the Duetz System

The E.colipGEc47ΔJ bioconversion of *n*-dodecane occurred in a 24-DSW MTP with the Duetz System during 48hours. It was tested the effects of the addition of surfactants (PPG and Triton X-100) in the product formation compared with the normal condition in that two different types of sandwich cover (soft spongy white silicone layer (A) and rigid black impermeable layer(B)). It was important to verify several parameters and conditions like if sandwich cover prevented spillage of the culture fluid during orbital shaking and ensured that exchange of headspace air is sufficient and occurs solely through the center holes and if that holes were not closed. Besides that it was also desirable to determine which sandwich cover provides the best product formation. Moreover, the key was to establish which culture conditions present the highest product formation.

The first observation is that was obtained more dodecanoic acid, in all culture conditions, than 1-dodecanol (which is the target product). The second is that the product disappears along with time. At 48hours there is no dodecanoic acid. These observations occurred in both sandwich covers. Moreover, the cell density (in both sandwich cover) was higher when the surfactants were added, revealing that the surfactant concentrations used were not toxic for the cells and the formation of interface is equal in all conditions.

In soft spongy white silicone layer of sandwich cover (A), the formation either 1-dodecanol either dodecanoic acid was higher in the organic phase than in the interface, in all culture conditions. However, in both phases the dodecanoic acid concentration was considerable higher than 1-dodecanol. The highest 1-dodecanol concentration was achieved with Triton X-100 (0,02g/L at 24hours). About the evaporation rate the wells with surfactant had in average 12%(v/v) and the wells in normal conditions had 16%(v/v). The interface formation was higher in the wells with normal conditions and with PPG 10%(v/v). In rigid black impermeable layer (B), there was a most high production of dodecanoic acid in organic phase, but 1-dodecanol was only in the organic phase in the wells with the normal culture conditions and with PPG and mainly in those with Triton X-100. Both 1-dodecanol and dodecanoic acid were in lower concentrations in the interface in comparison with the organic phase. The highest 1-dodecanol was achieved with Triton X-100 (0,3g/L at 48hours). The higher evaporation rate occurred in the wells with PPG, it was also in these wells that the interface formation was the highest. The low evaporation rate was with Triton X-100. The fact that the interface formation was higher in the wells without Triton X-100 is surprising accordingly with the pictuce of the SFs (Figure 31).

In a overall perspective the sandwich cover A had, in average, 13% (v/v) of evaporation rate and 10% (v/v) of interface formation compared, in average, with 12% (v/v) in the sandwich cover B and 11% (v/v) of interface formation. In summary, the evaporation rate and the interface formation are similar between phases. However, the addition of surfactants reduces the evaporation rate by decreasing the surface tension.

In conclusion, the addition of surfactants increases the 1-dodecanol formation through Triton X-100 was more efficient. The DCWs were all similar. Related to the choice of sandwich covers that goes to the rigid black impermeable layer, because dodecanoic acid concentration obtained in the organic phase and in the interface is lower (29%) which is fine for the downstream process, however the formation of 1-dodecanol was 46% lower (only considering the concentration in the organic phase) but the evaporation rate was also lower.

Another unexpected conclusion was that the The E.colipGEc47ΔJ bioconversion of *n*-dodecane in a 24-DSW MTP should not during more than 24hours. The fact that the products disappear may be for numerous reasons, one is that as the cell growth was at 37℃ and the boilling point of 1-dodecanol is 24℃ and 44℃ for dodecanoi c acid they evaporate. The same evaporation problem takes place on SFs

E.coli pGEc47ΔJ *n*-dodecane bioconversion in MTPs using Duetz sytem with permeable membranes

The E.colipGEc47ΔJ bioconversion of *n*-dodecane occurred in a 24-DSW MTP, which was covered by gas permeable membrane during 30hours. To ensure a more stability it was used the clamp system from Duetz system (Figure 32), e.g. it was use the Duetz system by instead of using the sandwich covers it was used permeable membrane. It was tested the effects of the addition of surfactants (PPG and Triton X-100) and also the effect of the bottom of the 24-DSW microwell: inverted inverted pyramid bottom (the one used in all other experiences) and half sphere in the product formation compared with the normal condition.

Although a 24-DSW with half sphere bottom mimic was not visualised with the high speed camera, it was jointly used with the inverted inverted pyramid bottom 24-DSW for *E.coli* pGEc47ΔJ bioconversion of *n*-dodecane 24-DSW MTPs. As a spherical bottom DoEs not have any cutting edges it is expected poorest mixing compared with a inverted inverted pyramid bottom. Therefore, in this experience accomplish to compare the method of cover of the MTPs and the difference between MTP bottoms.

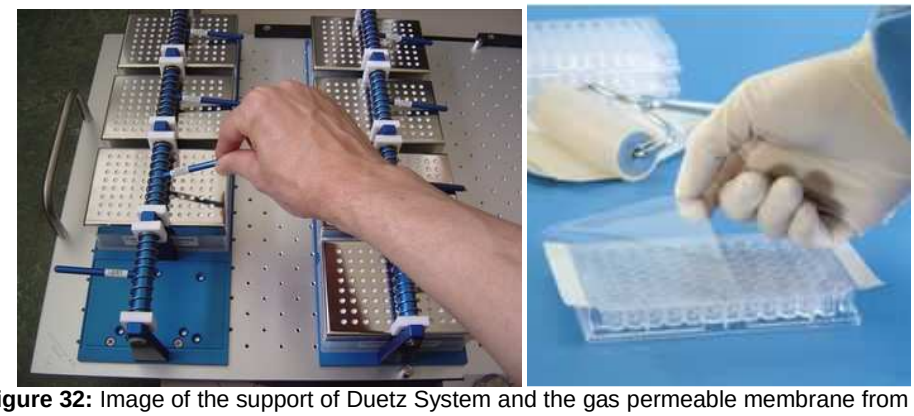

Figure 32: Image of the support of Duetz System and the gas permeable membrane from [3;6]

In the 24-DSW with inverted inverted pyramid bottom and with half sphere the DCW in all wells are similar, confirming again the fact that the surfactant concentration added are not toxic and increase with the fermentation time. In the 24-DSW with inverted inverted pyramid bottom 1-dodecanol was more in the organic phase then in the interface been the wells with Triton X-100 those who had less 1-dodecanol in the interface followed by the wells with normal culture conditions. Over again there was over-expression. In this case there was more dodecanoic acid in the organic phase that 1-dodecanol although in the interface happened the opposite. In the 24-DSW with half sphere bottom happened the same situation. In this the wells with PPG produced either 1-dodecanol or dodecanoic acid in a very small quantity. In the both MTPs the wells were it was verified the highest bioconversion was the ones that did not had any surfactants, inverted inverted pyramid bottom: 0,3g/L at 30hours and half sphere bottom: 0,2g/L at 24hours. In relation with the evaporation rate in this experience it was revealed the imprecision in measuring the volumes in the samples. In conclusion, in this new MTP attach method it is not need to add surfactants and the 24-DSW with the inverted inverted pyramid bottom is the best.

In summary, there was a higher bioconversion of *n*-dodecane into 1-dodecanol in the SFs, but assuming the maximum values, this superiority was three time higher. The addition of Triton X-100 to SFs and 24-DSW (inverted inverted pyramid bottom) with the Duetz system sandwiches cover improve the bioconversion into 1-dodecanol, both in the organic phase as in the interface. Although, the system of covering the 24-DSW with gas permeable membrane and put them in Duetz system clamp support, shows that the addition of surfactants is not necessary as, the 1-dodecanol in the organic phase and in the interface is equal or superior that when used Triton X-100 or PPG. A fact interesting is that the addition of PPG did not increase the bioconversion and its action is to put the product in the interface. About the over-expression, dodecanoic acid it is assumed in the organic phase and in the interface of all the different scales and conditions. The dodecanoic acid concentration is even higher or equal than the 1-dodecanol concentration in the major of the conditions. Therefore, the presence of dodecanoic acid can not be

ignoring.The over-expression of 1-dodecanol could be explain by the poor solubility of the *n*-dodecane in aqueous phase reduces access of the *n*-dodecane in the active site and so favors the conversion of the 1-dodeacnol to dodecanal (aldehyde) due to enhanced enzyme access to the more water soluble 1-dodecanol. Dodecanal is then rapidly converted to dodecanoic acid, shifting equilibrium to favour further dodecanal production.

Consequently, the interface is an important part in this two-liquid phase system as, it has product concentrations comparable with the organic phase.

Application of Design Expert (DoE)

Application of DoE on *E.coli* pGEc47ΔJ bioconversion of *n*-dodecane

Use of Design of experiences (DOE) enables the quality of information gained from an experience to be maximised whilst allowing the number of experiences to be minimised. It is a statistical approach to designing experiences which, rather than investigating one factor at a time, studies multiple factors simultaneously around a defined centre point. As well as speeding up the experienceation process, varying multiple factors simultaneously enables interactions between factors to be detected, which is not possible by the traditional method of investigating one factor at a time.

The DOE design for a given situation is dependant on the objective, number of factors and the expected noise (inherent variability) of the dataset. There are various options available. A 2-level full factorial design studies each factor over two levels (high and low) in combination with the high and low points of all other factors. The number of runs required to run such a design is the square of the number of factors (e.g. 3 factors = 3^2 = 8 runs). Normally, a number of centre-points, 4-6 would be necessary to predict the curvature of any relationships found and to give an indication of the inherent noise of the dataset.

The statistical power of the DoE design can be adjusted to suit the objective; if looking to screen many factors to rule out those which are unimportant, a 2-level fractional factorial is probably most suitable. A fractional factorial design will test only a certain fraction of the total possible combinations of high and low factors. The result is less experiences but that there will be aliased terms that may require follow up if an aliased term generates a significant response. If the objective is to optimise a process, a full factorial design at the least is recommended. It may even be desirable to study the factors over more than 2 levels, this is achieved by a response surface model.

Table 5: It is shown DCW (g/L), 1-dodecanol and dodecanoic acid concentrations (g/L) in organic phase and in the interface, the evaporation rate (% (v/v)) and interface formation (% (v/v)) in all the experiences realised in this section. The numbers in red are the evidence of the imprecision of measuring the volumes in the samples.

									Piramyd bottom						Duetz System with gas permeable membrane					
									Duetz System_ Sandwich Cover: A			Duetz System_ Sandwich Cover: B			Piramyd bottom 			Half Sphere Bottom 		
	Time Points (h)	1L SF	1L SF - DCPK	1L SF + PPG	1l SF +Triton X-100	500mL SF	500mL SF + PPG	500ml SF +Triton X-100	24-DSW	24-DSW+ PPG	24-DSW +Triton X-100	24-DSW	24-DSW+ PPG	24-DSW + Triton X-100	24-DSW	24-DSW+ PPG	24-DSW Triton X-100	24-DSW	24-DSW + PPG	24-DSW +Triton X-100
DCW (g/L)	6	1,6±0,6	3,3±1,3	0,6±1,1	1,2±1,3	0,8	0,7	0,2	n/a	n/a	n/a	n/a	n/a	n/a	3,6±2,0	3,6±1,9	7,3±2,6	4,9±1,7	3,0±0,5	3,6±4,0
	24	2,1±0,1	2,9±0,5	0,8±3,4	2,2±3,5	1,1	1,7	1,2	1,6±0,1	1,8±0,6	1,9±0,3	1,7±0,5	1,7±0,1	2,6±0,2	4,1±0,2	3,4±0,9	4,8±2,0	6,5±2,2	7,5±2,2	4,2±1,2
	30	2,3±0,4	3,9±1,2	1,7±2,9	2,8±3,3	1,6	1,6	1,0	n/a	n/a	n/a	n/a	n/a	n/a	7,0±1,7	7,8±3,7	5,1±1,3	6,2±2,3	6,6±3,6	4,1±0,2
	48	1,5±0,2	n/a	1,3±0,7	0,8±1,0	1,6	1,7	1,3	2,1±0,3	2,2±0,4	3,6	1,7±0,3	1,9±0,1	2,9±0,2	n/a	n/a	n/a	n/a	n/a	n/a
1_Dodecanol (g/L) (Organic Phase)	6	0	0	0	0	0	0	0	n/a	n/a	n/a	n/a	n/a	n/a	0	0	0	0,06	0	0,02
	24	0	0	0	0,2	0,08	0	0,8	0,004±0,003	0,007	0,02±0,01	0,003	0,005	0,01±0,27	0,04±0,002	0,03±0,08	0,05±049	0,2±0,2	0,09±0,08	0,1±0,06
	30	0,04	0	0,08	0,3	0,2	0,01	0,8	n/a	n/a	n/a	n/a	n/a	n/a	0,3±0,6	0,1±0,04	0,3±0,1	0,2±0,07	0,05±0,09	0,1±0,05
	48	0,2	n/a	0,3	0,8	0	0	0,006	0	0	0	0	0	0,3±0,3	n/a	n/a	n/a	n/a	n/a	n/a
1_Dodecanol (g/L) (Interface)	6	0	0	0	0	0,006	0	0,2	n/a	n/a	n/a	n/a	n/a	n/a	0	0	0	0	0	0
	24	0,01	0	0,01	0,06	0	0	0,5	0	0	0	0	0	0,004±0,003	0,04±0,001	4,1±0,2	0,02±0,02	0,6±0,5	0,4	0,2±0,1
	30	0,03	0	0	0,2	0,050	0,04	0,007	n/a	n/a	n/a	n/a	n/a	n/a	0,02	0,06±0,01	0	0,7±0,2	0,2±0,2	0,1±0,04
	48	0,07	0	0,4	0,2	0	0,09	0	0	0	0,01±0,01	0	0	0,008	n/a	n/a	n/a	n/a	n/a	n/a
Dodecanoic Acid (g/L) (Organic Phase	6	0,01	0	0,07	0,1	0,02	0,04	0,05	n/a	n/a	n/a	n/a	n/a	n/a	0,5±0,04	1,9±0,07	0,1±0,01	0,1±0,07	0	0,04
	24	0	0	0,004	03	0	0	0,8	0,04±0,04	0,2	0,7±0,3	0,2±0,2	0,2	0,5±0,4	0,1±0,03	0,09±0,05	0,1±0,04	0,6±0,3	0,08±0,06	0,5±0,1
	30	0	0	0,02	0,4	0	0,02	0,4	n/a	n/a	n/a	n/a	n/a	n/a	0,4±0,2	0,3±0,2	0,7±0,4	0,5±0,1	0,09±0,07	0,3±0,08
	48	0	0	0,002	0	0	0	0	0	0	0	0	0	0	n/a	n/a	n/a	n/a	n/a	n/a
Dodecanoic Acid (g/L) (Interface)	6	0,07	0	0,06	0,01	0,04	0,05	0	n/a	n/a	n/a	n/a	n/a	n/a	0	0	0,04±0,03	0	0	0,06±0,02
	24	0	0	0,6	0	0	0,8	0	0,01	0,03±0,01	0,4	0,02	0,03	0,09±0,01	0,02±0,003	0,04±0,004	0,04±0,01	0,4±0,2	0,04±0,03	0,2±0,07
	30	0	0	0,8	0	0,02	0,4	0	n/a	n/a	n/a	n/a	n/a	n/a	0,04±0,01	0,05±0,01	0,04±0,02	0,4±0,08	0,1±0,04	0,3±0,1
	48	0	0	0	0	0	0	0	0	0	0	0	0	0	n/a	n/a	n/a	n/a	n/a	n/a
Evaporation Rate (% (v/v))	6								n/a	n/a	n/a	n/a	n/a	n/a	42±16	29±20	43±5	58±8	64±25	58±23
	24								10	6	9	10±9	14	13±14	n/a	n/a	n/a	99±11	98±5	104
	30								n/a	n/a	n/a	n/a	n/a	n/a	n/a	n/a	n/a	105±7	100	100
	48								22±8	17±5	15±1	16±8	14±5	5±4	n/a	n/a	n/a	n/a	n/a	n/a
Interface Formation (% (v/v))	6								n/a	n/a	n/a	n/a	n/a	n/a	0	0	15±15	0	5±3	6±1
	24								11±1	12±10	9±2	9±2	20±6	13±2	6±1	14±6	9±4	5±3	6±1	0
	30								n/a	n/a	n/a	n/a	n/a	n/a	5±2	5±2	6±2	6±1	0	3±1
	48								9±1	9±6	8±3	8±2	8	7	n/a	n/a	n/a	n/a	n/a	n/a

In this work the goal is to discover what is or are the parameter or parameters relevant for enhance the 1-dodecaonol bioconversion and prevent the dodecanoic acid production. Therefore, it was used a powerful tool many times applied in scale-down studies, the design expert (DoE). The variables tested on a 2 level DoE design were:

-Volume of aqueous phase (mL) (min.: 1mL and max.: 3mL);

-Volume of n-dodecane (% (v/v)) ((min.: 9(% (v/vaq)) and max.: 26 (% (v/vaq)));

-Glucose concentration in the medium (g/L) (min.: 5g/L and max.: 15 g/L);;

-Surfactant (Triton X-100) Concentration (% (v/v)) (min.: 0,01(% (v/v)) and max.: 0,2 (% (v/v))).

These variables (inputs) seem those that could affect more the bioconversion. It was accepted all the DoE defaults parameters, like entering the responses it was not established any value for the “Sigma”, “Noise” and “Signal/Noise Ratio, it was only enter the name and the units and it was not established any number the Std Dev and adopted as advanced options: “Analyze as factorial” and POE options as “Use ANOVA Std Dev”.

Therefore, it was necessary to do 16 (2^4) runs (Table 6). Four centre points in the factorial block were used. With the centre points information on curvature is gaining and, enable the inherent system noise to be assessed. Once the data is collated, the Once the data is collated, the first stage in the analysis process is to predict which model best fits the relationship between the factors and each of the responses; i.e linear, quadratic, cubic. Only for a question of simplicity it was previously assumed that these four variables related with each other linearly. However, before do the model, it can be done a pre-analysis of the effects of data and simple scatter plots. This is the way to get a feel of the data before moving on to an in-depth analysis.

It can be done a pre-analysis of effects by making a plot of the response (y axis) versus the input (x axis) and it can be known the diverse correlations (Table 7). However, this is only a preliminary to more throrough analysis using much more sophisticated graphical and statistical tools. It begins with the half-normal plot effects, where the effects to be included in the model must be chosen (Appendix 3). It should start with the largest effect at the right side of the half-normal plot of effects and keep picking from right to left until the lines matches up with the majority of the effects near zero. The Design-Ease adjusts the line to exclusde the chosen effects. At the point where you should stop, this line jumps up, leaving a noticeable gap. In ANOVA analysis values of “Prob>F” less than 0.0500 indicate model terms are significant. Values greater than 0,1000 indicate the model terms are not significant. Therefore, in ANOVA it is known if the model is significant or not. However, it is the 3-D surface plots that helps to indetify the conditions of the parameters where the optimisation of a response is obtain.

Table 6: Inputs and the output obtain by using the culture condition stipulated by the DOE using the Triton X-100 as the surfactant. Aqueous phase: Wubbolts media.

Inputs							Experienceal Outputs					
									Organic Phase		Interface	
Run	Row	Line	Aqueous Phase (mL)	Triton X-100 (% v/v)	Glucose (g/L)	*n*-dodecane (% (v/v))	DCW (g/L)	Evaporation Rate (% (v/v))	1-dodecanol (g/L)	Dodecanoic Acid (g/L)	1-dodecanol (g/L)	Dodecanoic Acid(g/L)
1	A	1	1	0,01	15	9	0,8	0	0	0	0,03	1,1
2	A	2	1	0,2	15	26	0,8	0	0,06	0,4	0,03	0,2
3	A	3	1	0,01	15	26	1,5	4	0,09	0,9	0,08	0,5
4	A	4	1	0,01	5	26	3,2	11	0,2	0,8	0,03	0,1
5	A	5	3	0,2	5	26	2,4	23	0	0	0	0
6	A	6	1	0,2	5	26	2,7	3	0,2	0,3	0,2	0,4
7	B	1	1	0,2	15	9	1,8	11	0	0	0	0
8	B	2	3	0,2	15	26	1,2	0,6	0,02	0,08	0,02	0,04
9	B	3	2	0,11	10	17,5	2,5	15	0	0	0	0
10	B	4	1	0,2	5	9	3,2	15	0	0	0	0
11	B	5	1	0,01	5	9	3,7	14	0	0	0	0
12	B	6	3	0,2	15	9	1,3	3	0,05	0,4	0,04	0,4
13	C	1	3	0,2	5	9	1,7	0,2	0,2	0	0,09	0,4
14	C	2	3	0,01	15	26	1,5	8	0,1	0,3	0,02	0,1
15	C	3	3	0,01	5	26	3,9	15	0,2	0,8	0,02	0,2
16	D	1	3	0,01	5	9	2,2	8,	0	0	0,02	0,1
17	D	2	2	0,11	10	17,5	1,0	3	0	0	0,05	0,8
18	D	3	1	0,11	10	17,5	1,3	9	0	0	0,05	0,9
19	D	4	1	0,01	15	9	1,5	1	0,09	1,0	0,02	0,3
20	D	5	1	0,111	10	17,5	0,5	9	0	0	0,07	1,1

Table 7: Correlation values between the inputs and the responses. The negative signal reveals a indirect relation betweenthe parameters.

Correlation	DCW (g/L)	Evaporation Rate (% (v/v))	1-dodecanol (organic phase) (g/L)	Dodecanoic Acid (organic phase) (g/L)	1-dodecanol (interface) (g/L)	Dodecanoic Acid (interface) (g/L)
Aqueous Phase (mL)	0,051	0,091	0,115	-0,137	-0,159	-0,301
n-dodecane (% (v/v))	0,064	0,109	0,382	0,367	0,238	-0,118
Glucose (g/L)	-0,720	-0,545	-0,274	0,205	-0,107	0,215
Triton X-100 (% v/v)	-0,193	-0,049	-0,08	-0,423	0,174	-0,145

From the 3D surface plots obtained in the DoE (Appendix 3) the ones that give the conclusion are the those from the 1-dodecanol in the organic phase and in the interface (Figure 33 and Figure 34).

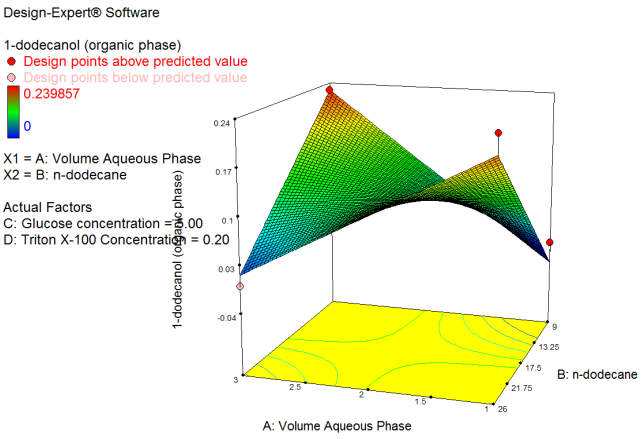

Figure 33: 3D surface plot showing that the higher 1-dodecanol concentration in the organic phase happens in two different situations. The one with maximum aqueous volume and the minimum of the *n*-dodecane. which correspond to higher evaporation rate (figure??). The other is the minimum aqueous volume and the *n*-dodecane maximum addition. The last it is the better conditions.

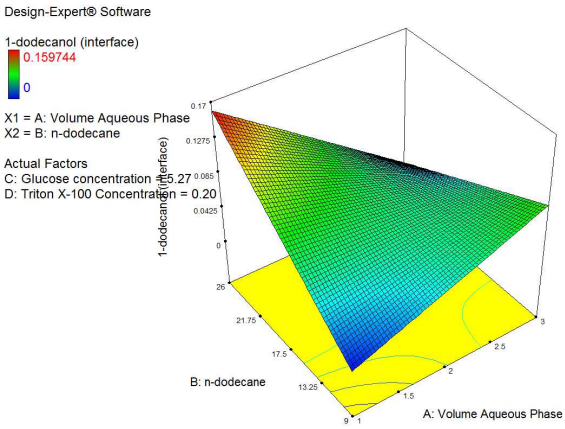

Figure 34: 3D surface plot showing that the highest 1-dodecanol concentration in the interface is reached combining the maximum of *n*-dodecane addition with the minimum of aqueous volume.

The conditions chosen to maximise the bionversion of n-dodecane into 1-dodecanol are: **volume of aqueous phase: 1mL and volume of n-dodecane: 26%(v/v)**

Verification of the DoE design experience

From the assumptions of the DoE it was performed *E.coli* pGEc47 ΔJ bioconversion of *n*-dodecane in 24-DSW MTP with the sandwich cover B (black rigid silicon layer) from The Duetz System during 48hours with DoE conditions and 0,01% of Triton X-100. It was also applied a new method (NW) of extraction at the same time points, where there is no separation of the phases and it is added ethyl acetate (Table 8).

In all the conditions the DCW along the time presents a parabolic curvature and the 1-dodecanol concentration, whatever the phase, is increasing. In the normal procedure of extraction with separation of phases the dodecanoic acid shears the same DCW behavior. In the new method is increasing. Except in the new method the dodecanoic acid concentration is higher in the organic phase and in the interface. Besides, with this method it is possible to rescue more 1-dodecanol and as it is diluted in ethyl acetate, it will be easily recovered. In addition, with the new method less dodecanoic acid is present, being a advantage.

The assumption of the Triton X-100 DoE was that with low volume of aqueous volume and high addition of *n*-dodecane the bioconversion would be improved. Analyzing the concentration of 1-dodecanol in organic phase did not increased, but in the interface that happened.

Table 8: It is shown the DCW (g/L), 1-dodecanol and dodecanoic acid in the organic phase, in the interface and in the new method of the verification experience of the DoE of the Triton X-100.

DCW (g/LTotal)			Dodecanol (g/Ltotal)	Dodecanoic Acid (g/Ltotal)
1,6		5	0,00	0,03±0,01
7,1±0,2	**Organic Phase**	19,5	0,2±0,03	1,8±0,3
6,0±0,2		30	0,2±0,07	1,2±0,2
2,7±0,3		48	0,3±0,07	0,6±0,1
1,6		5	0,004±0,1	0,2±0,2
7,1±0,6	**Interface**	19,5	0,6±0,5	8,5±0,5
6,0±0,4		30	0,4±0,3	5,2±0,5
2,7±0,9		48	0,9±0,1	2,7±0,8
1,8±0,04		5	0,04	0,03±0,0005
7,7±0,4	**NW**	19,5	0,4±0,03	0,3±0,02
6,5±1,0		30	0,9±0,6	0,8±0,5
2,9±1,0		48	1,1±0,7	0,9±0,6

Metrics from diverse E.coli pGEc47ΔJ bioconversion of *n*-dodecane experiences

It is extremely important to know the maximum total product concentration (PCL_{total}) and in which fermentation time for a determine condition where a fermentation is running. Therefore, in Table 9, it is shown the PCL_{total}, time PCL_{total} (h) and the cell density (DCW (g/L) of all the experiences done in this work and from fermentation in the 2l-fermenter with *n*-octane and *n*-dodecane.

Obviously, the Table 9 is crucial for a point a view for have the perspective which are the good and bad conditions or dimensions. And that is significant for the *E.coli* pGEc47ΔJ bioconversion of n-dodecane became industrially applied.

The first observation is that the bioconversion of n-dodecane into 1-dodecanol in the large scale is equal from the 1L SFs with PPG, Duetz system 24-DSW MTP with B sandwich cover where

Triton X-100 was added,24-DSW (inverted inverted pyramid bottom) with the gas permeable membrane with and without Triton X-100 and in the Duetz system 24-DSW with B sandwich cover consequence from the DoE experience with Triton X-100. Although, the 1L SF WITH Triton X-100 produced more 1-dodecanol that the 2L-fermenter (three times higher), faster and formed a plateau between 24hours to 30hours.

The condition that produced more dodecanoic acid in the organic phase was the 24-DSW (half sphere bottom) MTP with the gas permeable membrane with PPG and the Duetz system 24-DSW with B sandwich cover consequence from the DoE experience with Triton X-100.

In the interface, the highest 1-dodecanol concentration was achieved with it is the the 24-DSW (half sphere bottom) MTP with the gas permeable membrane with PPG and dodecanoic acid in the DoE experience with Triton X-100. Therefore, in the MTPs there is a higher tendency to accumulate the products in the interface.

Table 9: Maximum total product concentration (PCL_{total}) (g/L), time of PCL_{total} (h) and DCW (g/L) of all experiences done in this work and from fermentation in the 2l-fermenter with *n*-octane and *n*-dodecane. * This experiences were done before the start of this work. **The culture conditions were 10% (v/v) of Wubbolts media; 5% (v/v) of inoculum; 20% (v/v) of n-dodecane and 0,05% (v/v) of DCPK for the SFs and 0,1% (v/v) DCPK.

		2l-fermenter; *n*-octane; -DCPK *	2l-fermenter; *n*-dodecane; -DCPK *	2l-fermenter; *n*-dodecane; + DCPK *	1L SF + DCPK **	1L SF – DCPK **	1L SF + 0,01% (v/v) PPG (1:100) **	1l SF +0,1% Triton X-100 (1:10) **	500mL SF **	500mL SF + 0,01% (v/v) PPG (1:100) **	500ml SF +0,1% Triton X-100 (1:10) **	24-DSW (inverted inverted pyramid bottom) **	24-DSW (inverted inverted pyramid bottom) + 0,01% (v/v) PPG (1:100) **	24-DSW (inverted inverted pyramid bottom) + 0,1% Triton X-100 (1:10) **	24-DSW (inverted inverted pyramid bottom) **	24-DSW (inverted inverted pyramid bottom) + 0,01% (v/v) PPG (1:100) **	24-DSW (inverted inverted pyramid bottom) +0,1% Triton X-100 (1:10) **	24-DSW (inverted inverted pyramid bottom) **	24-DSW (inverted inverted pyramid bottom) + 0,01% (v/v) PPG (1:100) **	24-DSW (inverted inverted pyramid bottom) +0,1% Triton X-100 (1:10) **	24-DSW (half sphere bottom)**	24-DSW half sphere bottom)+ 0,01% (v/v) PPG (1:100) **	24-DSW half sphere bottom)+0,1% Triton X-100 (1:10) **	24-DSW (inverted inverted pyramid bottom) with TritoX-100 DoE**
												Duetz System: Sandwich Cover: A			Duetz System: Sandwich Cover: B			Duetz System with gas permeable membrane						
ORGANIC PHASE																									
1-dodecanol  [9]	DCW (g/L) at PCL_{tota}	2,4	10,0	10,7	1,5± 0,2		1,3± 0,7	0,8± 1,0	1,6	1,6	1,1± 0,1	1,6± 0,1	1,8± 0,6	1,9±0,3	1,7± 0,5	1,7± 0,1	2,9± 0,2	4,1± 0,2	7,8± 3,7	5,1±1,3	6,4±2,5	7,5±2,2	3,9±2,6	2,7± 0,3
	PCL_{total} (g/L)	0,8	0.3	0.3	0,2		0,3	0,8	0,2	0,01	0,8	0,004± 0,003	0,007	0,02± 0,01	0,003	0,005	0,3± 0,3	0,3± 0,6	0,1±0, 04	0,3±0,1	0,2±0,1	0,09± 0,08	0,1± 0,06	0,3± 0,07
	Time PCL_{total} (h)	11-24	29	48	48		48	48	30	30	24-30	24	24	24	24	24	48	30	30	30	24 -30	24	24-30	48
Dodecanoic Acid  [11]	DCW (g/L) at PCL_{tota}				1,6± 0,6		0,6± 1,1	2,8± 3,3	0,8	0,7	1,2	1,6±0,1	1,8± 0,6	1,9± 0,3	1,7± 0,5	1,7± 0,1	2,6± 0,2	3,6± 2,0	3,6±1, 9	5,1±1,3	6,5±2,2	6,6±3,6	4,2±1,2	7,1± 0,2
	PCL_{total} (g/L)				0,01		0,07	0,4	0,02	0,04	0,8	0,04± 0,04	0,2	0,7± 0,3	0,2±0, 2	0,2	0,5± 0,4	0,5±0, 04	1,9±0, 07	0,7±0,4	0,6±0,3	0,09± 0,07	0,5±0,1	1,8±0, 3
	Time PCL_{total} (h)			48	6		6	30	6	6	24	24	24	24	24	24	24	6	6	30	24	30	24	19,5
INTERFACE																									
1-dodecanol  [9]	DCW (g/L) at PCL_{tota}				1,5± 0,2		1,3± 0,7	1,8± 2,2	1,6	1,7	0,2						2,6± 0,2	7,0± 1,7	3,4± 0,9	4,8± 2,0	6,2±2,3	7,5±2,2	4,2±1,2	2,7± ,9
	PCL_{total} (g/L)				0,07		0,4	0,2	0,05	0,09	0,2						0,004± 0,003	0,02	4,1± 0,2	0,02± 0,02	0,7±0,2	0,4	0,2±0,1	0,9± 0,1
	Time PCL_{total} (h)				48		48	30 - 48	30	48	6						24	30	24	24	30	24	24	48
Dodecanoic Acid  [11]	DCW (g/L) at PCL_{tota}				1,6± 0,6		1,7± 2,9	1,2± 1,3	0,8	0,7		1,6± 0,1	1,8± 0,6	1,9±0,3	1,7± 0,5	1,7± 0,1	2,6±0,2	7,0± 1,7	3,4± 0,9	5,7± 2,0	6,4±2,3	6,6±3,6	4,1±0,2	7,1± 0,6
	PCL_{total} (g/L)				0,07		0,8	0,01	0,04	0,05		0,01	0,03±0, 01	0,4	0,02	0,03	0,09± 0,01	0,04± 0,01	0,04± 0,004	0,04± 0,02	0,4±0,1	0,1±0,04	0,3±0,1	8,5± 0,5
	Time PCL_{total} (h)				6		30	6	6	6		24	24	24	24	24	24	30	24	6-30	24-30	30	30	19,5

Conclusion

This work was about the qualitative characterisation of mixing in order to develop a scale-down approach for a two-liquid phase bio-oxidation reaction.

A qualitative characterisation of mixing visualisation of fluid hydrdynamics in 2L-fermenter, 500mL, 1LSfs, 24-DSW and 24-SRW mimics. In all these vessels the visualisation of the *n*-dodecane droplets was difficult.

In the 2L-fermenter there was observed that mass transfer limitations are present, as only after 24 hours the two-liquid media is completely emulsified. In the hope of solve this limitation it was added to the 2L-fermenter PPG, which is a emulsification agent, but its action was inconclusive, could be beneficial (due to increased liquid-.liquid interface) or detrimental (due to increased resistance) to mass transfer.

In SFs the visualisation of the fluid hydrodybanmics was by changing the throw diameter and the agitation rate. In this part it was analysed in the SFs the behavior of 10%(v/v) of Wubbolts media and 20% (v/v) at 25mm and 50mm of throw diameter. In both cases when the agitation rate was to high the formation of foaming and the turbulency was very elevated. In the SFs there was the problem of distinguishing a *n*-dodecane droplet from a air bubble. It was verified that the liquid motion was similar between the 500mL and 1L SFs. Therefore, for the 25mm throw diameter it was decided that 250rpm was a “ideal” agitation rate as provide enough turbulency for a good oxygen-mass transfer and the liquid heigth was not possible to wet the cotton cover. The same reasons determine the 150rpm “ideal” agitation rate for 50mm.

In the MTPS, it was used 24-DSW and 24-SRW mimics. The last was considered inadequated. It was concluded that as the throw diameter diminishe the thee turbulency is higher and the mixing is becaming better. However, with the addition of Triton X-100, a nonionic surfactant, a complete and homogenous two-liquid phase was achieved. Normally, durin a fermentation the cells release active-surface substances, therefore it was tested the effect of the addition of the emulsion (biosurfactant) to the media and the use of the fermentation broth. The conclusion was that the broth helped more than the biosurfactant, but the last improved more the mixing compared with those wells with the standard conditions.

Therefore, the major conclusion is that it was possible obbtain a homogenous phase in this system with the addition of chemical surfactant, which before it was not known. And so, allow the development of a scale-down approach.

As a result it was performed *E.coli* pGEc47ΔJ *n*-dodecane bioconversion in mini-bioreactors. SFs and MTPs. In MTPs is was tested two types of covers: Duetz system and a new and innovative system developed in this work, which consist in cover the MTPs with the usually used gas permeable membrane but they were put in the Duetz system clamp support. The last was testes in 24-DSW with inverted inverted pyramid and half sphere bottoms. In all the vessels it was

observed over-expression of the pGEc47ΔJ plasmid. Even the dodecanoic acid concentrations both in the organic phase and in the interface were higher than 1-dodecanol.

It was tested the effects of adding surfactants: PPG and Triton X-100. The addition of Triton X-100 to SFs and 24-DSW (inverted inverted pyramid bottom) with the Duetz system sandwiches cover improve the bioconversion into 1-dodecanol, both in the organic phase as in the interface. In the Duetz system it was tested 2 types of sandwich covers: soft spongy white silicone layer (A) and rigid black impermeable layer (B). The conclusion obtain was it is preferable use the B sandwich cover, because the dodecanoic acid concentration was lower also the evaporation rate and that in the Duetz system the bioconversion occurred only 24hours. In the innovative incubation process, the astonishing conclusion is that is not necessary to add surfactants to get good products concentrations. Obviously, the inverted inverted pyramid bottom 24-DSW was where the high yield was acquired.

From DoE design it was discovered that the 1-doddecanol concentration in both phase, organic and interface, reach the higher with the lowest aqueos volume (1mL) and the highest addition of n-dodecane (26 %(v/v)). It was done a verification experience with the normal concentration of Triton X-100, 1mL of Wubbolts media and 20% (v/v) of *n*-dodecane. In this it was concluded that the concentration of 1-dodecanol only improved in the interface. In this same experience, it was tried a new method of extraction. This consists in add ethyl acetate to the sample without any separation of phases. The goal was to extract the products from all the phases. With this method it was possible to recuver more 1-dodecanol and dodecanoic acid.

A overwhelming observation is that in all the different scales the concentrations of dodecanoic acid in both phases is equal or superior, which consist a problem. The reason for the over-expression of 1-dodecanol could be explain by the poor solubility of the *n*-dodecane in aqueous phase reduces access of the *n*-dodecane in the active site and so favors the conversion of the 1-dodeacnol to dodecanal (aldehyde) due to enhanced enzyme access to the more water soluble 1-dodecanol. Dodecanal is then rapidly converted to dodecanoic acid, shifting equilibrium to favour further dodecanal production.

Another crucial problem is the high evaporation rate, which leads to a loss of the 1-dodecanol. As the incubator is at 37℃ if the evapo ration rate is high there is loss of 1-dodecanol for the atmosphere. To avoid that it can turn to addition of surfactants, or use humidified atmosphere to increase the liquid pressure as a example of the several possibilities. Perhaps, it is the evaporation rate the reason that it was found more dodecanoic acid.

As was concluded since the beginning, by alanlysing the interface, in this two-liquid-phase it is necessary to count with the interface. Although, the recovery of the 1-dodecanol and/or dodecanoic acid is more difficult than in the organic phase, where, for example, a distillation could easly separate the two.

In conclusion, a scale-down approach was done as the bionversion yield of 1-dodecanol is equal in many conditions in SFs and MTP and superior in 1L Sf with 0,1 % (v/v) Triton X-100 (1:10).

Future Work

In order to perform a more accurate qualitative or quantitative characterisation of the mixing the solution, in particular, in SFs it goes by using a contrast substance, which has affinity for the *n*-dodecane combined with an Optical Reflectance Measurement (ORM).

The different 1-dodecanol and dodecanoic acid coefficient partition from aqueous phase, interface and organic phase to the ethyl acetate, for the extraction method, to aqueous phase-organic phase, aqueous phase-interface, interface-organic phase should be determined. With these values it facilitated the sample treatment as well as it will eliminate the inaccuracy of measuring the three phase volumes and a mass transfer model of this two-liquid system could be done. Other parameter that should be established is the optimal ethyl acetate volume to add in order to get a high extraction yield.

The method of quantification of the organic compounds in this work could also change. It could be used a gradient of solvents in the GC analysis or simply analyse the samples on HPLC

In the future DoE designs will certainly intensly be used in the optimisation of culture conditions and extraction methods.

About the overoxidation is caused by conversion to aldehyde by *alk*B and rapid conversion to dodecanoic acid by alkH. Therefore, must be removed.

References

Aires-Barros M. R. and *et. al*.. 2003. *Chapter 6: Biocatálise em meios não-convencionais*. Enzenharia Enzimática. Lidel-Edições Técnicas, Lda.

Ayala M., and *et. al*.. 2004. *Enzymatic activation of alkanes: constraints and prospective*. Applied Catalysis A: General, **272**: 1–13.

Betts J.I. and et. al. 2006. *Miniature bioreactors: current practices and future opportunities* Microbial Cell Factories, 2006, **5**: 1-14.

Bognolo G. 1999. *Biosurfactants as emulsifying agents for hydrocarbons*. Colloids and Surfaces A: Physicochemical and Engineering Aspects, **152**: 41–52.

Büchs J. and *et. al*.. 2007. *Calculating liquid distribution in shake flasks on rotary shakers at waterlike viscosities*. Biochemical Engineering Journal, **34**: 200–208.

Chan E-C, and *et. al*.. 1991. *Stimulation of n-alkane conversion to dicarboxylic acid by organic solvent- and detergent-treated microbes*. Appl. Microbiol Biotechnol, **34**: 772-737.

Chen Q, and *et. al*..1996. *Physiological Changes and alk Gene Instability in Pseudomonas oleovorans during Induction and Expression of alk Genes*. Journal of Bacteriology, **178**: 5508–5512.

Chen Q., and *et. al*.. 1995. *Effects of octane on the fatty acid composition and transition temperature of Pseudomonas oleovorans membrane lipids during growth in two-liquid-phase continuous cultures*. Enzyme and Microbial Technology, **17**:647-652.

Cull S.G and *et. al*.. 2002. *Scale-down studies on the hydrodynamics of two-liquid phase biocatalytic reactors*. Bioprocess Biosyst Eng, **25** 143–153.

Doig S. D. and *et. al*.. 1998. *A Membrane Bioreactor for Biotransformations of Hydrophobic Molecules*. Biotechnology and Bioengineering, **58**: 587-594.

Duetz W. A. and *et. al*.. 2001. *Using proteins in their natural environment: potential and limitations of microbial whole-cell hydroxylations in applied biocatalysis*. Current Opinion in Biotechnology, **12**: 419–425.

Duetz W. A.. 2007. *Microtiter plates as mini-bioreactors: miniaturization of fermentation methods*. TRENDS in Microbiology, **15**:469-475.

Duetz, W.A. and *et. al*.. 2000. *Methods for intense aeration, growth, storage, and replication of bacterial strains in microtiter plates*. Appl. Environ. Microbiol, **66**: 2641–2646.

Eggink G. and *et. al*..1987. *Controlled and Functional Expression of the Pseudomonas oleouorans Alkane Utilizing System in Pseudomonas putida and Escherichia coli*. The Journal of Biological Chemistry, **262:** 17712-17718.

Eggink G.S and *et. al*.. 1988. *Alkane Utilization inP seudomonas oleovorans: Structure and function of the regulatory locus alkR*. The Journal of Biological Chemistry, **263**: 13400-13405.

Favre-Bulle O. and *et. al*..1993. *Continuous Bioconversion of n-Octane to Octanoic Acid by Recombinant Escherichia coli (alk+) Growing in a Two-Liquid-Phase Chemostat.* Biotechnology and Bioengineering, **41**: 263-272.

Fonseca M.M. and Teixeira J. A. 2007. Chapter 4:Transferência de massa. Reactores Biológicos. Lidel – edições técnicas, lda.

Funhoff E.G. and *et. al*.. 2006. *CYP153A6, a Soluble P450 Oxygenase Catalyzing Terminal-Alkane Hydroxylation*. Journal of Bacteriology, **188**: 5220–5227.

Funke M. and *et. al*.. 2009. *The Baffled Microtiter Plate: Increased Oxygen Transfer and Improved Online Monitoring in Small Scale Fermentations*. Biotechnology and Bioengineering, **103**: 1118-1128.

Hoekstra, and et. al. 1976, B. *Release of outer membrane fragments from normally growing Escherichia coli. Biochim. Biophys. Acta*, **455:** 889–899.

Kok M and *et. al*.. 1989. *The Pseudomonas oleovorans Alkane Hydroxylase Gene Sequence and Expression*. The Journal of Biological Chemistry, **264**: 5435-5441.

Kollmer A. 1997. *Verfahrenstechnische Aspekte bei zwei-flüssing-phasigne Bioprozessen*. PhD thesis, Eidgeno□sische Technische Hochschule, Zürich, Switzerland.

Kollmer A and *et. al*.. 1999. *On liquid-liquid mass transfer in two-liquid-phase fermentations*. Bioprocess Engineering, **20:** 441-448.

Laane C and *et. al*.. 1987. *Rules for Optimization of Biocatalysis in Organic Solvents*. Biotechnology and Bioengineering, **30**: 81-87.

Lye G. J. and *et. al*.. 2003. *Accelerated design of bioconversion processes using automated microscale processing techniques.* TRENDS in Biotechnology, **21**: 29-37.

Lye G.L. and *et. al*.. 2001. Chapter 5: Advances in the selection and design of two-liquid phase biocatalytic reactors, Muliphase Bireactor Design, Taylor & Francis.

Mathys R. G., and *et. al*.. 1999. *Integrated Two-Liquid Phase Bioconversion and Product-Recovery Processes for the Oxidation of Alkanes: Process Design and Economic Evaluation*. Biotechnology and Bioengineering, **64**: 459-477.

Micheletti M. and *et. al*.. 2006. *Fluid mixing in shaken bioreactors: Implications for scale-up predictions from microlitre-scale microbial and mammalian cell cultures*. Chemical Engineering Science, **61**: 2939–2949.

Panke S., and *et. al*.. 1999. *An Alkane-Responsive Expression System for the Production of Fine Chemicals*. Applied and Environmental Microbiology, **65**: 2324–2332.1999.

Pavia D. and *et. al*.. 2006. *Introduction to Organic Laboratory Techniques*. Thomson Brooks/Cole.

Rojo F.. 2005. *Guest Commentaries. Specificity at the End of the Tunnel: Understanding Substrate Length Discrimination by the AlkB Alkane Hydroxylase.* Journal of Bacteriology, **187**: 19–22.

Rothen S. A., and *et. al*.. 1998. *Growth Characteristics of Escherichia coli HB101[pGEc47] on Defined Medium*. Biotechnology and Bioengineering, **58**: 92-100.

Schmid A and *et. al*.. 1998. *Developments towards large-scale bacterial bioprocesses in the presence of bulk amounts of organic solvents*. Extremophilos **2**: 249-256.

Schmid A. and *et. al*.. 1998. *Medium Chain Length Alkane Solvent-Cell Transfer Rates in Two-Liquid Phase, Pseudomonas oleovorans Cultures*. Biotechnology and Bioengineering, **60**: 10-23.

Schmid A. and *et. al*.. 1999. *Development of equipment and procedures for the safe operation of aerobic bacterial bioprocesses in the presence of bulk amounts of flammable organic solvents*. Bioprocess Engineering **20**: 91-100.

Schmid A., and *et. al*.. 1998a. *Effects of biosurfactant and emulsification on two-liquid phase Pseudomonas oleovorans cultures and cell-free emulsions containing n-decane*. Enzyme and Microbial Technology, **22**: 487–493.

Setti L. and *et. al*..1995. *Surface Tension as a Limiting Factor for Aerobic n-Alkane*. J. Chem. Tech. Biotechnol. **64:** 41-48

Singh A., and *et. al*.. 2007. *Surfactants in microbiology and biotechnology: Part 2. Application aspects*. Biotechnology Advances, **25:** 99–121.

Smet M-J and *et. al*..1981. *Synthesis of 1,2-Epoxyoctane by Pseudomonas oleovorans During Growth in a Two-Phase System Containing High Concentrations of 1-Octene*. Applied and Environmental Microbiology, **42**: 811-816.

Smits T. H. M. and *et. al*.. 2003. *Functional characterization of genes involved in alkane oxidation by Pseudomonas aeruginosa*. Antonie van Leeuwenhoek, **84**: 193–200.

Smits T. H. M., and *et. al*.. 1999. *Molecular screening for alkane hydroxylase genes in Gram-negative and Gram-positive strains*. Environmental Microbiology, **1**: 307—317.

Staijen I. E and *et. al*.. 2000. *Expression, stability and performance of the three-component alkane mono-oxygenase of Pseudomonas oleovorans in Escherichia coli.* Eur. J. Biochem, **267**: 1957-1965.

Staijen I. E. and *et. al*.. 1998. *Synthesis of Alkane Hydroxylase of Pseudomonas oleovorans Increases the Iron Requirement of alk+ Bacterial Strains*. Biotechnology and Bioengineering, **57**: 228-237.

Staijen I.E. and *et. al*.. 1997. *The AlkB monooxygenase of Pseudomonas oleovorans Synthesis, stability and level in recombinant Escherichiu coli and the native host*. Eur. J. Biochem, **244**: 462-470.

van Beilen J. B and *et. al*.. 2001. *Analysis of Pseudomonas putida alkane degradation gene clusters and flanking insertion sequences: evolution and regulation of the alk genes.* Microbiology, **147**: 1621–1630.

van Beilen J. B. and *et. al*. 2005. *Identification of an Amino Acid Position That Determines the Substrate Range of Integral Membrane Alkane Hydroxylases*. Journal OF Bacteriology, **187:** 85–91.

van Beilen J. B. and *et. al*.. 2005. *Expanding the alkane oxygenase toolbox: new enzymes and applications*. Current Opinion in Biotechnology, **16**: 308–314.

van Beilen J. B. and *et. al*.. 2007. *Alkane hydroxylases involved in microbial alkane degradation.* Appl Microbiol Biotechnol **74**:13–21.

van Beilen J. B., and *et. al*.. 1994. *Genetics of alkane oxidation by Pseudomonas oleovorans*. Biodegradation, **5**: 161-174.

van Beilen J.B and *et. al*.. 2003. *Practical issues in the application of oxygenases*. TRENDS in Biotechnology, **21**: 170-177.

Van Beilen J.B and *et. al*.. 2004. Chapter 14: Alkane Degradation by Pseudomonads. Pseudomonas: Biosynthesis of Macromolecules and Molecular Metabolism. Klumer Academic/Plenum Piblishers.

Van Hamme J. D. and *et. al*.. 2006. *Physiological aspects Part 1 in a series of papers devoted to surfactants in microbiology and biotechnology.* Biotechnology Advances, **24**: 604–620.

Wentzel A., and *et. al*.. 2007. *Bacterial metabolism of long-chain n-alkanes*. Appl Microbiol Biotechnol, **76**:1209–1221.

Wubbolts M.G. and *et. al*.. 1996. *Biosynthesis of Synthons in Two-Liquid-Phase Media*. Biotechnology and Bioengineering, **52:** 301-308.

Zhang H. and *et. al*.. 2008. *Engineering characterisation of a single well from 24-well and 96-well microtitre plates*. Biochemical Engineering Journal, **40**: 138–149.

Web Sites

1. http://www.apczech.cz/pdf/DF-Novaspec-Plus.pdf
2. http://www.sigmaaldrich.com/

3. http://www.enzyscreen.com/Manual_system_duetz_May_2008.pdf
4. http://www.emsdiasum.com/microscopy/products/preparation/plates.aspx
5. http://www.visionresearch.com/
6. http://www.emsdiasum.com/microscopy/products/preparation/plates.aspx
7. http://www.jtbaker.com/msds/englishhtml/d8784.htm
8. http://www.statease.com/dx7descr.html DOE7
9. http://chemicalland21.com/industrialchem/solalc/lauryl%20alcohol.htm
10. http://www.chemblink.com/products/112-40-3.htm
11. http://chemicalland21.com/industrialchem/organic/LAURIC%20ACID.htm
12. http://www.researchandmarkets.com/reports/648687

Appendix

Appendix 1: Method of determination of dry cell weight (DCW) and concentration of 1-dodecanol and dodecanoic acid

1. Determination of total DCW

After the determination of the dry cell pellet in the eppendorfs, this value is divided by its aqueous volume. The unit of this concentration is gL_{aq}^{-1}. However, it is desirable to have a total DCW (gL_{Total}^{-1}.). So, it was used the equation 1.

$$\boldsymbol{DCW\ gL_{Total}^{-1} = DCW\ gL_{aq}^{-1} * \frac{V_{aq}}{V_{Total}}} \qquad \textbf{Equation 1}$$

2. Determination of the concentration of 1-dodecanol and dodecanoic acid

As the standards of dodecanoic acid are prepared with the units g/L, because it is solid and also because is the units that are most wanted. It is necessary to convert the units of the 1-dodecanol standards, as it is liquid and so the units used was % (v/v), for that the equation 2 is used.

$$\boldsymbol{g/L_{1-dodecanol} = 1 - dodecanol\ \%(v/v) * Specific\ mass_{1-dodecanol}\ (g/cm^3) * 10} \quad \textbf{Equation 2}$$

After the GC analysis of the standards it was made a standard curve for 1-dodecanol and other for dodecanoic acid. The standard curves represented the concentration of 1-dodecanol (g/L) or dodecanoic acid (g/L) in order to the coefficient of the GC peak area of 1-dodecanol or dodecanoic acid and the GC peak area of *n*-dodecane. In this way it is eliminated any errors like measuring the volume for the dilutions.

So, throughout the standards curves it was obtained the concentrations of 1-dodecanol and dodecanoic acid in the organic samples or in the interface samples (equation 3 and equation 4).

$$\boldsymbol{1 - Dodecanol\ (g/L_{organic/interface}) = \frac{1-Dodecanol\ Peak\ Area\ (\mu V.s)}{Dodecane\ Peak\ Area\ (\mu V.s)} * \Delta_{1-Dodecanol\ standard\ curve}} \quad \textbf{Equation 3}$$

$$\boldsymbol{Dodecanoic\ Acid\ (g/L_{organic/interface}) = \frac{Dodecanoic\ Acid(\mu V.s)}{Dodecane\ Peak\ Area\ (\mu V.s)} * \Delta_{Dodecanoic\ Acid\ standard\ curve}} \quad \textbf{Equation 4}$$

On the other hand, it is crucial to have these metrics as total metrics. In this step, there is a differentiation between the treatments of the data of the organic samples from the interface samples. For the organic samples the calculation of total 1-dodecanol and dodecanoic acid concentrations is very simple (equation 5 and 6).

$$\boldsymbol{1 - Dodecanol\ (g/L_{Total\ (organic\ phase)}) = 1 - Dodecanol\ (g/L_{organic}) * \frac{V_{organic}}{V_{Total}}} \quad \textbf{Equation 5}$$

$$\boldsymbol{Dodecanoic\ Acid}\ (\boldsymbol{g/L_{Total\ (organic\ phase)}}) = \boldsymbol{Dodecanoic\ Acid}\ (\boldsymbol{g/L_{organic}}) * \frac{\boldsymbol{V_{organic}}}{\boldsymbol{V_{Total}}}\quad \textbf{Equation 6}$$

However, the calculation of the final concentrations are very difficult because it is not known the partition coefficient of 1-dodecanol and dodecanoic acid between the interface and ethyl acetate. The interface is an emulsion of organic and aqueous components. Measurement of the volume of organic liquid "freed" after ethyl acetate addition indicates the relative proportions of aqueous and organic liquid in the interface. Experiments have indicated that his averages to be a 50:50 split of organic and aqueous phase in the interface. So, it was assumed that the interface measured is made up of half organic phase (an assumption based upon measurement of the breakdown following interface extraction) (equation 7 and 8).

$$\boldsymbol{g/L_{Total_{1-dodecanol_{Interface}}}} = \frac{\boldsymbol{1-Dodecanol\ Peak\ Area\ (\mu V.s)}}{\boldsymbol{Dodecane\ Peak\ Area\ (\mu V.s)}} * \frac{\boldsymbol{V_{Ethyl\ Acetate}}}{\boldsymbol{V_{Interface}}} * \frac{\boldsymbol{V_{Interface}}}{\boldsymbol{V_{Total}}} * \boldsymbol{0,5}\quad \textbf{Equation 7}$$

$$\boldsymbol{g/L_{Total_{Dodecanoic\ Acid_{Interface}}}} = \frac{\boldsymbol{Dodecanoic\ Acid\ Peak\ Area\ (\mu V.s)}}{\boldsymbol{Dodecane\ Peak\ Area\ (\mu V.s)}} * \frac{\boldsymbol{V_{Ethyl\ Acetate}}}{\boldsymbol{V_{Interface}}} * \frac{\boldsymbol{V_{Interface}}}{\boldsymbol{V_{Total}}} * \boldsymbol{0,5}\quad \textbf{Equation 8}$$

Appendix 2: DoE Case Study: Fermentation Process Optimisation: Characterisation and Optimisation of Soluble Recombinant Protein Expression in E.coli.

Christopher Grant
Research Engineer
UCL Dept of Biochemical Engineering
Advanced Centre for Biochemical Engineering

Introduction to DoE

Use of Design of experiments (DoE) enables the quality of information gained from an experiment to be maximised whilst allowing the number of experiments to be minimised. It is a statistical approach to designing experiments which, rather than investigating one factor at a time, studies multiple factors simultaneously around a defined centre point. As well as speeding up the experimentation process, varying multiple factors simultaneously enables interactions between factors to be detected, which is not possible by the traditional method of investigating one factor at a time.

The DOE design for a given situation is dependant on the objective, number of factors and the expected noise (inherent variability) of the dataset. There are various options available. A 2-level full factorial design studies each factor over two levels (high and low) in combination with the high and low points of all other factors. The number of runs required to run such a design is the square of the number of factors (e.g. 3 factors = 3^2 = 8 runs). Normally, a number of centre-points, 4-6 would be necessary to predict the curvature of any relationships found and to give an indication of the inherent noise of the dataset.

The statistical power of the DOE design can be adjusted to suit the objective; if looking to screen many factors to rule out those which are unimportant, a 2-level fractional factorial is probably most suitable. A fractional factorial design will test only a certain fraction of the total possible combinations of high and low factors. The result is less experiments but that there will be aliased terms that may require follow up if an aliased term generates a significant response. If the objective is to optimise a process, a full factorial design at the least is recommended. It may even be desirable to study the factors over more than 2 levels, this is achieved by a response surface model.

Introduction to the Expression System

Optimisation of the production of recombinant proteins using expression systems in *E.coli* is often dependent on a myriad of factors which will vary depending on the nature of the protein in question as well as factors such as the expression system and host strain used.

In this study, such an *E.coli* expression system has undergone initial screening, in microwells, of the effect of ten factors on cell density (post induction OD) and protein concentration

(log_{10}yield). From these initial ten, three factors were identified as important: growth agitation, growth period and induction agitation.

DOE goal

The aim of this second screening design is to find the optimum conditions to maximise protein production and to characterise the design space surrounding this optimum so the effect of any deviation from this optimum can be quantified.

The high and low levels of the three factors, growth agitation, growth period and induction agitation, are to be changed in light of the results of the initial screen. Firstly, this will determine whether the optima may lie beyond the levels of the original design space; secondly, it may give an indication of whether any relationship between a factor and a response is linear or experiences curvature.

Optimisation design to be used

A response surface design was employed to confirm the suspected location of the optimum; specifically, a face-centred central composite design was used. This is an extension of the full factorial design that requires 6 additional runs, one in the centre (axis) of each face of the cubic design space (Figure 35). 20 runs were necessary; these were studied in a factorial block of 12 and axial block of 8 runs. Four centre points in the factorial block were used and 2 for the axial block. As well as being essential for gaining information on curvature, the centre points enable the inherent system noise to be assessed, as well as any noise shifts between the two blocks to be quantified and discounted if necessary. The following factors and levels were used in the design (Table 10).

Table 10: Factors considered in this case study: growth agitation, growth period and induction agitation and the levels applied in the design of experiments.

Factor	High Level	Low Level
Growth agitation (rpm)	50	250
Growth Period (h)	2	6
Induction agitation (rpm)	200	400

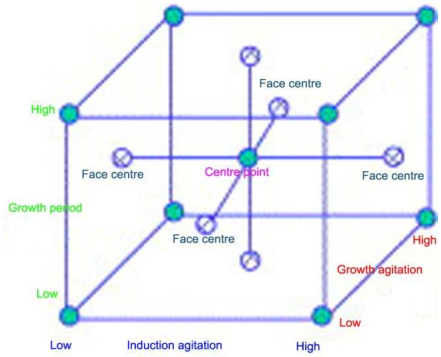

Figure 35: Schematic of face-centred composite design used. This is an extension of the full factorial design that requires 6 additional runs, one in the centre (axis) of each face of the cubic design space.

Data Analysis

Predicted Model Choice

Once the data is collated, the first stage in the analysis process is to predict which model best fits the relationship between the factors and each of the responses; i.e linear, quadratic, cubic. The effect blocking should also be quantified.

This Fit summary for the relationship in the design space of the factors upon log_{10}yield suggests a quadratic model best fits the data but warns that the cubic model is aliased and therefore there is not enough unique design points to estimate all the cubic model coefficients.

The quadratic model is suggested for both responses based on data in three tables:

(i) sequential model sum of squares

(ii) lack of fit tests

(iii) Model summary statistics.

All three suggest a quadratic model. These are explained below with reference to the post-ind OD model.

The sequential model sum of squares provides a table showing the statistical significance of adding various model terms to those terms already in the model. The F value (test of significance) for the effect of adding quadratic terms to the previous two-factor interaction model is 10.29; the P value that this significance is wrong is 0.0029 ($P<0.05$ = significant) and is the lowest P value of all models. The lack of fit test compares residual error to the pure error from replicate values. The F factor for lack of fit in the quadratic model is 0.33; the lowest of all models. The P factor that the F factor is wrong 0.8738 and therefore very unlikely. The model summary statistics for the quadratic model indicate the model has the smallest standard deviation (0.43) and the R-squared value closest to the ideal of 1 (0.8951). The adjusted R-squared is lower (0.7903) due to adjustment accounting for the number of terms in the model relative to the number of design points.

For the Log_{10}Yield model, the suggested model was also quadratic, however the lack of fit probability was much lower at 0.26. Also, the predicted R-squared was only 0.273, some way off the adjusted R-squared of 0.78. This may indicate a large block effect or possible problem with either the model or data.

ANOVA

The ANOVA (analysis of variance) is checked to determine the F value of the model fit and the p value indicating the probability that the model F value occurs due to noise. The F value is the mean square of the term divided by the mean square of the residual. A high F value therefore indicates significance. The importance of factors on the response is also determined by looking at these two metrics. A P-value of less than 0.05 indicates a very low probability that the factor is not significant.

The Adequate precision value measures the signal to noise ratio. Greater than 4 is desirable; both responses have an adequate precision value of ~10 indicating confidence that the results will not be misleading due to noise.

Table 11: Table showing ANOVA for response 2, Post-ind OD for response surface quadratic model.

Analysis of variance table [Partial sum of squares - Type III]

Source	Sum of Squares	df	Mean Square	F Value	p-value Prob > F	
Block	9.901E-005	1	9.901E-005			
Model	1.03	9	0.11	8.10	0.0023	significant
A-Growth Agi	*0.19*	*1*	*0.19*	*13.41*	*0.0052*	
B-Growth Per	*0.26*	*1*	*0.26*	*18.25*	*0.0021*	
C-Ind Agitatic	*0.022*	*1*	*0.022*	*1.60*	*0.2379*	
AB	*0.046*	*1*	*0.046*	*3.25*	*0.1047*	
AC	*0.11*	*1*	*0.11*	*8.14*	*0.0190*	
BC	*0.048*	*1*	*0.048*	*3.38*	*0.0989*	
A^2	*0.036*	*1*	*0.036*	*2.55*	*0.1450*	
B^2	*0.076*	*1*	*0.076*	*5.39*	*0.0454*	
C^2	*0.21*	*1*	*0.21*	*14.86*	*0.0039*	
Residual	0.13	9	0.014			
Lack of Fit	*0.097*	*5*	*0.019*	*2.60*	*0.1874*	*not significan*
Pure Error	*0.030*	*4*	*7.434E-003*			
Cor Total	1.15	19				

The Model F-value of 8.10 implies the model is significant. There is only a 0.23% chance that a "Model F-Value" this large could occur due to noise.

Table 12*: Table showing ANOVA for response 2, Post-ind OD for response surface quadratic model*

Analysis of variance table [Partial sum of squares - Type III]

Source	Sum of Squares	df	Mean Square	F Value	p-value Prob > F	
Block	2.99	1	2.99			
Model	14.26	9	1.58	8.54	0.0019	significant
A-Growth Agi	*0.12*	*1*	*0.12*	*0.63*	*0.4479*	
B-Growth Per	*8.12*	*1*	*8.12*	*43.77*	*< 0.0001*	
C-Ind Agitatic	*3.386E-003*	*1*	*3.386E-003*	*0.018*	*0.8955*	
AB	*0.14*	*1*	*0.14*	*0.75*	*0.4082*	
AC	*0.094*	*1*	*0.094*	*0.50*	*0.4957*	
BC	*0.054*	*1*	*0.054*	*0.29*	*0.6028*	
A^2	*0.41*	*1*	*0.41*	*2.23*	*0.1691*	
B^2	*1.95*	*1*	*1.95*	*10.51*	*0.0101*	
C^2	*0.029*	*1*	*0.029*	*0.16*	*0.7028*	
Residual	1.67	9	0.19			
Lack of Fit	*0.49*	*5*	*0.097*	*0.33*	*0.8738*	*not significant*
Pure Error	*1.18*	*4*	*0.30*			
Cor Total	18.92	19				

The Model F-value of 8.54 implies the model is significant. There is only a 0.19% chance that a "Model F-Value" this large could occur due to noise.

Table 13: Showing significant factors and interactions for each response. Where, A = Growth agitation, B=Growth Period, C=Induction Agitation.

Response	Log_{10}Yield	Post-ind OD
Significant factors	A B AC B^2 C^2	B B^2

Diagnostic plots

Firstly, the normality of residuals is determined by checking the Normal probability vs studentised residuals plot. The residuals are studentised to reduce the effect of residual size changing at different positions in the model. The plot should show the residuals in good correlation with the line of best fit. If they indicate a sigmoid curve, a transformation is likely to be required.

The plot of studentised residuals vs predicted values should show all data points are scattered randomly; if not, a transformation may be required.

The externally studentised residuals vs run is useful to identify outliers and investigate them to see if the data point is wrong or the model!

The Box-cox plot should be checked to determine if any power transformations are recommended.

One data point had an externally studentised residual of 3.5, this was a potential outlier since it was close to the upper threshold of 4.3 and higher than the calculated internal residual of 2.5. This point could be the cause of the discrepancy observed between the predicted and adjusted R-squared values fro this response mentioned earlier. The outlier was not close to the maximum of either response so is unlikely to significantly impact on the choice of operating conditions.

For both responses, outputs from the diagnostic plots indicated that the dataset and model selected were statistically acceptable to draw conclusions from the results.

Model Graphs and optimisation

With confidence in the statistical significance of the model and results it is possible to interpret the results using the model graphs.

The 2D interaction plots are useful to isolate individual interactions and determine how they each of the two (or more) factors involved in an interaction are affected. This is particularly useful for trying to quantify relationships but the purposes of selecting optimal process conditions the contour and 3d surface plots are most useful to determine regions where the responses are optimal and equally importantly regions where fluctuations from these optima will not incur significant changes to the key responses.

The optimisation section enables criteria to be set (e.g. maximise yield, OD to be in certain range) and the software feeds back a set of solutions that best fulfil the set criteria. The solutions are ranked according to a desirability scale of 0 to 1; predicted responses are also given. The point prediction tool predicts the range of values in which you can expect the process average to fall into

95% of the time under the set process conditions. This is given as 95% CI (confidence interval) high and low values. The 95% PI (prediction interval) is the range in which you'd expect any individual point to fit into 95% of the time.

Final Optimised operating conditions

Growth Period

The optimal conditions for maximising log_{10}yield of protein show that the optimal growth period to choose is the lowest tested, 2hours. The shape of the 3-D surface (Figure 36) toward the low value for the growth period indicate no sign of a plateau and it could therefore be advisable to follow up this work by extending the design space to include lower growth periods.

For maximising post-induction OD, the highest growth period of 6hours is best. Prioritising one factor over another or compromise is therefore required to choose the most appropriate growth period.

As the ultimate aim must be to maximise the yield of recombinant protein rather than maximising the post induction OD reached by the cells; the conditions predicted to achieve maximum protein yield should be prioritised. This may in-fact lead to further benefits in any case since a lower cell density is usually preferable for downstream processing.

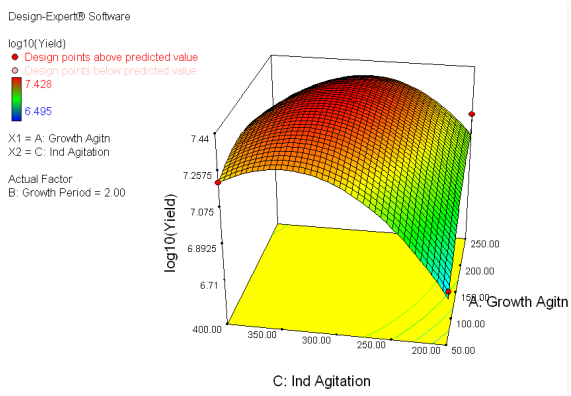

Figure 36: Showing a flat plateau region for achieving maximum yield exists with a growth period of 2hours, an induction agitiaton in the range of 275-325rpm and a growth agitation of 150rpm to 225rpm.

Growth agitation

Involved in an interaction with induction agitation with respect to log_{10}yield, it becomes less important as induction OD increases and growth period is kept low. At an induction agitation of 300rpm and growth period of 2hours varying the growth agitation between 125 and 225 rpm produces little difference in yield. This therefore makes a sensible operating range for achieving process consistency (Figure 36:).

For maximising Post ind OD at the low growth period of 2h, this factor should be kept between 185 and 250 rpm, this range is also flat and thus beneficial for achieving consistency (**Error! Reference source not found.**Figure 37).

Induction agitation

Under the growth period and growth agitation recommended above a plateau region indicating an area where $\log_{10}$yield can be maximised exists in the range of 275 to 325rpm induction agitation (Figure 36). With respect to post induction OD, the Induction agitation has little effect over the range of 200 to 400rpm at a growth agitation of 185rpm where an OD of approximately 6 is estimated with 2hours growth period (Figure 37).

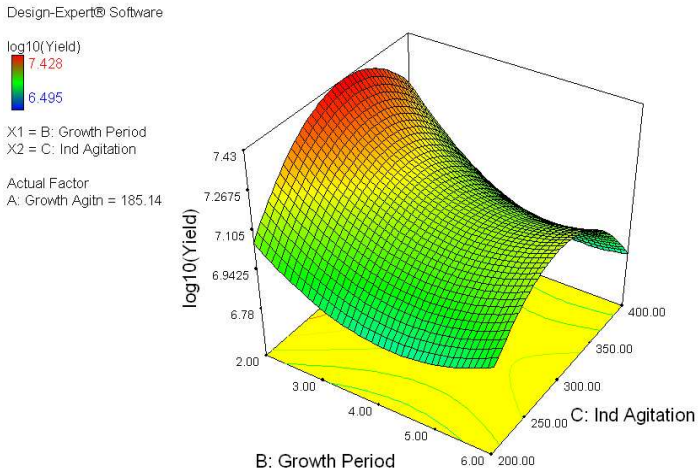

Figure 37: 3D surface plot showing how further reduction in growth period may lead to increased yield; fluctuations in growth period may also be expected to change the yield since the relationship is not flat around this region of the plot. The contour plot indicates that for maximum consistency an induction agitation of 310rpm should be used with a growth agitation of 185rpm.

The conditions chosen to maximise yield are: **Growth Period: 2hours**; **Growth agitation: 185rpm and Induction agitation: 310rpm**.

Appendix 3: Raw Data from on E.colipGEc47∆J bioconversion of n-dodecane

Description of laboratorial experiences

Experience 1: Effect of the SF Volume on E.colipGEc47 ∆J bioconversion of *n*-dodecane

It was performed *E.coli* pGEc47 ∆J bioconversion of *n*-dodecane in three 500mL SF and three 1L. The culture conditions was 10 % (v/v) Wubbolts media, 5% (v/v) inoculum, 20% (v/v) *n*-dodecane and 0,05 % (v/v) DCPK (inducer) The SFs were put into a incubator at 37℃ , 250rpm and 25mm of throw diameter for 48hours. The samples were taken in 3 time points (6, 24 and 48h) and the cell density and 1-dodecanol in organic phase were analysed on duplicate.

Experience 2: Effect of SF volume on three different E.colipGEc47∆J bioconversion of *n*-dodecane cultures conditions.

By the observation of the effect that the surfactant, Triton X-100, had in the mixing of the two liquid phases in MTPs. It was decided to visualize if the surfactants could improve the bioconversion. Therefore, it was performed *E.coli* pGEc47 ∆J bioconversion of *n*-dodecane in in three 500mL SF and three 1L. However, opposite to previous experience each SF had a different culture condition. This experience, work in parallel, one 500mL and 1L had the usually (normal) culture conditions (10 % (v/v) Wubbolts media, 5% (v/v) inoculum, 20% (v/v) *n*-dodecane and 0,05 % (v/v) DCPK (inducer)), other 2 SFs had the addition of 0,01% of PPG (1:100) (1mL) and the remains had the addition of 0,1% of Triton X-100 (1:10) (1mL). The six SFs were put in the incubator at 37℃ , 250rpm and 25mm of throw diamet er for 48hours. Unique samples of 5mL were taken in 4 time points (6, 24, 30 and 48h) and the cell density and 1-dodecanol and dodecanoic acid in organic phase and in the interface were GC analysed. For the interface method of extraction is was used 1mL

Experience 3: E.colipGEc47∆J bioconversion of *n*-dodecane in 1L SFs.

The experience 2 was repeated, but now only using only the 1L SFs. The reasons for that is to have statistical importance by collect the samples in triplicate. However, the bioconversion was performed until the 30hours. Besides, it was also used a 1L SF with 10 % (v/v) Wubbolts media, 5% (v/v) inoculum and 20% (v/v) *n*-dodecane and it was used the same method of collecting the samples. For the interface method of extraction is was used 1mL

Experience 4: *E.coli* pGEc47∆J bioconversion of *n*-dodecane in the thermomixer

After the bioconversion in SFs it was decided to do *n*-dodecane bioconversion in 24-DSW MTP covered by a gas permeable membrane in the thermomixer at 1000rpm and with a 3mm of throw diameter inside of the incubator to maintaining the temperature (37℃) constant for 24h. It was used 10% (v/v) of Wubbolts medium, 5% (v/v) inoculum, 20% (v/v) of *n*-dodecane and 0,1%

(v/v) of DCPK. No data was collected because the excessive turbulency, splashing and elevated evaporation rate. Nevertheles, samples from the organic phase of all wells were collected and analysed, but no product were there.

Experience 5: Effect of different Duetz Sandwich covers on the *E.coli* pGEc47∆J bioconversion of *n*-dodecane on 24-DSW MTPs.

Consequently, it was clear, by the experience 4, that evaporation rate is very serious in a two liquid system and the splashing present when the bioconversion is performed in MTPS. So, it was necessary to obtain a solution for this problem. These two factors cause losses of the product, as 1-dodecanol is volatile at the incubation temperature, and the contamination of wells. Therefore, it was used in this experience the Duetz system in order to try to solve the problem.

The E.colipGEc47∆J bioconversion of *n*-dodecane occurred in a 24-DSW MTP (piramyd bottom) two different sandwich covers soft spongy white silicone layer (A) and rigid black impermeable layer (B)) from the Duetz System using. It was used 10% (v/v) of Wubbolts medium, 5% (v/v) inoculum, 20% (v/v) of *n*-dodecane and 0,1% (v/v) of DCPK. The incubation occurred at 37℃, 250rpm and 25mm (throw diameter). Besides, as a consequence of the visualization of the surfactant effect o the liquid hydrodynamic in MTPs, it was tested the effects of the addition of surfactants (0,01% PPG (1:100) and 0,1% Triton X-100 (1:10)) in the product formation compared with the normal condition. It was measured the cell density, the 1-dodecanol and dodecanoic acid concentrations in organic phase and in the interface, evaporation rate and interface formation at two time points (24h and 48h). For the interface method of extraction is was used 1mL

Experience 6: *E.coli* pGEc47∆J bioconversion of *n*-dodecane 24-DSW MTPs permeable membrabes.

In this experience it was used the same culture conditions (10% (v/v) of Wubbolts medium, 5% (v/v) inoculums, 20% (v/v) of *n*-dodecane and 0,1% (v/v) of DCPK) of Experience 5 in 24 MTPs using the same support device (figure???), but instead of cover the MTPs with sandwich covers it was covers with the normally used gas permeable membrane (figure???). It was analysed the cell density, 1-dodecanol and dodecanoic acid in organic phase and in the interface, evaporation rate and interface formation at three time points (6, 24 and 48hours). For the interface method of extraction is was used 0,15mL

Experience 7: Design Experience (DoE) with *E.coli* pGEc47∆J bioconversion of *n*-dodecane in 24-SDW with Duetz System.

After all these experiences there were 4 factors that seem to have an important role in the bioconversion of *n*-dodecane. There are the volume of aqueous phase, volume of n-dodecane, concentration of glucose on the Wubbolts media and the concentration of surfactant (Triton X-100). These factors affect the evaporation rate then with the bioconversion of *n*-dodecane. Another,

problem to understand is the over expression. Therefore, with help of design expert (DOE) 7.1.6 from Stat-Ease®, it is expected to discover what the optimum conditions are and those are irrelevant. Therefore, it was realised two DOE experiments in 24-DSW MTPs (inverted inverted pyramid bottom) with the black silicon (B) sandwich cover of the Duetz system. It was used 10% (v/v) of Wubbolts medium, 5% (v/v) inoculums, 20% (v/v) of *n*-dodecane and 0,1% (v/v) of DCPK. The MTPs were in the incubator at 37℃, 250rpm and 25mm of throw diameter for 24hours.For the interface method of extraction is was used 0,15mL

The Table 14 indicates the inputs of the DoE experiments. The responses were the DCW (g/L), Evaporation rate (% (v/v)), 1-dodecanol (organic phase) (g/L), dodecanoic acid (organic phase) (g/L), 1-dodecanol (interface) (g/L) and dodecanoic acid (interface) (g/L).

Table 14: Inputs and the output obtain by using the culture condition stipulated by the DOE using the Triton X-100 as the surfactant

			Inputs			
Run	Row	Line	**Aqueous Phase (mL)**	**Triton X-100 (% v/v)**	**Glucose (g/L)**	***n*-dodecane (% (v/v))**
1	A	1	1	0,01	15	9
2	A	2	1	0,2	15	26
3	A	3	1	0,01	15	26
4	A	4	1	0,01	5	26
5	A	5	3	0,2	5	26
6	A	6	1	0,2	5	26
7	B	1	1	0,2	15	9
8	B	2	3	0,2	15	26
9	B	3	2	0,11	10	17,5
10	B	4	1	0,2	5	9
11	B	5	1	0,01	5	9
12	B	6	3	0,2	15	9
13	C	1	3	0,2	5	9
14	C	2	3	0,01	15	26
15	C	3	3	0,01	5	26
16	D	1	3	0,01	5	9
17	D	2	2	0,11	10	17,5
18	D	3	1	0,11	10	17,5
19	D	4	1	0,01	15	9
20	D	5	1	0,111	10	17,5

1. DCW model

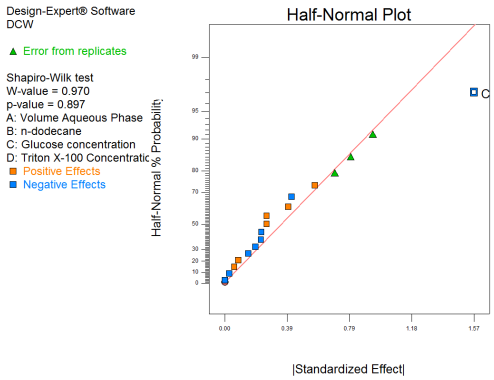

Figure 38: DCW half-normal plot of effects, where it is chosen the effects to be included in the model.

Table 15: Table showing ANOVA for response 1: DCW. The model is significant.

Response 1 DCW

ANOVA for selected factorial model

Analysis of variance table [Partial sum of squares - Type III]

Source	Sum of Squares	df	Mean Square	F Value	p-value Prob > F	
Model	9.87	1	9.87	23.18	0.0002	significant
C-Glucose cc	*9.87*	*1*	*9.87*	*23.18*	*0.0002*	
Curvature	1.92	1	1.92	4.52	0.0484	significant
Residual	7.23	17	0.43			
Lack of Fit	*5.60*	*14*	*0.40*	*0.73*	*0.7065*	*not significant*
Pure Error	*1.64*	*3*	*0.55*			
Cor Total	19.02	19				

The Model F-value of 23.18 implies the model is significant. There is only a 0.02% chance that a "Model F-Value" this large could occur due to noise.

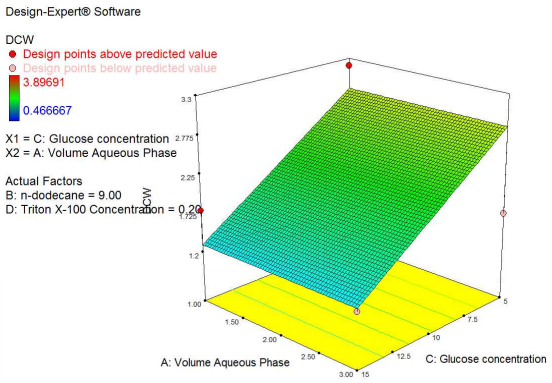

Figure 39: 3D surface plot showing the weak relationship between the parameters. It seems that with the higher concentration of glucose the DCW is higher.

2. Evaporation rate model

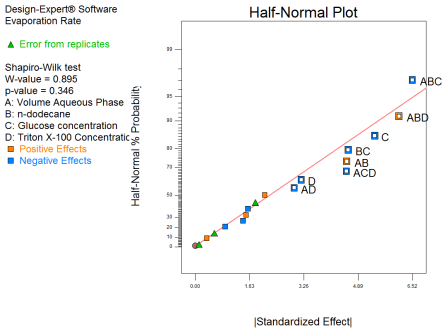

Figure 40: Evaporation rate half-normal plot of effects, where it is chosen the effects to be included in the model.

Table 16: Table showing ANOVA for response 2: Evaporation rate. The model is not significant.

Response 2 **Evaporation Rate**

Hierarchical Terms Added after Manual Regression

A B AC BD CD

ANOVA for selected factorial model

Analysis of variance table [Partial sum of squares - Type III]

Source	Sum of Squares	df	Mean Square	F Value	p-value Prob > F	
Model	737.62	13	56.74	3.37	0.0936	not significant
A-Volume Aqueous Phase	*23.33*	*1*	*23.33*	*1.39*	*0.2918*	
B-n-dodecane	*6.57*	*1*	*6.57*	*0.39*	*0.5594*	
C-Glucose concentration	*60.07*	*1*	*60.07*	*3.57*	*0.1173*	
D-Triton X-100 Concentration	*39.92*	*1*	*39.92*	*2.37*	*0.1840*	
AB	*41.69*	*1*	*41.69*	*2.48*	*0.1762*	
AC	*14.75*	*1*	*14.75*	*0.88*	*0.3919*	
AD	*39.54*	*1*	*39.54*	*2.35*	*0.1857*	
BC	*74.53*	*1*	*74.53*	*4.43*	*0.0892*	
BD	*2.75*	*1*	*2.75*	*0.16*	*0.7025*	
CD	*13.63*	*1*	*13.63*	*0.81*	*0.4092*	
ABC	*151.35*	*1*	*151.35*	*9.00*	*0.0301*	
ABD	*135.04*	*1*	*135.04*	*8.03*	*0.0365*	
ACD	*80.13*	*1*	*80.13*	*4.77*	*0.0808*	
Curvature	0.038	1	0.038	2.232E-003	0.9641	not significant
Residual	84.08	5	16.82			
Lack of Fit	*10.08*	*2*	*5.04*	*0.20*	*0.8257*	*not significant*
Pure Error	*74.00*	*3*	*24.67*			
Cor Total	821.74	19				

The Model F-value of 3.37 implies there is a 9.36% chance that a "Model F-Value" this large could occur due to noise.

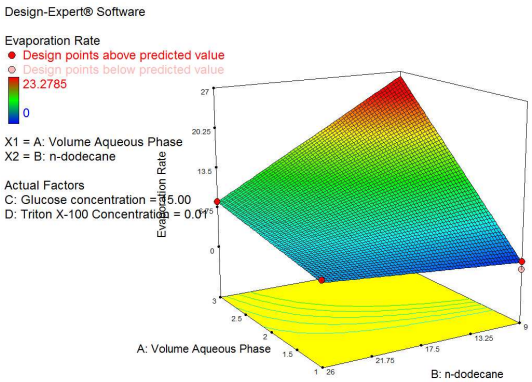

Figure 41: 3D surface plot showing that the higher evaporation rate is achieved at the maximum aqueous volume and the minimum *n*-dodecane volume.

3. 1-Dodecanol in the organic phase model

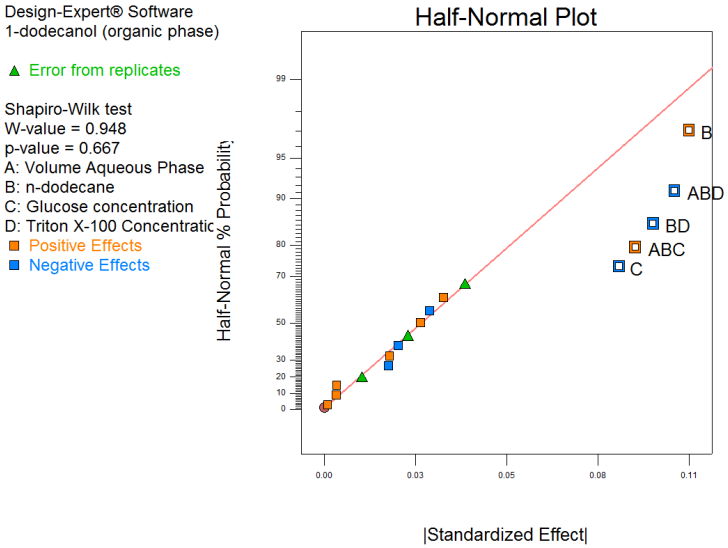

Figure 42: 1-dodecanol in the organic phase half-normal plot of effects, where it is chosen the effects to be included in the model.

Table 17: Table showing ANOVA for response 3: 1-dodecanol in the organic phase. The model is significant.

Response 3 **1-dodecanol (organic phase)**

Hierarchical Terms Added after Manual Regression

A D AB AC AD BC

ANOVA for selected factorial model

Analysis of variance table [Partial sum of squares - Type III]

Source	Sum of Squares	df	Mean Square	F Value	p-value Prob > F	
Model	0.12	11	0.011	4.39	0.0302	significant
A-Volume Aqueous Phase	*5.003E-004*	*1*	*5.003E-004*	*0.20*	*0.6697*	
B-n-dodecane	*0.032*	*1*	*0.032*	*12.72*	*0.0091*	
C-Glucose concentration	*0.020*	*1*	*0.020*	*7.96*	*0.0257*	
D-Triton X-100 Concentration	*3.546E-004*	*1*	*3.546E-004*	*0.14*	*0.7190*	
AB	*5.037E-003*	*1*	*5.037E-003*	*1.99*	*0.2008*	
AC	*8.042E-004*	*1*	*8.042E-004*	*0.32*	*0.5902*	
AD	*2.854E-003*	*1*	*2.854E-003*	*1.13*	*0.3231*	
BC	*9.410E-005*	*1*	*9.410E-005*	*0.037*	*0.8524*	
BD	*0.026*	*1*	*0.026*	*10.13*	*0.0154*	
ABC	*0.025*	*1*	*0.025*	*10.08*	*0.0156*	
ABD	*0.033*	*1*	*0.033*	*13.00*	*0.0087*	
Curvature	6.632E-003	1	6.632E-003	2.63	0.1492	not significant
Residual	0.018	7	2.526E-003			
Lack of Fit	*0.014*	*4*	*3.390E-003*	*2.47*	*0.2420*	*not significant*
Pure Error	*4.121E-003*	*3*	*1.374E-003*			
Cor Total	0.15	19				

The Model F-value of 4.39 implies the model is significant. There is only a 3.02% chance that a "Model F-Value" this large could occur due to noise.

4. Dodecanoic Acid in the organic phase model

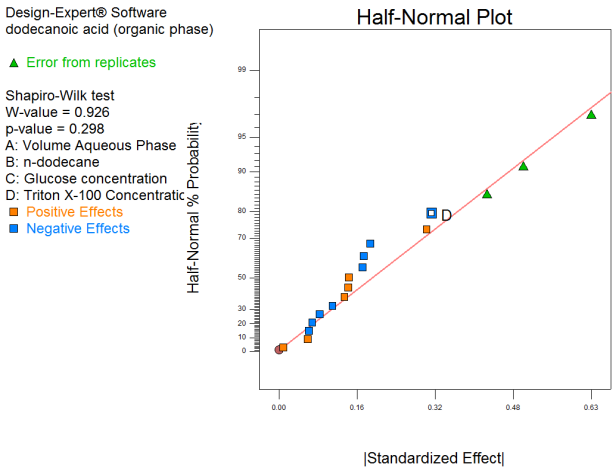

Figure 43: 1-dodecanol in the organic phase half-normal plot of effects, where it is chosen the effects to be included in the model.

Table 18: Table showing ANOVA for response 4: dodecanoic acid in the organic phase. The model is not significant.

Response 4 dodecanoic acid (organic phase)

ANOVA for selected factorial model

Analysis of variance table [Partial sum of squares - Type III]

Source	Sum of Squares	df	Mean Square	F Value	p-value Prob > F	
Model	0.42	1	0.42	4.41	0.0510	not significant
D-Triton X-100 Concentration	*0.42*	*1*	*0.42*	*4.41*	*0.0510*	
Curvature	0.31	1	0.31	3.26	0.0887	not significant
Residual	1.62	17	0.095			
Lack of Fit	*1.13*	*14*	*0.080*	*0.49*	*0.8481*	*not significant*
Pure Error	*0.50*	*3*	*0.17*			
Cor Total	2.35	19				

The Model F-value of 4.41 implies there is a 5.10% chance that a "Model F-Value" this large could occur due to noise.

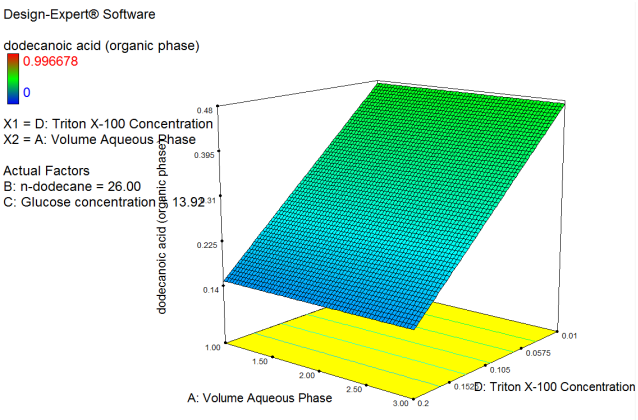

Figure 44: 3D surface plot showing the weak relationship between the parameters.

5. 1-dodecanol in the interface model

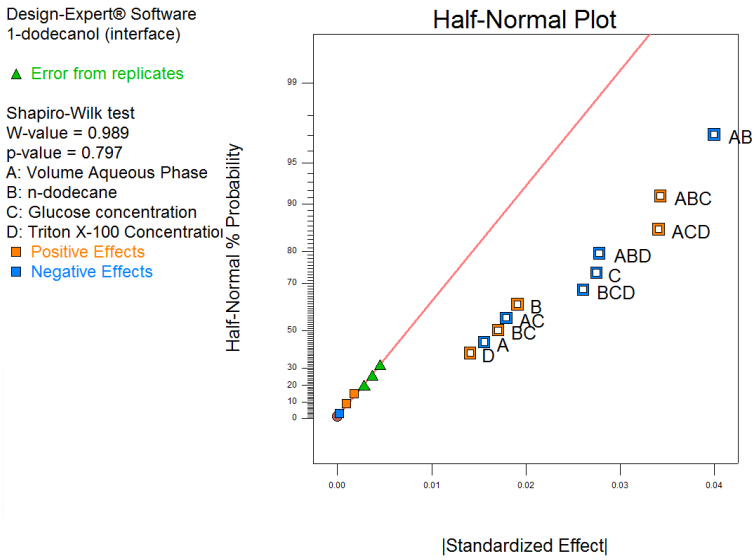

Figure 45: 1-dodecanol in the organic phase half-normal plot of effects, where it is chosen the effects to be included in the model.

Table 19: Table showing ANOVA for response 5: 1-dodecanol in the interface. The model is not significant.

Response 5 **1-dodecanol (interface)**

Hierarchical Terms Added after Manual Regression

AD BD CD

ANOVA for selected factorial model

Analysis of variance table [Partial sum of squares - Type III]

Source	Sum of Squares	df	Mean Square	F Value	p-value Prob > F	
Model	0.027	14	1.910E-003	3.66	0.1097	not significant
A-Volume Aqueous Phase	*4.096E-003*	*1*	*4.096E-003*	*7.84*	*0.0488*	
B-n-dodecane	*5.481E-003*	*1*	*5.481E-003*	*10.50*	*0.0317*	
C-Glucose concentration	*3.333E-003*	*1*	*3.333E-003*	*6.38*	*0.0649*	
D-Triton X-100 Concentration	*4.361E-003*	*1*	*4.361E-003*	*8.35*	*0.0446*	
AB	*5.208E-004*	*1*	*5.208E-004*	*1.00*	*0.3745*	
AC	*1.415E-003*	*1*	*1.415E-003*	*2.71*	*0.1751*	
AD	*1.737E-003*	*1*	*1.737E-003*	*3.33*	*0.1422*	
BC	*1.284E-003*	*1*	*1.284E-003*	*2.46*	*0.1920*	
BD	*1.762E-003*	*1*	*1.762E-003*	*3.37*	*0.1401*	
CD	*1.881E-007*	*1*	*1.881E-007*	*3.603E-004*	*0.9858*	
ABC	*5.172E-003*	*1*	*5.172E-003*	*9.90*	*0.0346*	
ABD	*6.698E-003*	*1*	*6.698E-003*	*12.83*	*0.0231*	
ACD	*5.119E-003*	*1*	*5.119E-003*	*9.80*	*0.0352*	
BCD	*2.997E-003*	*1*	*2.997E-003*	*5.74*	*0.0747*	
Curvature	3.385E-005	1	3.385E-005	0.065	0.8116	not significant
Residual	2.089E-003	4	5.222E-004			
Lack of Fit	*5.495E-004*	*1*	*5.495E-004*	*1.07*	*0.3769*	*not significant*
Pure Error	*1.539E-003*	*3*	*5.131E-004*			
Cor Total	0.029	19				

The "Model F-value" of 3.66 implies the model is not significant relative to the noise. There is a 10.97 % chance that a "Model F-value" this large could occur due to noise.

6. Dodecanoic acid in the interface model

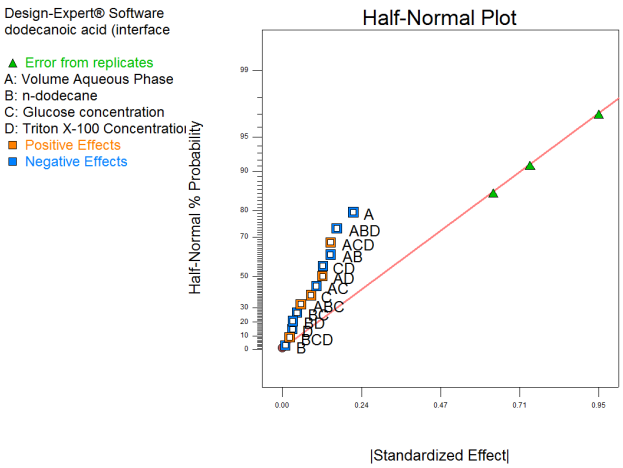

Figure 46: 1-dodecanol in the organic phase half-normal plot of effects, where it is chosen the effects to be included in the model.

Table 20: Table showing ANOVA for response 6: dodecanoic acid in the interface. The model is not significant.

Response 6 **dodecanoic acid (interface**

ANOVA for selected factorial model

Analysis of variance table [Partial sum of squares - Type III]

Source	Sum of Squares	df	Mean Square	F Value	p-value Prob > F	
Model	0.85	14	0.060	0.15	0.9967	not significant
A-Volume Aqueous Phase	*0.096*	*1*	*0.096*	*0.24*	*0.6503*	
B-n-dodecane	*1.981E-004*	*1*	*1.981E-004*	*4.952E-004*	*0.9833*	
C-Glucose concentration	*0.016*	*1*	*0.016*	*0.039*	*0.8528*	
D-Triton X-100 Concentration	*2.015E-003*	*1*	*2.015E-003*	*5.037E-003*	*0.9468*	
AB	*0.044*	*1*	*0.044*	*0.11*	*0.7568*	
AC	*0.022*	*1*	*0.022*	*0.055*	*0.8262*	
AD	*0.031*	*1*	*0.031*	*0.077*	*0.7952*	
BC	*4.139E-003*	*1*	*4.139E-003*	*0.010*	*0.9239*	
BD	*2.082E-003*	*1*	*2.082E-003*	*5.204E-003*	*0.9460*	
CD	*0.031*	*1*	*0.031*	*0.078*	*0.7937*	
ABC	*6.572E-003*	*1*	*6.572E-003*	*0.016*	*0.9042*	
ABD	*0.057*	*1*	*0.057*	*0.14*	*0.7259*	
ACD	*0.044*	*1*	*0.044*	*0.11*	*0.7560*	
BCD	*1.030E-003*	*1*	*1.030E-003*	*2.574E-003*	*0.9620*	
Curvature	0.036	1	0.036	0.090	0.7797	not significant
Residual	1.60	4	0.40			
Lack of Fit	*0.91*	*1*	*0.91*	*3.97*	*0.1402*	*not significant*
Pure Error	*0.69*	*3*	*0.23*			
Cor Total	2.48	19				

The "Model F-value" of 0.15 implies the model is not significant relative to the noise. There is a 99.67 % chance that a "Model F-value" this large could occur due to noise.

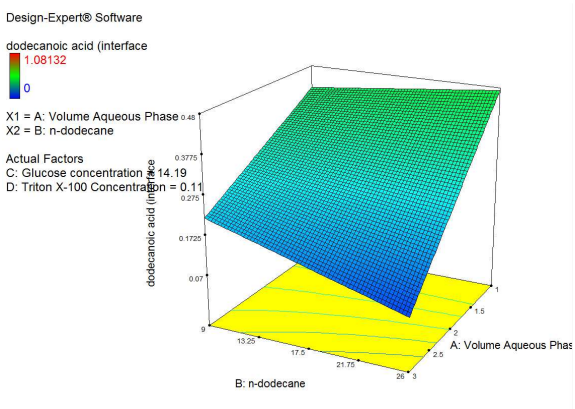

Figure 47: 3D surface plot showing the weak relationship between the parameters. It seems that with the higher concentration of glucose the DCW is higher.

Experience 8*: E.coli* pGEc47ΔJ bioconversion of *n*-dodecane in 24-SDW with Duetz System and Triton X-100.

As a consequence of the results from the DOE of the Triton X-100, it was performed a *.coli* pGEc47ΔJ bioconversion of *n*-dodecane in 24-SDW (inverted inverted pyramid bottom) MTPs with the black silicon (B). In each well (19) 1mL of Wubbolts media without glucose, 5% (v/v) inoculum, 20% (v/v) of *n*-dodecane , 10µL of glucose and 0,1% TritonX-100 (mL) (1:10). Despite the culture conditions were all the same in the nineteen wells the sample treatment of the wells were divided in two. In eleven wells the sample treatment were the previously used, it was taken in triplicate on the 5, 30 and 48 hours and in duplicate at 19,5hours. At the rest of the wells the sample were done in duplicate at the same time points. It was measured the cell density and 1-dodecanol and dodecanoic acid in organic phase, in the interface and in the sample. For the interface method of extraction is was used 0,8mL

GC Chromatograms

1-Dodecanol and Dodecanoic GC Standards

Table 21: GC Chromatogram (50 % (v/v) sample/ethyl acetate)of the 1-Dodecanol Standards of Experience 1. Blue: Ethyl acetate, Orange: *n*-dodecane GC peak area and Pink: 1-Dodecanol peak area. t:time (minutes)and peak area: peak area (µV s).

v/v 1-dodecanol/ *n*-dodecane prepared (%)	t	Peak Area	t	Peak Area	t	Peak Area	t	Peak Area	t	Peak Area	t	Peak Area	t	Peak Area	t	Peak Area	t	Peak Area
0,01	1,631	4123281,72	2,128	28132,11	2,17	4984481,73	2,86	13785,10	3,35	924,51								
0,05	1,633	3891303,81	2,127	29043,15	2,17	5209960,16	2,85	31461,48	3,34	8115,54								
0,10	1,633	3976287,63	2,127	28515,24	2,17	4961050,17	2,38	163548,63	2,86	28626,22	3,342	11419,32						
0,50	1,63	3968118,08	2,125	27369,00	2,17	5048157,46	2,85	21429,97	3,34	41883,33								
1,00	1,63	4015365,85	1,849	121242,98	2,13	10814,30	2,17	4894200,06	2,38	137275,96	2,856	4812,59	3,348	80900,56	3,949	132,87	4,736	116,55

Table 22: GC Chromatogram (50 % (v/v) sample/ethyl acetate) of the 1-Dodecanol Standards of Experience 2. Blue: Ethyl acetate, Orange: *n*-dodecane GC peak area and Pink: 1-Dodecanol peak area. t:time (minutes)and peak area: peak area (µV s).

v/v 1-dodecanol / *n*-dodecane prepared (%)	t	Peak Area	t	Peak Area	t	Peak Area	t	Peak Area	t	Peak Area	t	Peak Area	t	Peak Area	t	Peak Area	t	Peak Area	t	Peak Area
0,01	1,842	4029835,07	2,396	32553,7	2,437	5574638	2,783	177915,5	3,194	22187,44	3,723	184,83								
0,05	1,843	4092652,46	2,398	31701,5	2,441	5469412	2,785	171787,07	3,197	14564,26	3,724	3221,5								
0,10	1,856	2957231,31	2,395	29578,6	2,431	6543650	2,783	181312,29	3,2	33237,59	3,2	33238	3,724	12288						
1,00	1,847	3873694,08	2,399	32256,3	2,441	5640251	2,786	177963,89	3,199	15943,38	3,371	13421	3,742	154080	4,367	312,08	5,191	348,67		

Table 23: GC Chromatogram (20 % (v/v) sample/ethyl acetate) of the Dodecanoic Acid of Experience 2. Blue: Ethyl acetate, Orange: *n*-dodecane GC peak area and Green: Dodecanoic Acid peak area. t:time (minutes)and peak area: peak area (µV s).

v/v Dodecanoic Acid/ *n*-dodecane prepared (g/L)	t	Peak Area	t	Peak Area	t	Peak Area	t	Peak Area	t	Peak Area	t	Peak Area
0,01	1,846	4040238,23	2,401	32163,5	2,441	5575539	2,788	178471,7	3,2	17479,24		
0,05	1,847	3871992,1	2,399	30790,6	2,444	5336688	2,787	161680,31	3,198	14334,63	4,247	425,6
0,1	1,848	3788842,78	2,401	30898,5	2,441	5729853	2,788	167639,99	3,203	18268,76	4,248	971,94
1	1,848	3853054,24	2,399	24209,5	2,441	5655047	2,786	124716,36	3,2	421,2	4,262	8663,4

Table 24: GC Chromatogram (20 % (v/v) sample/ethyl acetate) of the 1-Dodecanol Standards from experiences 3, 6 and 7 . Blue: Ethyl acetate, Orange: *n*-dodecane GC peak area and Pink: 1-dodecanol peak area. t:time (minutes)and peak area: peak area (µV s).

v/v 1-dodecanol/ *n*-dodecane prepared (%)	**t**	**Peak Area**	**t**	**Peak Area**	**t**	**Peak Area**	**t**	**Peak Area**	**t**	**Peak Area**	**t**	**Peak Area**	**t**	**Peak Area**
0,01	**1,559**	**5342791,32**	**2,131**	**3023717,96**										
0,01	**1,561**	**4782823,44**	**2,131**	**2816795,53**										
0,01	**1,545**	**4283834,72**	**2,108**	**26616048,76**										
0,05	**1,561**	**5517774,67**	**2,136**	**2885480,48**	**3,273**	**1213,98**								
0,05	**1,53**	**6212497,09**	**2,113**	**3270294,2**	**3,251**	**1627,89**								
0,05	**1,541**	**4429527,98**	**2,106**	**2560807,3**	**3,23**	**1311,86**								
0,1	**1,56**	**5596640,79**	**2,138**	**2831047,74**	**3,272**	**2681,42**								
0,1	**1,558**	**5023530,19**	**2,132**	**2677149,63**	**3,262**	**2815,46**								
0,1	**1,544**	**4511524,51**	**2,11**	**2553740,08**	**3,234**	**3071,95**								
1	**1,537**	**7313035,4**	**2,123**	**3576829,54**	**3,272**	**80873,51**	**3,79**	**698,01**	**4,643**	**112,47**				
1	**1,558**	**5273010,64**	**2,126**	**2966930,44**	**2,933**	**209,66**	**3,267**	**73988,22**	**3,777**	**133,15**	**4,638**	**102,87**		
1	**1,547**	**4520272,24**	**2,105**	**28322430,56**	**2,752**	**260,05**	**2,911**	**229,81**	**3,243**	**81728,5**	**3,754**	**101,11**	**3,826**	**130,94**

Table 25: GC Chromatogram (20 % (v/v) sample/ethyl acetate) of the Dodecanoic Acid Standards from experiences 3, 6 and 7. Blue: Ethyl acetate, Orange: *n*-dodecane GC peak area and Green: Dodecanoic Area Peak area. t:time (minutes)and peak area: peak area (µV s).

v/v Dodecanoic Acid/ *n*-dodecane prepared (g/L)	t	Peak Area	t	Peak Area	t	Peak Area	t	Peak Area
0,01	1,559	5389927,34	2,134	2886475,27				
0,01	1,558	4733679,51	2,126	2841242,1	2,772	139,76		
0,01	1,548	3859469,98	2,096	30265665,77	2,747	164,7		
0,05	1,524	7361416,82	2,11	4343120,55	3,767	149,01		
0,05	1,559	4802823,07	2,13	2745458,87	3,779	196,37		
0,05	1,541	4225341,43	2,103	2655435,08	3,748	146,81		
0,1	1,561	5505309,33	2,138	2759942,53	3,794	349,38		
0,1	1,576	3188668,75	2,102	4521997,11	2,776	1013,45	3,782	1104,67
0,1	1,618	1444737,1	2,073	9036,96	2,136	1846761	3,766	1856,22
1	1,561	5109176,8	2,126	3184743,44	3,795	3441,36		
1	1,562	4510780,85	2,124	3061622,93	3,784	3538,82		
1	1,544	3812751,82	2,09	3134338,19	2,743	224,73	3,752	4410,43
10	1,563	5295174,42	2,133	2965827,16	3,858	36171,43		
10	1,56	4670475,27	2,126	2944743,04	3,849	40221,49		
10	1,545	3902802,04	2,094	3027952,84	2,744	182,75	3,829	52990,96

Table 26: GC Chromatogram (20 % (v/v) sample/ethyl acetate) of the 1-Dodecanol Standards at 24hours from experience 5. Blue: Ethyl acetate, Orange: *n*-dodecane GC peak area and Pink: 1-Dodecanol peak area. t:time (minutes)and peak area: peak area (µV s).

v/v 1-dodecanol/ *n*-dodecane prepared (%)	t	Peak Area	t	Peak Area	t	Peak Area	t	Peak Area	t	Peak Area
0,01	1,896	5894478	2,564	3046106,86						
0,05	1,896	5988146	2,563	3133050,78	3,855	1350,82				
0,1	1,893	6110139	2,58	3090937,38	3,848	3058,74				
1	1,882	6474126,47	2,542	3585602,54	3,852	121442,9	4,371	259,11	4,492	111,26

Table 27: GC Chromatogram (20 % (v/v) sample/ethyl acetate) of the 1-Dodecanol Standards at 48hours from experience 5. Blue: Ethyl acetate, Orange: *n*-dodecane GC peak area and Pink: 1-Dodecanol peak area. t:time (minutes)and peak area: peak area (µV s).

v/v 1-dodecanol/ *n*-dodecane prepared (%)	**t**	**Peak Area**	**t**	**Peak Area**	**t**	**Peak Area**	**t**	**Peak Area**	**t**	**Peak Area**
0,01	1,904	4698229	2,573	2546428,31						
0,05	1,902	4998254	2,572	2602441,33	3,863	1246,91				
0,1	1,903	5099990	2,576	2509831,51	3,864	2522,45				
1	1,858	6810636	2,545	3229624,36	3,861	131607,16	4,499	121,86	5,332	148,03

Table 28: GC Chromatogram (20 % (v/v) sample/ethyl acetate) of the Dodecanoic Acid Standards at 24hours from experience 5. Blue: Ethyl acetate, Orange: *n*-dodecane GC peak area and Green dodecanoic peak area. t:time (minutes)and peak area: peak area (µV s).

v/v Dodecanoic Acid/ *n*-dodecane prepared (g/L)	t	Peak Area	t	Peak Area	t	Peak Area
0,01	1,896	6062461	2,566	3078298,78		
0,05	1,902	5868527	2,57	3067534,23	4,39	246,68
0,1	1,899	5899553	2,567	3048292,27	4,387	323,37
1	1,9	5851170	2,565	3205024,21	4,395	3549,01
10	1,896	5947171	2,565	3078805	4,457	38483,63

Table 29: GC Chromatogram (20 % (v/v) sample/ethyl acetate) of the Dodecanoic Acid Standards at 48hours from experience 5. Blue: Ethyl acetate, Orange: *n*-dodecane GC peak area and Pink: 1-Dodecanol peak area. t:time (minutes)and peak area: peak area (µV s).

v/v Dodecanoic Acid/ *n*-dodecane prepared (g/L)	**t**	**Peak Area**	**t**	**Peak Area**	**t**	**Peak Area**
0,01	1,93	425491,85	1,952	695888,41		
0,05	1,902	5364723	2,569	2.726136.87		
0,1	1,898	5355545	2,568	2679276,05	4,393	304,35
1	1,899	5393435	2,566	2752628,46	4,396	3149,74
10	1,898	5247104	2,567	2712658,13	4,456	34014,21

Table 30: GC Chromatogram (20 % (v/v) sample/ethyl acetate) of the 1-Dodecanol Standards from experience 7. Blue: Ethyl acetate, Orange: *n*-dodecane GC peak area and Pink: 1-Dodecanol peak area. t:time (minutes)and peak area: peak area (µV s).

v/v 1-dodecanol/ *n*-dodecane prepared (%)	t	Peak Area	t	Peak Area	t	Peak Area	t	Peak Area	t	Peak Area
0,01	1,568	5225042	2,138	2689071	3,269	217,3				
0,1	1,542	6682582	2,119	3509551	2,77	57223,31	3,251	15181,85		
0,5	1,569	5065944	2,137	2701741	2,781	203	3,259	17964,2	3,748	232,21
1	1,564	5200878	2,133	2704998	3,255	36071,7				

Table 31: GC Chromatogram (20 % (v/v) sample/ethyl acetate) of the Dodecanoic Acid Standards from experience 7. Blue: Ethyl acetate, Orange: *n*-dodecane GC peak area and Green dodecanoic peak area. t:time (minutes)and peak area: peak area (µV s).

v/v Dodecanoic Acid/ *n*-dodecane prepared (g/L)	t	Peak Area	t	Peak Area	t	Peak Area
0,1	1,538	6858997	2,117	4058414	3,729	285,65
1	1,57	5181876	2,139	2709896	3,754	4414,25
5	1,57	5198115	2,139	2693411	3,787	22597,33
10	1,567	5232816	2,137	2673290	3,811	43359,85

Table 32: GC Chromatogram (20 % (v/v) sample/ethyl acetate) of the 1-Dodecanol Standards from experience 8. Blue: Ethyl acetate, Orange: *n*-dodecane GC peak area and Pink: 1-dodecanol peak area. t:time (minutes)and peak area: peak area (µV s).

v/v Dodecanoic Acid/ *n*-dodecane prepared (g/L)	t	Peak Area	t	Peak Area	Peak Area	Peak Area	t	Peak Area	t	Peak Area	t	Peak Area
0,025	1,539	7.047.696,76	2,137	3.828.565,88								
0,25	1,579	5.061.820,63	2,157	2.598.409,70	3,294	8.235,47						
2,50	1,576	4.987.082,29	2,154	2.652.273,32	3,305	96.585,60	3,813	99,06	3,891	162,65	4,671	156,81

Table 33: GC Chromatogram (20 % (v/v) sample/ethyl acetate) of the Dodecanoic Acid Standards from experience 8. Blue: Ethyl acetate, Orange: *n*-dodecane GC peak area and Green: Dodecanoic Area Peak area. t:time (minutes)and peak area: peak area (µV s).

v/v Dodecanoic Acid/ *n*-dodecane prepared (g/L)	t	Peak Area	t	Peak Area	t	Peak Area
0,25	1,55	4927699,25	2,115	2792078,93	3,759	727,26
2,5	1,551	5010285	2,212	2656408,27	3,778	7527,32
25	1,551	5028234,53	2,123	2626159,74	3,876	84955,15

Samples

Table 34: GC Chromatogram (50 % (v/v) sample/ethyl acetate) of the samples of the 1L SFs at the different time points from experience 1. Blue: Ethyl acetate, Orange: *n*-dodecane GC peak area, Pink: 1-Dodecanol peak and Green: Dodecanoic Acid (proved later). t: time and peak area: peak area (µV s).

	Time Point (h)	t	Peak Area	t	Peak Area	t	Peak Area	t	Peak Area	t	Peak Area	t	Peak Area	t	Peak Area	t	Peak Area	t	Peak Area	t	Peak Area
1L	6	1,622	3618639,85	1,83	2115,11	1,91	106601,07	2,11	12101,70	2,15	5202467,82	2,354	159364,79	2,838	22209,31	3,817	445,19				
1L	6	1,621	3789468,66	1,84	58109,51	1,91	97103,51	2,11	11654,45	2,15	5032757,22	2,359	137903,65	2,686	23290,73	2,837	21811,28	3,814	463,83		
1L	24	1,626	2448020,18	1,90	80938,16	2,10	7479,09	2,15	4288892,06	2,82	7358,2	3,312	345,53	3,809	3601,75						
1L	24																				
1L	48	1,646	3688858,44	1,941	105853,83	2,141	12339,56	2,184	5048984,52	2,869	28073,71	3,361	2655,13	3,858	5742,09	5,421	110,96				
1L	48	1,645	3741753,18	1,829	71196,7	1,941	85260,22	2,143	11289,64	2,187	4960661,35	2,361	151899,38	2,876	4430,12	3,369	1167,3	3,869	6878,06	5,425	122,32

Table 35: GC Chromatogram (50 % (v/v) sample/ethyl acetate) of the samples of the 1L SFs at the different time points from experience 1. Blue: Ethyl acetate, Orange: *n*-dodecane GC peak area, Pink: 1-Dodecanol peak and Green: Dodecanoic Acid (proved later). t:time (minutes)and peak area: peak area (µV s).

.	Time Point (h)	t	Peak Area	t	Peak Area	t	Peak Area	t	Peak Area	t	Peak Area	t	Peak Area	t	Peak Area	t	Peak Area	t	Peak Area	t	Peak Area	t	Peak Area
500 mL	6	1,627	3461280,44	1,838	2295,2	1,916	105802,41	2,114	12073,5	2,154	5348113,66	2,364	163794,41	2,841	15014,18	3,818	503,71						
500 mL	6	1,626	3791574,37	1,844	275,6	1,919	112911,13	2,117	12438,7	2,161	5045171,08	2,369	137784,09	2,699	23169,61	2,845	22002,53	3,821	463,52				
500 mL	24	1,626	3350516,12	1,917	100462,62	2,116	9315,31	2,164	4398808,65	2,441	70625,77	2,837	3258,21	3,325	333,93	3,825	5384,12						
500 mL	24	1,611	4171984,73	1,907	116136,76	2,105	11533,04	2,151	5030876,92	2,829	17187,7	2,987	2422,71	3,314	3219,77	3,822	7952,64						
500 mL	48	1,646	3865410,32	1,945	11814,52	2,148	2619,03	2,191	4714113,63	2,37	63286,33	2,514	26040,18	2,88	435,61	3,3038	328,15	3,37	3842,56	3,879	10465,31	5,43	108,4
500 mL	48	1,648	4018301,55	1,947	114349,38	2,15	12360,5	2,194	4866691,8	2,886	24018,6	3,039	5731,94	3,127	8251,48	3,371	5740,26	3,879	10184,51	5,429	116,85		

Table 36: GC Chromatogram (20 % (v/v) sample/ethyl acetate) of the 1L SFs samples of organic phase at the different time points from experience 2. Blue: Ethyl acetate, Orange: *n*-dodecane GC peak area, Pink: 1-Dodecanol peak and Green: Dodecanoic Acid. t:time (minutes)and peak area: peak area (µV s).

.	Time Point (h)	t	Peak Area	t	Peak Area	t	Peak Area	t	Peak Area	t	Peak Area	t	Peak Area	t	Peak Area	t	Peak Area	t	Peak Area	t	Peak Area
Normal	6	1,835	3862639	2,167	107204	2,386	13815,62	2,427	5763262	2,771	185090	3,181	24209	4,223	606,36						
	24	1,837	3654725	2,166	104709	2,385	14086,57	2,424	5944474	2,768	183064	3,18	13829	3,354	11030,45						
	30	1,836	3633298	2,164	103122	2,383	14049,38	2,424	6153579	2,696	13,28	2,767	175693	3,179	16008,84	3,353	15244,21	3,706	1578,15		
	48	1,83	3719463	2,113	357,69	2,159	77127,02	2,379	11041,57	2,417	6E+06	2,7	38258	2,762	119290,3	3,173	418,85	3,344	405,17	3,697	4959,86
PPG	6	1,84	3556622	2,169	102687	2,387	14123,67	2,427	5923617	2,773	185853	3,185	25622	4,229	2063,66						
	24	1,841	3426887	2,168	104347	2,387	13862,82	2,424	5992939	2,772	188244	3,187	14019	3,358	11087,36	4,224	183,4				
	30	1,841	3702407	2,171	114490	2,391	14123,27	2,431	5822852	2,776	200213	3,188	15877	3,362	16015,06	3,718	2018,89	4,227	965,48		
	48	1,836	3732039	2,165	104320	2,385	14100,46	2,424	5793317	2,77	196129	3,182	17447	3,354	17041,08	3,708	8714,51	4,222	138,38		
Triton X-100	6	1,832	3908118	2,162	105174	2,381	13135,83	2,424	5225067	2,764	183029	3,175	14482	3,343	9226,13	4,217	2325,87	4,855	39,27		
	24	1,833	3834610	2,163	103267	2,381	13661,31	2,424	5353358	2,766	178743	3,176	9867,9	3,353	17027,44	3,699	13401,23	4,305	57232,01		
	30	1,824	4278808	2,158	119027	2,376	15811,73	2,411	5993506	2,762	213188	3,176	12344	3,354	21127,34	3,7	21127,46	4,298	51882,65		
	48	1,84	3822796	2,17	107162	2,391	13711,87	2,431	5434668	2,776	185463	3,187	11177	3,365	12615,49	3,71	19397,36				

Table 37: GC Chromatogram (20 % (v/v) sample/ethyl acetate) of the 500mL SFs samples of organic phase at the different time points from experience 2. Blue: Ethyl acetate, Orange: *n*-dodecane GC peak area, Pink: 1-Dodecanol peak and Green: Dodecanoic Acid. t:time (minutes)and peak area: peak area (µV s).

.	Time Point (h)	t	Peak Area	t	Peak Area	t	Peak Area	t	Peak Area	t	Peak Area	t	Peak Area	t	Peak Area	t	Peak Area	t	Peak Area	t	Peak Area
Normal	6	1,835	4050558	2,168	97193,6	2,387	13232,18	2,431	5710904	2,772	157563	3,182	4761,5	4,222	999,16						
	24	1,836	3676485	2,164	100967	2,382	14163,82	2,421	6119429	2,768	184515	3,182	16787	3,354	16526,12	3,71	1912,38				
	30	1,831	4001849	2,162	100260	2,381	14025,38	2,421	5790165	2,765	182969	3,173	14719	3,349	14629,79	3,701	2977,16				
	48	1,818	4734833	2,154	111825	2,373	15736,53	2,411	6237134	2,758	219433	3,173	19243	3,345	18913,05	3,7	10826,39				
PPG	6	0,542	10,21	0,987	11,15	1,839	3956767,41	2,172	99819,46	2,392	12413	2,437	5E+06	2,778	149914,2	3,187	4975,65	4,228	876,02		
	24	1,84	3873878	2,172	106686	2,39	13807,09	2,431	5755296	2,777	181421	3,189	14562	3,361	10695,38						
	30	1,838	3937734	2,171	105062	2,389	13690,62	2,431	5691947	2,775	2E+06	3,187	12468	3,36	6614,99	3,715	212,67	4,227	831,26	4,613	15,61
	48	1,797	5731734	2,14	106433	2,391	7385827,3	2,746	258958,5	3,334	588,8	3,688	6694								
Triton X-100	6	1,841	3971916	2,173	101813	2,393	13572,87	2,434	5582345	2,779	177177	3,19	13419	3,363	9665,08	4,239	3269,01				
	24	1,838	4069930	2,172	88443,1	2,393	10937,13	2,437	5436948	2,78	117531	3,19	365,96	3,368	7912,26	3,715	19488,97	4,314	47824,29		
	30	1,843	3778376	2,173	101283	2,392	14356,5	2,431	5792989	2,778	185653	3,189	14665	3,367	27613,95	3,713	28549,95	4,293	36712,8		
	48	1,836	4072729	2,168	87480,8	2,388	12315,76	2,427	5908658	2,776	140371	3,364	2742,2	3,721	463,38						

Table 38: GC Chromatogram (20 % (v/v) sample/ethyl acetate) of the 1L SFs samples of interface at the different time points from experience 2. Blue: Ethyl acetate, Orange: *n*-dodecane GC peak area, Pink: 1-Dodecanol peak and Green: Dodecanoic Acid. t:time (minutes)and peak area: peak area (µV s).

.	Time Point (h)	t	Peak Area	t	Peak Area	t	Peak Area	t	Peak Area	t	Peak Area	t	Peak Area	t	Peak Area	t	Peak Area
Normal	6																
	24	1,824	5900383	2,466	3423888	2,787	1,28E+05	3,367	449,67	3,725	719,5						
	30	1,837	4428971	2,175	112180	2,441	5,05E+06	2,782	199740,3	3,192	10558	3,368	4610,6	3,723	1307,99	3,986	98,14
	48	1,838	5326934	2,467	3992222	2,797	1,03E+05	3,202	341,75	3,38	248,94	3,737	3003,4	4,257	197,93		
PPG	6																
	24	1,823	6061872	2,47	3119674	2,788	1,17E+05	3,364	210,39	3,725	156,53						
	30	1,841	7337889	2,48	1899078	2,774	1,18E+05										
	48	1,839	3417012	2,164	113377	2,384	1,43E+04	2,421	6151211	2,769	198137	3,182	17759	3,355	15766,94	3,707	6740,14
Triton X-100	6	1,813	7079312	2,492	1723843	2,785	1,60E+05	4,226	485,11								
	24	1,82	621488,51	1,83	5907458,73	2,48	2679215,79	2,79	106873,52	3,37	3165,58	3,71	4436,59	4,27	21012,83		
	30	1,824	186686,36	2,487	2359358,64	2,792	1,21E+05	3,373	2836,31	3,721	6233,39	4,286	20560,73				
	48	1,824	5905855,19	2,468	2643803,35	2,778	1,30E+05	3,356	2106,68	3,702	7754,75	4,219	244	4,437	41,93		

Table 39: GC Chromatogram (20 % (v/v) sample/ethyl acetate) of the 500mL SFs samples of interface at the different time points from experience 2. Blue: Ethyl acetate, Orange: *n*-dodecane GC peak area, Pink: 1-Dodecanol peak and Green: Dodecanoic Acid. t:time (minutes)and peak area: peak area (µV s).

.	Time Point (h)	t	Peak Area	t	Peak Area	t	Peak Area	t	Peak Area	t	Peak Area	t	Peak Area	t	Peak Area	t	Peak Area	t	Peak Area	t	Peak Area	t	Peak Area
Normal	6																						
	24	1,828	7025177	2,507	2010126	2,806	1,53E+05	3,744	170,47														
	30	1,816	7136550	2,498	1743538	2,792	1,56E+05	3,724	305,73														
	48	1,823	6700808	2,494	2243793	2,797	1,02E+05	3,73	1119,63														
PPG	6																						
	24	1,822	7259180	2,506	1699988	2,8	1,63E+05	4,252	73,17	4,786	80,98												
	30	1,822	7214164	2,507	1712308	2,802	1,62E+05	4,254	92,26														
	48	1,828	6719224	2,499	2242780	2,802	1,09E+05	3,738	947,8														
Triton X-100	6	1,788	9568370	2,495	1395848	2,784	2,00E+05	3,721	604,73	4,237	381,86												
	24	1,82	6926476	2,494	2175087	2,795	1,53E+05	3,374	1617,09	3,723	5956,4	4,287	20610										
	30	1,866	2267388	2,177	76952,1	2,397	9,29E+03	2,431	6936147	2,786	145427	3,207	504,32	3,385	12288,49	3,737	45012,14	4,367	86237,14	4,621	191		
	48	1,828	5746786	2,465	3501655	2,787	1,22E+05	3,368	895,81	3,725	332,03	4,235	275,41	4,957	104,39								

Table 40: GC Chromatogram (20 % (v/v) sample/ethyl acetate) of the 1L SFs samples of organic phase at the different time points from experience 3. Blue: Ethyl acetate, Orange: *n*-dodecane GC peak area, Pink: 1-Dodecanol peak and Green: Dodecanoic Acid. t:time (minutes)and peak area: peak area (µV s).

.	Time Point (h)	t	Peak Area	t	Peak Area	t	Peak Area	t	Peak Area	t	Peak Area	t	Peak Area
Normal	6	1,559	5410832	1,876	106914,3	2,136	2936746	3,788	677,04				
	24	1,553	4625709	1,866	120412	2,108	4002422	2,929	26615,77				
	30	1,568	4215624	1,884	102246,6	2,14	2637847	2,951	6654,27				
PPG	6	1,56	5300082	1,877	99549,4	2,135	2966391	3,789	691,05				
	24	1,558	4865208	1,874	98170,54	2,132	2814096	2,938	6801,95				
	30	1,596	3165325	1,902	99898,18	2,144	3336846	2,984	12964,72				
Triton X-100	6	1,557	4782849	1,875	102500,3	2,131	2950808	2,937	9544,59	3,263	1068,29	3,782	1912,21
	24	1,557	4618201	1,873	100047,5	2,128	3020734	2,94	10418,44	3,26	6946,98	3,802	9888,09
	30	1,55	5059636	1,875	81795,99	2,126	3170746	2,952	9704,23	3,273	7738,82	3,863	40549,58

Table 41: GC Chromatogram (20 % (v/v) sample/ethyl acetate) of the 1L SFs samples in the interface at the different time points from experience 3. Blue: Ethyl acetate, Orange: *n*-dodecane GC peak area, Pink: 1-Dodecanol peak and Green: Dodecanoic Acid.t:time (minutes)and peak area: peak area (µV s).

.	Time Point (h)	t	Peak Area	t	Peak Area	t	Peak Area	t	Peak Area	t	Peak Area
Normal	6										
	24	1,546	581786,4	2,149	1455932						
	30										
PPG	6										
	24										
	30	1,57	5068463	2,189	892497,5						
Triton X-100	6	1,548	5522344	2,141	2272541	3,779	1547,36				
	24	1,517	8089887	2,143	1018007	2,918	13511,94	3,242	2878,04	3,769	2455,22
	30										

Table 42: GC Chromatogram (20 % (v/v) sample/ethyl acetate) of the well samples at 24hours in the organic phase from experience 5. Blue: Ethyl acetate, Orange: *n*-dodecane GC peak area, Pink: 1-Dodecanol peak and Green: Dodecanoic Acid. t:time (minutes)and peak area: peak area (µV s).

Sandwich cover		t	Peak Area	t	Peak Area	t	Peak Area	t	Peak Area	t	Peak Area	t	Peak Area
A	Normal	1,899	5490334	2,273	118378,4	2,571	2697362	3,501	431,59	3,864	293,86	4,395	308,57
		1,904	5031953	2,275	118987,2	2,572	2804197	3,504	838,93	3,866	199,58	4,403	4439,66
	PPG												
		1,904	2576123	1,971	2399235	2,275	118052,1	2,573	2573195	3,502	724,74	3,863	369,19
	Triton X-100	1,905	528291,5	2,276	126070,8	2,571	2963335	3,506	1997,35	3,866	1144,05	4,438	19069,3
		1,905	4930549	2,278	113678,8	2,576	2535074	3,506	1423,66	3,867	789,92	4,426	13676,81
B	Normal	1,903	4929553	2,275	115791,7	2,573	2594273	3,503	549,31	4,407	5442,77		
		1,902	2751253	1,973	2437961	2,274	116375,1	2,572	2601253	3,503	808,58	3,865	252,45
	PPG	1,911	5303295	2,273	112759,9	2,573	2822801	3,504	867,23	3,865	1014,35	4,408	5083,15
		1,906	5077128	2,278	116488,1	2,576	2729732	3,508	1831,59	3,869	1044,57	4,446	22396,89
	Triton X-100	1,902	3307313	2,002	1747053	2,273	117421	2,57	2859459	3,501	857,67	3,863	219,09
		1,905	5143596	2,277	118249	2,574	2580965	3,507	1783,05	3,868	1203,8	4,455	28909,6

Table 43: GC Chromatogram (20 % (v/v) sample/ethyl acetate) of the well samples at 24hours in the interface from experience 5. Blue: Ethyl acetate, Orange: *n*-dodecane GC peak area, Pink: 1-Dodecanol peak and Green: Dodecanoic Acid. t:time (minutes)and peak area: peak area (µV s).

Sandwich cover		t	Peak Area	t	Peak Area	t	Peak Area	t	Peak Area	t	Peak Area	t	Peak Area
A	Normal	1,877	7434999	2,601	489867								
		1,878	2815364	1,958	3886014	2,601	1778627	4,397	1607,05				
	PPG	1,873	3976233	2,044	2723184	2,577	792322,7	2,638	401457,6	4,414	1248,89		
		1,8141	9426389	2,575	1274153	4,38	1442,89						
	Triton X-100												
		1,872	6640804	2,578	116404,5	3,461	6207,29	4,37	2907,51				
B	Normal	1,87	6930799	2,58	1202481	4,368	1279,71						
	PPG												
		1,881	6176959	2,258	143077	2,569	2195039	3,472	3262,53	4,379	3625,92		
	Triton X-100	1,876	6217657	2,252	123237,2	2,5715	1775715	3,4685	2253,94	3,826	360,44	4,3865	8579,47
		1,8565	636717	1,874	6377986	2,5485	398064,5	4,332	2009,865				

Table 44: GC Chromatogram (20 % (v/v) sample/ethyl acetate) of the well samples at 48hours in the organic phase from experience 5. Blue: Ethyl acetate, Orange: *n*-dodecane GC peak area, Pink: 1-Dodecanol peak and Green: Dodecanoic Acid. t:time (minutes)and peak area: peak area (µV s).

Sandwich cover		t	Peak Area	t	Peak Area	t	Peak Area	t	Peak Area
A	Normal								
	PPG								
	Triton X-100								
B	Normal								
	PPG								
	Triton X-100	1,896	6228981	2,579	2535470	3,499	2130,74	3,855	3220,45
		1,848	8620341	2,547	3896344	3,47	54474,33	3,829	19033,31

Table 45: GC Chromatogram (20 % (v/v) sample/ethyl acetate) of the well samples at 48hours in the interface from experience 5. Blue: Ethyl acetate, Orange: *n*-dodecane GC peak area, Pink: 1-Dodecanol peak and Green: Dodecanoic Acid. t:time (minutes)and peak area: peak area (µV s).

Sandwich cover	MTP Line	t	Peak Area	t	Peak Area	t	Peak Area	t	Peak Area
A	Normal	1,883	7636722	2,606	731540				
		1,886	7734214	2,61	660091,2				
	PPG	1,894	7614100	2,613	481496,2				
		1,891	7475060	2,606	908902,5				
	Triton X-100	1,877	8054299	2,604	642470,1	3,854	301,22		
		1,882	7659545	2,606	670867,6	3,49	12558,23	3,855	1645,97
B	Normal	1,847	9666009	2,582	622995,4				
		1,856	9269457	2,59	648962,9				
	PPG	1,884	771836,9	2,609	539003,3				
		1,887	7729907	2,61	598515,8				
	Triton X-100	1,849	9482120	2,584	608285,1	3,837	413,57		
		1,887	7671328	2,611	680862,9	3,861	384,17		

Table 46: Average GC Chromatogram (20 % (v/v) sample/ethyl acetate) of the well samples in the organic phase from experience 6. Blue: Ethyl acetate, Orange: *n*-dodecane GC peak area, Pink: 1-Dodecanol peak and Green: Dodecanoic Acid. t:time (minutes)and peak area: peak area (µV s).

Bottom Type		Time points (h)	t	Peak Area	t	Peak Area	t	Peak Area	t	Peak Area	t	Peak Area	t	Peak Area
Inverted inverted pyramid	Normal	6	1,548	5438790	2,1285	2665359	3,774	684,815						
		24	1,5575	5131759	2,1355	2684044	2,939	186,095	3,266	671,13	3,791	3309,885		
		30	1,596	3332439	2,139	3574386	2,983	3140,66	3,307333	6401,863	3,855333	11854,39	5,408	150,83
	PPG	6	1,556	4879181	2,131333	2608388	3,778	1506,047						
		24	1,5565	4818936	2,13	2775748	3,098	603,025	3,5225	1785,065				
		30	1,595333	3793417	2,153	3176827	2,986333	1414,463	3,311	2426,507	3,857	10897,23		
	Triton X-100	6	1,5565	4938681	2,132	2576441	3,355	699,03	3,778	1098,75				
		24	1,55775	5230858	2,06725	2233979	2,737	749823	3,183	2536,608	3,789333	4618,123		
		30	1,599333	3461818	2,065	2268269	2,703333	1331009	3,204	3787,987	3,680667	12990,73		
Half sphere	Normal	6	1,593333	3862026	2,034667	1352808	2,987333	1925419	3,268	7076,933				
		24	1,593667	3105538	2,057333	2230689	2,698667	1278990	3,199333	9758,257	3,688333	16291,75	4,886	3892,88
		30	1,595667	3175404	2,147333	3067440	3,094333	1341,737	3,492	9608,773	3,6285	188,855	3,8815	23702,95
	PPG	6	1,597333	3167224	1,902333	54414,52	2,142	3543365						
		24	1,597667	3005495	2,142	3346589	3,201	1319,697	3,661333	1894,397				
		30	1,5975	3474931	2,144	3592904	3,311	2000,47	3,7305	786,49				
	Triton X-100	6	1,595	4047160	1,904	27055,12	2,158	3166515	2,987	10579,11	3,313	946,34	3,839	1983,77
		24	1,586667	2803864	1,965333	3088277	2,698	1215518	3,198333	5132,65	3,675	11111,5		
		30	1,599	2854531	2,138	3521999	2,984667	2386,59	3,311	4088,22	3,863	13519,91		

Table 47: Average GC Chromatogram (20 % (v/v) sample/ethyl acetate) of the well samples in the interface from experience 6. Blue: Ethyl acetate, Orange: *n*-dodecane GC peak area, Pink: 1-Dodecanol peak and Green: Dodecanoic Acid. t:time. and peak area: peak area (µV s).

Bottom Type		Time point (h)	t	Peak Area	t	Peak Area	t	Peak Area	t	Peak Area	t	Peak Area	t	Peak Area	t	Peak Area	t	Peak Area
Inverted inverted pyramid	Normal	6																
		24	1,5505	5794290	2,1525	1608391	3,257	209,145	3,78	1352,04								
		30	1,5745	5204800	2,198	626899,4	3,5745	674,3	3,839	1009,14								
	PPG	6																
		24	1,538	5786647	2,121	2955197	3,249	1578,355	3,7785	4049,805								
		30	1,58625	4578413	2,12525	790322,9	3,07175	1005350	3,174667	37869,05	3,365	1841,705	3,627	156,32	3,855	9765,31	5,407	176,25
	Triton X-100	6	1,543	6287511	2,151	798818	3,774667	469,17										
		24	1,5466	5789252	2,1462	1661169	3,2908	1397,976	3,648	2463,905	3,783	5015,98						
		30	1,572	5259702	2,194333	472276,9	3,656667	620,72	3,84	4290,14								
Half sphere	Normal	6																
		24	1,562333	24624965	2,190333	1033649	3,484	1341,09	3,847	3081,7								
		30	1,569333	5120922	2,186333	719164,8	3,472667	1500,32	3,83	2440,555								
	PPG	6																
		24	1,575333	5268215	2,195333	1011314	3,5735	819,37										
		30	1,58	5036084	2,2005	1165711	3,3145	720,64	3,8455	704,525								
	Triton X-100	6	1,577	5066220	2,197	847616	3,8385	194,175										
		24	1,565333	4982815	2,184333	981871,3	3,295667	468,8133	3,822	1364,633								
		30	1,573667	5078294	2,193333	762708,7	3,479667	401,9867	3,834	1357,545								

Table 48: GC Chromatogram (20 % (v/v) sample/ethyl acetate) of the well samples in the organic phase from experience 7. Blue: Ethyl acetate, Orange: *n*-dodecane GC peak area, Pink: 1-Dodecanol peak and Green: Dodecanoic Acid. t:time (minutes)and peak area: peak area (µV s).

Run	t	Peak Area	t	Peak Area	t	Peak Area	t	Peak Area	t	Peak Area	t	Peak Area	t	Peak Area
1	1,502	1255661	1,776	1817915	2,036	38177,58	2,303	191408,5						
2	1,563	5169078	2,138	2669198	2,945	602,17	3,267	2613,29	3,825	19108,3				
3	1,559	5140627	2,133	2654131	2,94	718,98	3,261	2175,37	3,821	21095,27				
4	1,565	4641212	2,125	2938135	2,944	5364,22	3,263	6273,9	3,821	20768,61				
5														
6	1,559	5096181	2,135	2638564	2,943	3607,69	3,262	6793,73	3,796	8183,94				
7														
8	1,5605	4966280	2,1325	14400059	2,9395	457,12	3,2635	2811,41	3,798	9111,395	3,882	80256,59		
9														
10														
11														
12	1,562	4831598	2,131	2529015	2,936	382,49	3,257	5406,2	3,83	37674,48	3,802	12845,61	3,823	35515,23
13	1,578	3441759	2,104	4118981	2,779	30285,73	2,942	24210,41	3,264	31483,72				
14	1,563	4889651	2,134	2629170	2,8585	6300,83	3,1015	8027,095	3,5325	9225,905	4,568	2514,96		
15	1,562	4784012	2,134	2468224	2,941	1281,97	3,261	6329,05	3,82	26605,19				
16	1,563	4555217	1,947	59695,99	2,12	2966632	2,455	42739,45	2,935	1835,95				
17														
18														
19	1,561	4942906	2,132	2568696	2,935	385,64	3,257	4841,98	3,846	51228,36				
20														

Table 49: GC Chromatogram (20 % (v/v) sample/ethyl acetate) of the well samples in the interface from experience 7. Blue: Ethyl acetate, Orange: *n*-dodecane GC peak area, Pink: 1-Dodecanol peak and Green: Dodecanoic Acid. t:time. and peak area: peak area (µV s).

Run	t	Peak Area	t	Peak Area	t	Peak Area	t	Peak Area	t	Peak Area	t	Peak Area	t	Peak Area	t	Peak Area	t	Peak Area
1	1,544	6345552	2,151	879770,7	3,244	969,85	3,787	29202,12										
2	1,565	5123100	2,141	2637000	2,947	600,5	3,271	5336,87	3,834	31414,71								
3	1,558	5486228	2,137	2362696	2,925	12396,15	3,169	3047,81	3,25	3315,31	3,771	16819,7						
4	1,546	6223172	2,15	1084682	2,92	4579,76	3,243	789,55	3,74	3585,14								
5																		
6	1,566	4517496	2,124	2968222	2,774	304,43	2,938	4836,43	3,257	14542,53	3,808	31157,08						
7																		
8	1,5725	18150183	1,979	2316913	2,445	1625457	2,848	23284,28	3,09	9033,365	3,247	4798,16	3,775	19556,71	5,289	143,83		
9	1,562	5485979	2,153	2123790	2,946	2216,34	3,266	12172,94	3,845	49717,84								
10																		
11																		
12	1,557	5364566	2,135	2343768	3,245	5299,62	3,85	94792,67	4,93	85,93	5,283	211,46						
13	1,566	4637799	2,001	1422622	2,528	1574857	2,984	20075,43	3,316	45377,72	3,681	7465,525	4,282	12538,5	3,892	99266,91	4,449	287,09
14	1,556	5573247	2,1405	1329943	2,9385	359,355	3,2625	2434,285	3,795	11093,14								
15	1,554	6047851	2,1565	1489836	3,104	885,725	3,529	6888,05	4,154	13177,48	4,481	204,43						
16	1,5615	5490290	2,1515	2142125	2,9455	5816,16	3,2675	2990,175	3,813	18504,06								
17	1,558	4707044	1,864	107700,6	2,115	2946746	2,92	813,88	3,24	8020,94	3,859	119905	4,4	160,59	5,276	341,23		
18	1,556	4890379	1,861	101179,8	2,121	2732881	2,921	761,15	3,24	6879,88	3,855	110784,9	4,858	66,92	5,277	309,78		
19	1,561	5097060	1,879	121235,5	2,143	2329038	2,941	195,41	3,264	4287,03	3,851	44808,45	5,347	116,2				
20	1,571	4475582	1,881	119652,5	2,131	3024450	2,943	717,62	3,27	9598,92	3,934	152629,8	4,977	155,78	5,353	736,76		

Table 50: GC Chromatogram (20 % (v/v) sample/ethyl acetate) of the well samples in the organic phase from experience 8. Blue: Ethyl acetate, Orange: *n*-dodecane GC peak area, Pink: 1-Dodecanol peak and Green: Dodecanoic Acid. t:time (minutes)and peak area: peak area (µV s).

Time Point (h)	t	Peak Area	t	Peak Area	t	Peak Area	t	Peak Area	t	Peak Area	t	Peak Area
5	1,543	5566635,75	2,12	3030709,13	3,795	581,17						
5	1,559	4905081,82	2,134	2654349,3	3,8	374,79						
5	1,562	4894405,73	2,137	2672703	3,805	411,08						
19,5	1,543	5848461,41	2,142	1849580,57	2,933	1257,34	3,257	2974,07	3,823	17501,67		
19,5	1,553	5716955,73	2,152	1822251,29	2,942	9716,94	3,267	3825,06	3,827	14002,03		
30	1,55	4966137,42	2,126	2524196,01	2,707	183,78	2,931	2465,79	3,253	6121,06	3,831	26832,58
30	1,521	6631190,21	2,11	3588743,56	2,917	28183,82	3,24	16695,01	3,817	30648,56		
30	1,528	6709204,14	2,134	2219162,36	2,928	16432,27	3,252	7579,2	3,817	16768,96		
48	1,552	4965833,87	2,126	2.537.894	2,713	981,85	2,932	1874,68	3,254	9313,6	3,804	10230,34
48	1,552	5073323,92	2,134	2298591,29	2,715	802,76	2,935	1525,43	3,257	7722,92	3,803	8421,25
48	1,525	6521475,25	2,115	3322421,35	2,707	24.736	2,927	19.205	3,249	17926,48	3,809	16687,91

Table 51: GC Chromatogram (20 % (v/v) sample/ethyl acetate) of the well samples in the interface from experience 8. Blue: Ethyl acetate, Orange: *n*-dodecane GC peak area, Pink: 1-Dodecanol peak and Green: Dodecanoic Acid. t:time (minutes)and peak area: peak area (µV s).

Time Point (h)	t	Peak Area	t	Peak Area	t	Peak Area	t	Peak Area	t	Peak Area	t	Peak Area	t	Peak Area	t	Peak Area	t	Peak Area	t	Peak Area	t	Peak Area
5	1,549	5.689.777,64	2,142	2.066.671,790	3,401	147,730	3,775	1.440,770	4,474	92,440	4,871	68,270	5,017	137,910								
5	1,547	5.970.335,79	2,149	1.592.638,670	3,777	1.322,830	4,873	53,770														
5	1,551	5.442.261,46	2,144	2.098.972,610	3,257	140,530	3,403	143,010	3,790	2.048,620												
19,5	1,555	4.708.390,93	2,125	2.724.126,080	2,713	649,390	2,935	3.064,060	3,122	25,140	3,257	9.548,570	3,405	275,570	3,874	61602,09	4,874	113,81	4,966	97,14	5,268	151,22
19,5	1,554	4.482.051,06	2,113	3.028.367,100	2,708	355,230	2,929	3.327,580	3,251	10.557,070	3,402	328,540	3,871	63.018,080	4,87	125,27	4,96	89,91	5,263	125,47		
30	1,533	6.224.858,04	2,117	3.108.838,570	2,699	21.991,010	2,926	19.610,490	3,246	895,910	3,839	41.675,050	4,867	182,060								
30	1,552	5.501.432,45	2,141	2.315.526,400	2,714	10.002,540	2,938	4.920,590	3,259	6.097,420	3,841	30.313,120	4,876	97,210								
30	1,554	4.974.508,64	2,128	2.636.770,560	2,714	684,380	2,935	2.707,400	3,257	8.262,010	3,852	40.792,940	4,482	71,700	4,965	123,53	5,267	105,44				
48	1,555	4.883.574,95	2,124	2.770.494,390	2,713	2.919,900	2,933	2.295,460	3,253	15.569,480	3,825	26.624,830	4,474	155,890	4,959	217,81	5,257	128,19				
48	1,549	5.699.737,52	2,144	1.975.863,590	2,712	23.606,370	2,934	9.781,680	3,254	8.423,860	3,800	10.016,680										
48	1,555	4.773.678,74	2,121	2.899.123,340	2,714	2.359,960	2,933	2.383,570	3,254	15.802,160	3,819	21.276,800	4,960	72,820								

Table 52: GC Chromatogram (20 % (v/v) sample/ethyl acetate) of the well samples by a new extraction method from experience 8. Blue: Ethyl acetate, Orange: *n*-dodecane GC peak area, Pink: 1-Dodecanol peak and Green: Dodecanoic Acid. t:time (minutes)(minutes) and peak area: peak area (µV s).

Time Point (h)	t	Peak Area	t	Peak Area	t	Peak Area	t	Peak Area	t	Peak Area	t	Peak Area	t	Peak Area	t	Peak Area	t	Peak Area
5	1,551	5498384,21	2,136	2381241,49	3,402	329,54	3,77	795,18	4,792	91,3	4,868	182,26	5,014	316,05	5,087	160,47	5,186	107,95
5	1,552	5453124,24	2,135	2365845,96	3,249	110,61	3,4	323,18	3,768	1179,54	4,789	76,83	4,867	171,01	5,014	269,27	5	154,04
19,5	1,549	5476644,81	2,135	2250123,98	2,929	1531,63	3,248	4473,39	3,816	25397,37								
19,5	1,548	5696369,23	2,14	2083148,55	2,93	1429,41	3,25	3791,88	3,813	21569,38								
30	1,51	7696958,45	2,112	3630290,54	2,902	36747,85	3,225	30930,7	3,788	34387,01								
30	1,548	5352397	2,13	2401919,76	2,698	15199,46	2,926	12334	3,245	7010,89	3,813	25340,27						
48	1,545	5686951,9	2,137	2019307,72	2,701	23194,89	2,925	9625,03	3,244	7532,23	3,777	7347,4						
48	1,545	5.922.380	2,141	1.799.711	2,701	15431,29	2,925	9722,61	3,245	6671,75	3,776	6904,23						

Cell Density and Volume of the aqueous phase, interface and organic phase.

Table 53: Cell Density on the samples from experience 2

SF	Condition	Time Points (h)	DCW (g/L)
1L	Normal	6	1,1
		24	1,1
		30	1,3
		48	1,5
	PPG	6	0,5
		24	1,4
		30	1,3
		48	1,3
	Triton X-100	6	0,2
		24	1,1
		30	0,8
		48	0,8
500mL	Normal	6	0,8
		24	1,1
		30	1,6
		48	1,6
	PPG	6	0,7
		24	1,7
		30	1,6
		48	1,7
	Triton X-100	6	0,2
		24	1,2
		30	1,0
		48	1,3

Table 54: Cell Density on the samples from experience 3

Condition	Time Points (h)	DCW (g/L)
Normal	6	2,0
	24	3,2
	30	3,3
PPG	6	2,0
	24	6,1
	30	5,5
Triton X-100	6	2,2
	24	3,2
	30	4,7
Normal without Inducer	6	3,3
	24	2,9
	30	3,9

Table 55: Volume of the three separated phases on the samples from experience 5

			Aquous phase (mL)	Interface (mL)	Organic phase (mL)
A	24	NONE	1,5±0,1	0,2	0,2±0,05
		PPG	1,5±0,3	0,2±0,2	0,3±0,05
		Triton X-100	1,5±0,2	0,2±0,05	0,3±0,03
	48	NONE	1,4±0,2	0,1	1,5±0,2
		PPG	1,5	0,1±0,05	0
		Triton X-100	1,5	0,2±0,08	0,04±0,05
B	24	NONE	1,5±0,02	0,2±0,03	0,3±0,2
		PPG	1,3±0,05	0,3±0,1	0,04±0,05
		Triton X-100	1,3±0,3	0,2	0,2
	48	NONE	1,5	0,1±0,03	0,04±0,05
		PPG	1,5±0,05	0,1	0,04±0,05
		Triton X-100	1,6±0,03	0,1	0,1±0,1

Table 56: Final volumes of the three phases from experience 6.

Bottom Type			Aqueous phase (mL)	Interface (mL)	Organic phase (mL)
Inverted inverted pyramid	Normal	6	1,0±0,5	0	0,2±0,2
		24	1,7	0,1±0,02	0,3±0,04
		30	1,5±0,04	0,1±0,04	0,3±0,04
	PPG	6	1,2±0,4	0	0,3±0,04
		24	1,6±0,08	0,3±0,1	0,1±0,1
		30	1,5±0,04	0,1±0,04	0,2±0,04
	Triton X-100	6	0,75±0,1	0,2±0,2	0,2±0,2
		24	1,6±0,1	0,2±0,08	0,3±0,07
		30	1,5±0,08	0,1±0,04	0,3±0,07
Half sphere	Normal	6	1,0±0,3	0	0,1±0,07
		24	1,4±0,6	0,05±0,04	0,3±0,04
		30	1,6±0,3	0,1±0,02	0,3±0,07
	PPG	6	1,4±0,6	0,02±0,04	0,2±0,1
		24	1,2±0,6	0,04±,0,04	0,3±0,1
		30	1,7±0,1	0,07	0,3±0,04
	Triton X-100	6	1,3±0,3	0,06±0,04	0,2±0,09
		24	1,1±,08	0,07±0,07	0,4
		30	1,7	0,07	0,3

Table 57: Final volumes of the three phases from experience 7.

Run	**Aqueous phase (mL)**	**Interface (mL)**	**Organic phase (mL)**
1	1,3	0,1	0,1
2	1,0	1,5	0,3
3	1,0	0,1	0,3
4	0,9	0,1	0,2
5	3,0	0,1	0,0
6	1,0	0,1	0,2
7	0,9	0,2	0,0
8	2,8	0,6	0,8
9	2,0	0,0	0,0
10	0,8	0,2	0,0
11	0,9	0,1	0,0
12	2,8	0,6	0,1
13	2,7	0,6	0,2
14	2,9	0,3	0,6
15	2,8	0,3	0,4
16	3,1	0,4	0,3
17	1,9	0,4	0,0
18	1,9	0,3	0,0
19	2,9	0,4	0,3
20	1,9	0,3	0,0

Table 58: Final volumes of the three phases from experience 8.

Time Point (h)	Aqueous phase (mL)	Interface (mL)	Organic phase (mL)	Evaporation rate (% (v/v))
5	0,9	0,2±0,1	0,2±0,1	-3,4
19,5	0,9	0,1	0,2	5,9
30	0,9	0,1	0,2	0,3
48	1,0	0,1	0,1	0,36